

8-2015

# PRIMARY FLEXION AXIS SELECTION IN TOTAL KNEE REPLACEMENTS USING COMPUTATIONAL ANALYSIS

Nicholas Marais

*Clemson University*, [ncmarais@cox.net](mailto:ncmarais@cox.net)

Follow this and additional works at: [https://tigerprints.clemson.edu/all\\_theses](https://tigerprints.clemson.edu/all_theses)



Part of the [Engineering Commons](#)

---

## Recommended Citation

Marais, Nicholas, "PRIMARY FLEXION AXIS SELECTION IN TOTAL KNEE REPLACEMENTS USING COMPUTATIONAL ANALYSIS" (2015). *All Theses*. 2215.

[https://tigerprints.clemson.edu/all\\_theses/2215](https://tigerprints.clemson.edu/all_theses/2215)

This Thesis is brought to you for free and open access by the Theses at TigerPrints. It has been accepted for inclusion in All Theses by an authorized administrator of TigerPrints. For more information, please contact [kokeefe@clemson.edu](mailto:kokeefe@clemson.edu).

PRIMARY FLEXION AXIS SELECTION IN TOTAL KNEE REPLACEMENTS  
USING COMPUTATIONAL ANALYSIS

---

A Thesis  
Presented to  
the Graduate School of  
Clemson University

---

In Partial Fulfillment  
of the Requirements for the Degree  
Master of Science  
Bioengineering

---

by  
Nicholas Christopher Marais  
August 2015

---

Accepted by:  
Dr. John DesJardins, PhD, Committee Chair  
Dr. Martine LaBerge, PhD  
Dr. Guigen Zhang, PhD

## ABSTRACT

Total knee replacements (TKR) are one of the most frequently implanted medical devices, with over 600,000 procedures performed in the United States in 2012. In order to ensure TKR longevity, wear tests are frequently conducted on these implants prior to patient implantation. Variations in implant geometry, material, and surface treatments are all tested, however, TKR alignment may also play a role in the long-term success of the knee implant. When testing knee designs with complex tibial and femoral geometries it is essential that the implant be aligned as the implant manufacturers intended so as to best represent the function of the implant system. Although critical, a key alignment variable that is largely overlooked is femoral axis selection. Currently, femoral axis alignment is simply selected so as to minimize its effect on implant mechanics during walking simulation; a result that might completely misrepresent the implant designer's intent.

The purpose of this study was to create a computational model to determine the effect of femoral axis selection on contact-point bearing migration prior to simulator fixation and examine trends in femoral axis selection based on implant geometry. Using 3D optical scans of seven femurs, 3Matic STL for model remeshing, and COMSOL Multiphysics for simulation this study recreated the single-axis rotation of each femoral component in a wear simulator. The lowest femoral contact point was then tracked between 0° and 120° flexion over four hundred possible femoral axes alignment options.

The computational model was verified statistically and calculated the location of the ideal axes of rotation for all seven femurs. Reduction of P/D lowest contact-point translation during simulator flexion was found to be dependent on the range of flexion.

Single-axis knee designs were found to exhibit a lower tolerance to varied femoral axes of rotation, but still maintained lower mean P/D displacements. Anterior/posterior translation patterns during simulator flexion were found to vary significantly with femoral axis selection. Interestingly, A/P translation patterns were more consistent between varying flexion axes in implants with multiple axes of curvature compared to single-axis designs.

TKR alignment in single-axis simulators clearly affects proximal/distal and anterior/posterior lowest contact-point migration and thus possibly implant mechanics during functional testing. An implant that incorporates a geometry that is minimally affected by malalignment should enhance clinical outcomes and provide more consistent functional measures during simulation and use.

## DEDICATION

To those that aspire for greatness regardless of circumstance:

God did not give us a spirit of timidity, but a spirit of power, of love and of self-discipline.

## ACKNOWLEDGMENTS

The completion of this work was done using the knowledge and experience of a countless number of individuals. First, I must thank my advisor, Dr. John DesJardins, without whom I would not have found my place in the wonderful field of bioengineering. It is largely because of his boundless enthusiasm and excitement for engineering that I found myself in both his lab and the DEN, two aspects of my academic career that have defined my aspirations moving forward. I thank Dr. Martine LaBerge, the foundation of this extraordinary program, for her relentless passion for each and every student's success. I must also thank my final committee member, Dr. Guigen Zhang, for always keeping an open door and encouraging me to consider the bigger picture every time I stumbled in to his office confused. Recognition must be given to the rest of the Laboratory of Orthopaedic Design and Engineering for the help in various aspects of my project as well as helping me keep my sanity through the year. I would also like to thank Tim Pruett for his help with the 3D scans, Mike Jaeggli for his help and enormous patience as I learned 3Matic, and lastly Sam Bearden and Yu Zhao for guidance as I navigated COMSOL. An enormous thank you must be given to my parents who have always driven me to success while loving me no matter what, my sister and brother-in-law, Natassia and Spencer, for reminding me to make the most of life, my nieces, Peyton and soon to be Paisley, for lighting up my days, and finally my girlfriend, Jillian, for her endless support and encouragement to be the best person that I can.

Thank you all.

## TABLE OF CONTENTS

	Page
TITLE PAGE .....	i
ABSTRACT .....	ii
DEDICATION .....	iv
ACKNOWLEDGMENTS .....	v
LIST OF TABLES .....	ix
LIST OF FIGURES .....	x
CHAPTER	
1. GENERAL INTRODUCTION .....	1
1.1. Aims of the Study .....	1
1.2. Clinical Significance .....	2
2. KNEE ANATOMY AND PATHOLOGY .....	3
2.1. Knee Joint Anatomy .....	3
2.2. Knee Joint Kinematics .....	6
2.3. Common Knee Joint Pathologies .....	7
2.4. Treatment Options .....	9
3. TOTAL KNEE REPLACEMENTS .....	11
3.1. Surgical Procedure .....	11
3.2. Different TKR Designs and Functions .....	14
3.2.1. Fixed Bearing Implants vs. Mobile Bearing Implants .....	14
3.2.2. PCL Retaining vs. PCL Substituting .....	16
3.2.3. Medial Pivot Implants .....	17
3.2.4. High Flexion Implants .....	18
3.2.5. Constraint in Total Knee Replacements .....	19
3.2.6. Unicompartmental Implants .....	21
3.3. Femoral Design Features .....	23
3.3.1. Single-Axis vs. Multi-Axis Designs .....	23
3.3.2. The Extensor Mechanism .....	24
3.3.3. Posterior Femoral Rollback .....	25
3.3.4. Ligament Interactions .....	27
3.4. Anatomical and Surgical Alignment .....	28

Table of Contents (Continued)

	Page
3.4.1. Surgical Alignment .....	28
3.4.2. Known Errors in Surgical Alignment .....	31
3.4.3. Methods to Advance Alignment Precision .....	33
3.5. TKR Testing.....	35
3.5.1. Standards.....	36
3.5.2. TKR Simulation (cadaver, computational) .....	38
3.5.3. Instron Stanmore Knee Simulator.....	40
3.5.4. Design Variables Known to Affect Longevity .....	41
3.5.5. Summary of Aims and Introduction .....	43
4. MATERIALS.....	44
4.1. TKR Implants.....	44
4.2. NextEngine 3D Scanner.....	46
4.3. 3Matic STL .....	46
4.4. COMSOL Multiphysics Model .....	46
4.4.1. Model Physics.....	47
4.5. MATLAB.....	49
4.6. Knee Alignment Jig .....	49
5. METHODS .....	50
5.1. NextEngine 3D Scanner.....	50
5.2. 3Matic STL .....	51
5.3. COMSOL Multiphysics Model .....	55
5.4. MATLAB Post Processing .....	60
5.5. Alignment of the Femoral Component for Wear Testing.....	61
6. RESULTS .....	63
6.1. Mathematical Model Comparison.....	63
6.2. Ideal Axes of Femoral Rotation.....	65
6.3. P/D and A/P Translation at Varying Femoral Axes.....	73
7. DISCUSSION .....	77
7.1. Verification of 3D Model and Simulation Model.....	77
7.2. Location of Ideal Axes of Femoral Rotation .....	80
7.3. Relationship between P/D and A/P Translation on Varying Implants .....	83
7.4. Future Research .....	87
8. CONCLUSION.....	89



Table of Contents (Continued)

	Page
9. APPENDICES .....	90
1. Model Verification.....	91
2. A/P Translation.....	95
10. REFERENCES .....	102

## LIST OF TABLES

Table		Page
4.1	Femoral Component Descriptions .....	44
6.1	Computational versus measured proximal/distal bearing migration with the associated correlation value between the two sets of data .....	72
6.2	Proximal/Distal translation at ideal axis for each implant and flexion range.....	73
6.3	Anterior/Posterior translations at ideal axis based on minimum P/D translation for each implant and flexion range .....	74

## LIST OF FIGURES

Figure	Page
2.1	Structure of the knee joint (Drake, 2009) ..... 5
2.2	The knee with 6 degrees of freedom (Shenoy, Pastides, & Nathwani, 2013)..... 7
3.1	Bony referencing technique: (a) Alignment of the femoral cutting block for femoral resection based on the TEA (b) tibial insert alignment based on the femoral resection (“Surgical Technique for TKR - Wheelless’ Textbook of Orthopaedics,” n.d.) ..... 12
3.2	Ligament referencing technique: (a) Intraoperative photograph of a flexion gap tensioning jig placed into the flexion gap, tensioning the gap, and positioned parallel to the transepicondylar axis before the anterior and posterior femoral resections are performed (b) Intraoperative photograph demonstrating placement of the anteroposterior femoral cutting block parallel to the resected proximal tibia with each collateral ligament tensioned to create a rectangular flexion gap (Daines & Dennis, 2014) ..... 13
3.3	PCL retaining implant with tibial post (right) and PCL substituting implant (left) (MicroPort Orthopedics)..... 17
3.4	Tibial insert of a medial pivot total knee replacement showing the spherical medial condyle and cylindrical lateral condyle (Moonot, Mu, Railton, Field, & Banks, 2009) ..... 18
3.5	Unicompartmental Knee Implant (Arthrex) ..... 22
3.6	Anatomical and mechanical axes of the leg (Shenoy et al., 2013) ..... 30
4.1	Alignment jig used to align femoral components on simulator bracket..... 49
5.1	Bad edge located in difficult to scan areas of the implants need to be fixed in order to create a defined mesh ..... 52

List of Figures (Continued)

Figure	Page
5.2 Two-tone mesh created to keep the file size small while having a fine mesh over the area of analysis .....	54
5.3 Estimated geometrical axes for CenterPulse NKII .....	58
5.4 Visualized displacement of CenterPulse NKII at P/D 2 mm and A/P -8 mm .....	59
6.1 Graphic for measuring P/D migration of circle at ideal axis of rotation .....	64
6.2 Mathematically determined P/D displacement of single-axis implant at 0° - 90° flexion for 81 possible femoral axes with the ideal axis highlighted .....	64
6.3 P/D Displacement of 400 possible axes of rotation of Wright Medical Advance® Knee System at 0° - 90° flexion with ideal axis highlighted .....	65
6.4 Femoral axes of Natural Knee I .....	66
6.5 Femoral axes of Natural Knee II knee .....	67
6.6 Femoral axes of Biomet Maxim knee .....	67
6.7 Femoral axes of Wright Medical knee .....	68
6.8 Femoral axes of Ortho Development knee .....	68
6.9 Femoral axes of Stryker Triathlon knee .....	69
6.10 Femoral axes of Zimmer knee .....	69
6.11 Proximal/distal displacements at each possible femoral axis in 3-D for all seven implant .....	71
6.12 A/P displacement at the ideal axes and translated axes for 120 degrees flexion for the Zimmer knee .....	75

List of Figures (Continued)

Figure	Page
6.13 A/P displacement at the ideal axes and translated axes for 120 degrees flexion for the NKI (multi-axis) and Wright (single-axis) knee designs.....	76
A.1 A/P displacement of Wright Medical Advance® Knee System between 0° - 60° flexion with ideal axis highlighted. ....	91
A.2 P/D displacement of Wright Medical Advance® Knee System between 0° - 60° flexion with ideal axis highlighted. ....	92
A.3 A/P Displacement at ideal femoral axis between 0° - 60° flexion for Wright Medical Advance® Knee System. ....	93
A.4 Point of lowest contact in reference to knee geometry at 0° flexion. This can be plotted at each degree of flexion to recognize patterns. ....	93
A.5 Two meshes created in order to determine if bumpy surface was a result of mesh creation .....	94
B.1 A/P displacement of NKI at ideal axes for 60 and 120 degrees flexion.....	95
B.2 A/P displacement of NKII at ideal axes for 60 and 120 degrees flexion.....	96
B.3 A/P displacement of Biomet Maxim knee at ideal axes for 60 and 120 degrees flexion.....	97
B.4 A/P displacement of Ortho Development knee at ideal axes for 60 and 120 degrees flexion.....	98
B.5 A/P displacement of Stryker Triathlon knee at ideal axes for 60 and 120 degrees flexion.....	99
B.6 A/P displacement of Zimmer Knee at ideal axes for 60 and 120 degree flexion .....	100

List of Figures (Continued)

Figure	Page
B.7 A/P displacement of Wright Medical knee at ideal axes for 60 and 120 degrees flexion.....	101

## CHAPTER ONE: GENERAL INTRODUCTION

The knee is a synovial hinge joint made up by the femur, tibia, and patella that provides essential movement for many everyday activities. Chronic pain and reduced mobility due to damage of this articulation may result in the need for a replacement procedure to be conducted to regain functionality. Total knee replacements (TKR's) are a common procedure with high success rates. Variations in geometry between TKR's exist to satisfy different mechanisms of action. This thesis will discuss the effect that varying geometry may have on bearing contact migration. It will focus specifically on femoral lowest contact point translation (note: translation and displacement are used interchangeably in this work). This work includes a literature review on the anatomy, pathology, and treatment methods of the knee.

### *1.1 Aims of the Study*

This study seeks to determine the effect of femoral axis alignment on bearing migration in multiple TKR geometries. Previously studied femoral components provide a large and varied sample of implant geometries. The first aim will be to develop 3D models of these implants using 3-D scans. Next this study intends to use a computational model to measure proximal/distal, medial/lateral, and anterior/posterior translations of the lowest point of contact in the articulation during 120 degrees of flexion. This study will provide a comprehensive analysis of possible axes of rotation for the femoral component at varying angles of flexion, something that no other study has previously considered.

Using this analysis we hope to identify the ideal femoral axis of rotation, and translate that axis into a usable axis for our TKR wear testing procedures. This will help ensure that our wear testing is consistent between each implant, and that significant proximal/distal bearing migration does not damage our simulator. It is also a goal of the study to recognize any patterns between the geometry of the implants and minimized bearing migration.

### *1.2 Clinical Significance*

Although our three direct aims of this study are intended to produce a repeatable method of properly aligning femoral components for wear testing, the data outputted will allow for a comprehensive analysis of the effects of geometry on bearing migration. Because proper alignment of the implant during surgery is critical to the success of the procedure, it is of interest to understand if certain geometries minimize risk of aberrant bearing migration. Because many different knee geometries exist to satisfy separate elements, bearing migration can vary significantly between designs. However, the ability of the surgeon to actually attain accurate implant alignment is not guaranteed, which could result in detrimental functional consequences. It would be ideal if the surgeon had a larger range of femoral axis selection in which the implant would still be effective. Therefore, a geometry that would allow for multiple axes of rotation to provide very similar migration outcomes may be more effective for widespread use.



## CHAPTER TWO: KNEE ANATOMY AND PATHOLOGY

It is essential to understand the anatomy of the knee joint to understand the associated problems. The knee joint is a synovial hinge joint essential for everyday functions, most particularly walking. Because of the frequency of use many people suffer with ailments related to the knee, some of which can negatively affect function. Although this hinge joint is simple in concept, the human knee is actually made up of many different and complex components. This chapter focuses on the background of the knee joint and the associated pathologies.

### *2.1 Knee Joint Anatomy*

The knee joint is commonly referred to as the tibiofemoral joint, as the main articulation is a connection between the tibia and the femur. However, it is made up of both the tibiofemoral joint and the patellofemoral joint, or the connection between the patella and femur (Blackburn & Craig, 1980). As depicted in Figure 2.1 the bones that make up these two joints are the femur, the tibia, and the patella. The unique shape of each of these bones influences both the motion and strength of the knee (Blackburn & Craig, 1980). It is the ligaments, capsule, and musculature that provide stability to the knee (Goldblatt & Richmond, 2003), however the applied joint load is also an essential component to knee stability (Flandry & Hommel, 2011). Articular cartilage surrounds the bones at the points of intersection to provide a surface for the knee to smoothly rotate.

The tibiofemoral joint can be broken up into medial and lateral compartments, an articulation of the femoral condyles and the tibial plateaus (Goldblatt & Richmond, 2003). The femoral condyles are most easily compared to a cam, when looked at laterally. The medial and lateral condyles of the femur are asymmetrical, with the lateral condyle being smaller than the medial condyle (Goldblatt & Richmond, 2003). This plays a significant role in the valgus alignment of the knee. The medial compartment of the knee is supported in part by muscles in the thigh, including the extensor retinaculum, sartorius, gracilis, adductor magnus, vastus medialis, rectus femoris, and semitendinosus muscles (Blackburn & Craig, 1980). Capsular ligaments lie deep to the tibia collateral ligament (Figure 2.1) and provide stability to the knee through their thickened structures (Blackburn & Craig, 1980). The medial collateral ligament acts as a stabilization force by resisting valgus rotation forces. The posterior cruciate ligament is also found in the medial compartment and acts a significant stabilizer to the knee by resisting posterior displacement of the tibia on the femur. The posterior cruciate ligament tightens as the tibia internally rotates, and so it has an effect on knee motion. As depicted in Figure 1 the lateral and medial menisci lie in between the tibiofemoral articulation to enhance the conformity of the joint as well as aid in the flexion of the knee (Goldblatt & Richmond, 2003). The menisci aid in both lubrication of the knee for a smooth gliding surface and shock absorption to decrease joint loads.

The lateral compartment of the knee is also supported by musculature, including the iliotibial band, iliotibial tract, rectus femoris, biceps femoris, and vastus lateralis tendon (Blackburn & Craig, 1980). Capsular ligaments also exist laterally to stabilize the

joint. The lateral collateral ligament acts against varus rotational forces. The anterior cruciate ligament resists rotational loads during knee rotation by resisting anterior displacement of the tibia on the femur, also helping with overall knee stabilization (Duthon et al., 2006).

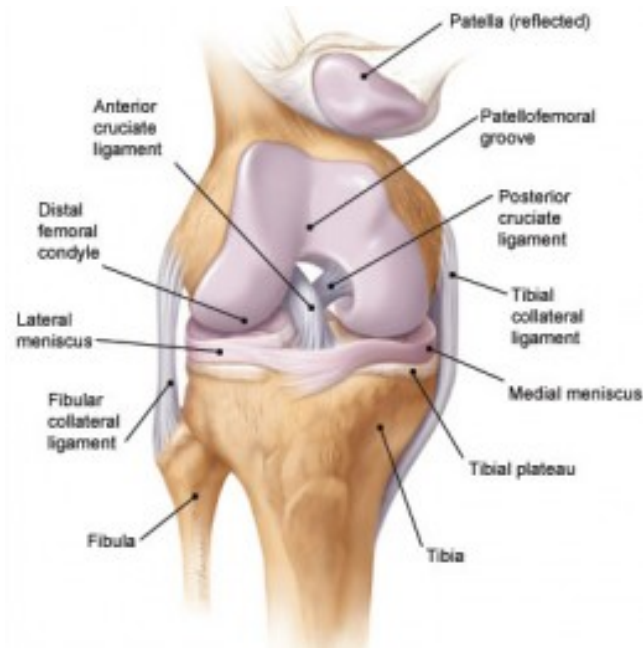


**Figure 2.1** Structure of the knee joint (Drake, 2009)

The patellofemoral joint is a sellar joint formed by the articulation of the patella and the femur. This joint's primary responsibility is the stability of the knee. The patella meets the femur at the patellofemoral groove and is held in place by a combination of ligaments and muscles. The patella acts as an aid to the extensor muscles by transmitting the outputted extensor force across the knee joint at a farther distance from the axis of rotation (Goldblatt & Richmond, 2003). This produces an increased moment arm ultimately reducing the required force to extend the knee.

## *2.2 Knee Joint Kinematics*

To fully understand this thesis it is necessary to understand the mechanisms via which the knee moves. This section will summarize normal knee movement during a range of flexion. Asano et al conducted a three-dimensional study on knee kinematics using a biplanar image-matching technique (Asano, Akagi, Tanaka, Tamura, & Nakamura, 2001). Shenoy et al published a mini-symposium on knee kinematics that summarizes many of Asano's results, as well as that of other studies.

The knee allows up to 160 degrees of flexion, with variations in the degree with different movements. Walking typically involves approximately 60 degrees of flexion, while there is 80 degrees for stair climbing, 90 degrees to walk down stairs, and approximately 115 degrees to sit down with up to 130 degrees for a full squat (Shenoy et al., 2013). The knee allows for six degrees of freedom (Figure 2.2) including flexion and extension, 25 – 30 degrees of rotation, 6-8 degrees of valgus and varus movement, 5 – 10 mm of anteroposterior translation, 1 -2 mm of mediolateral translation, as well as the articular cartilage and menisci allowing 2 -5 mm of joint compression (Shenoy et al., 2013).

Initial flexion (20 degrees) involves some posterior tibiofemoral translation via a rolling movement (Shenoy et al., 2013). As flexion continues lateral tibiofemoral translation is observed. The center of the medial femoral condyle translates slightly anteriorly, while the center of the lateral femoral condyle translates significantly posteriorly (Asano et al., 2001). This motion is known as posterior femoral rollback and will be discussed in greater detail in chapter three. The rotational motion occurring is

similar to that of a “screw home” motion of the knee around the tibial knee axis. This motion can more simply be described as a rotation of the knee along the medial condyle, with a posterior translation in the lateral condyle (Moonot et al., 2009).

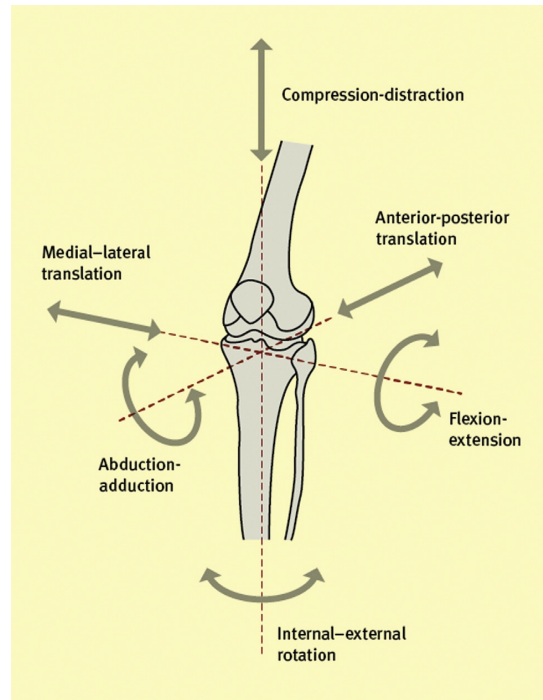


**Figure 2.2** The knee with 6 degrees of freedom (Shenoy et al., 2013)

### *2.3 Common Knee Joint Pathologies*

Because the knee joint is the largest joint in the body and one of the most relied upon joints it is at a high risk for injury. Many knee pathologies exist due to both spontaneous injury and degradation over time. Because there exists an expansive list of knee pathologies, this section seeks only to highlight some of the more prevalent injuries that may reduce function.

Injury to ligaments in the knee is very common and can often be debilitating. Damage to the anterior cruciate ligament typically occurs when the tibia slides anteriorly on the femur until rupture. This injury can be both painful and may also put the patient at significant risk for subsequent injury because of the lack of stability (Beynnon, Johnson, Abate, Fleming, & Nichols, 2005). Injury to the posterior cruciate ligament is more likely to occur when the knee is subjected to a direct load applied anteriorly during knee flexion (Voos, Mauro, Wente, Warren, & Wickiewicz, 2012). Medial collateral ligament injury is very common amongst young athletic patients and most commonly occurs with a high valgus stress or extreme external rotation (Phisitkul, James, Wolf, & Amendola, 2006). Lateral collateral ligament injuries are not as common, but can occur under high varus stress (Espregueira-Mendes & Vieira Da Silva, 2006).

Damage to the meniscus is often a serious concern because of the longevity of the injury. The meniscus is torn most commonly when a large force is applied while the knee is undergoing internal or external rotation (Rodkey, 2000). Because the meniscus is not penetrated by blood vessels, it does not heal. Therefore, potentially small injuries may become degenerative causing pain and deterioration of function (Rodkey, 2000).

Patellar injury is very common amongst athletes and may be the cause of chronic pain in the knee. Patellofemoral pain syndrome is frequently diagnosed although no consensus exists about its etiology (Collado & Fredericson, 2010). The pain frequently presents itself anteriorly, and so it is believed to be the result of deterioration of the articular cartilage behind the patella (Collado & Fredericson, 2010). Other patellar injuries include patellar fracture, dislocation, and patellar tendon rupture.

One of the most common knee pathologies, especially in older adults, is osteoarthritis. Osteoarthritis is characterized by cartilage loss over time resulting in degeneration of the articulation. This degeneration specifically causes thinning of the articular cartilage which can result in joint capsule narrowing (Das & Farooqi, 2008). Although significant damage is occurring osteoarthritis is typically not associated with intraarticular inflammation, but may result in synovitis (Goldring & Goldring, 2007). Changes in the peri-articular and subchondral bone may also occur during the reparative process (Das & Farooqi, 2008; Goldring & Goldring, 2007). Osteoarthritis is of significant concern because of the marked rise in incidences over recent years (Liddle, Pegg, & Pandit, 2013). This can be attributed to a larger aging population and longer life spans.

#### *2.4 Treatment Options*

The treatment of knee injuries varies significantly because of the variety of types of injury. Most treatment options require surgery and subsequent rehabilitation.

The treatment of ligamentous injuries are handled on a case by case basis with the primary object being to stabilize the knee to prevent further and future injury. Damage but not rupture to any of the ligaments in the knee could potentially be dealt with through rehabilitation exercises. This is the most effective method in treatment of medial collateral ligament damage, as direct intervention has been shown to have no significant positive effect (Woo, Chan, & Yamaji, 1997). If surgical intervention is required, repair of the ligament is the first priority. Unfortunately, if surgery is required it is typically

indicative of a ligament that cannot be repaired, and in this case an autograft or allograft will be used (Woo et al., 1997). Surgery is most commonly done to repair the anterior cruciate ligament.

Repair of the meniscus is difficult because of the lack of vascularization. However, preserving the meniscal tissue is incredibly important to the long term health of the joint. If the repair fails meniscal transplantation exists as an option (Noyes, Heckmann, & Barber-Westin, 2012). Although damage to the meniscus is not appealing, most damage is not significant remaining at the edge of the meniscus, where it can be cut away or more easily repaired because of increased vascularization near the edges (Noyes et al., 2012).

Patellar injury and pain is most commonly caused by patellofemoral pain syndrome (PFPS). Unfortunately PFPS is very common in athletes and no simple treatment option exists. The most effective solution is a rehabilitation regime to improve quadriceps muscle imbalances (Fagan & Delahunt, 2008).

Treatment of osteoarthritis is often a long term endeavor as the damage is progressive. Because of increased patient life there exists a large population living with osteoarthritis, and treatment has become extremely common. Treatment options include physical therapy and weight loss, nonsteroidal anti-inflammatory drugs to decrease inflammation and swelling, intra-articular corticosteroids, viscosupplementation, and intra-articular injections of hyaluronic acid to decrease pain (Snibbe & Gambardella, 2005). However, the most effective treatment for long term function remains a total knee replacement.



## CHAPTER THREE: TOTAL KNEE REPLACEMENTS

Total knee replacements are one of the most common orthopaedic surgical procedures performed each year. The principal objective of a total knee replacement is to restore functional movement to the knee joint. Indications for total knee replacements may include any damage to the articular surface of the knee, but is most commonly osteoarthritis in older patients (Shenoy et al., 2013). A TKR intends to restore the functional anatomy of the knee which includes the alignment of the knee, the soft tissue, and the joint line or mechanical axis (Shenoy et al., 2013).

### *3.1 Total Knee Replacement Surgical Procedure*

Total knee replacements are an invasive procedure that involves the removal of the entire natural articulation. To begin, the surgeon accesses the joint through a midline incision, typically about 8 to 10 inches in length, on the anterior face of the leg. The patella and extensor mechanism are rotated outside the knee joint so that access can be gained to the joint(Liddle et al., 2013). At this point two surgical techniques are commonly used to complete the procedure.

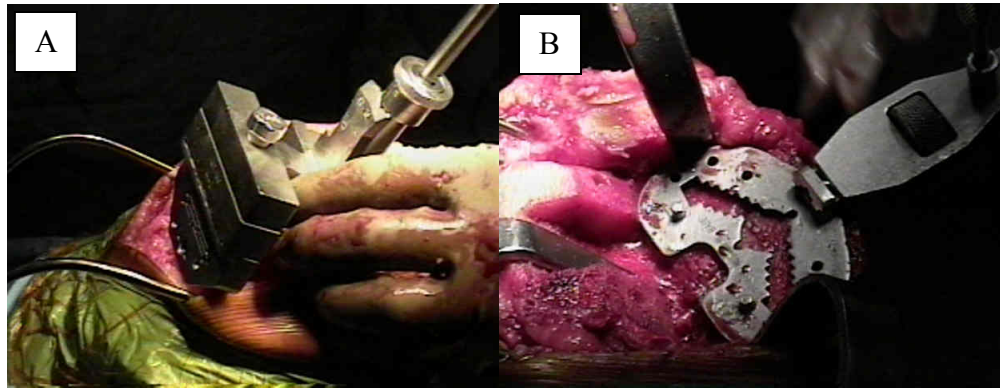


**Figure 3.1:** Bony referencing technique: (a) Alignment of the femoral cutting block for femoral resection based on the TEA (b) tibial insert alignment based on the femoral resection (“Surgical Technique for TKR - Wheelless’ Textbook of Orthopaedics,” n.d.)

The more conventional technique is commonly referred to as the bone referencing technique (Figure 3.1). In this instance bony landmarks are used to determine both the size of the implant required as well as where the cuts should be made (Bellemans, Vandenneucker, & Vanlauwe, 2005). The first cut will be made on the femur using a specialized alignment jig. These femoral joint surfaces are cut transversely to form the base for the femoral component (Liddle et al., 2013). The next cut will be a horizontal cut along the tibial surface, again using an alignment jig to ensure proper knee joint alignment. In this technique soft tissue balancing occurs after all of the cuts are made (Bellemans et al., 2005). After the metal femoral component is placed, the polyethylene tibial insert replaces the tibial surface. An optional addition may be a resurfacing of the patellofemoral joint if patellofemoral osteoarthritis exists (Liddle et al., 2013). The other method is known as the ligament referencing technique and simply involves a different

order of steps (Figure 3.2). In this technique ligament balancing is used to determine the bone cuts, with the tibial cuts being made first. This technique is used to ensure that adequate soft tissue equilibrium is reached prior to any extensive bone loss from cutting the femoral surface (Bellemans et al., 2005). Both techniques are commonly used and considered effective, with the significant controversy lying in the rotational positioning of the femoral component (Bellemans et al., 2005). To complete the procedure the surgeon will flex the knee to ensure proper alignment and rotation and will then close the patient.

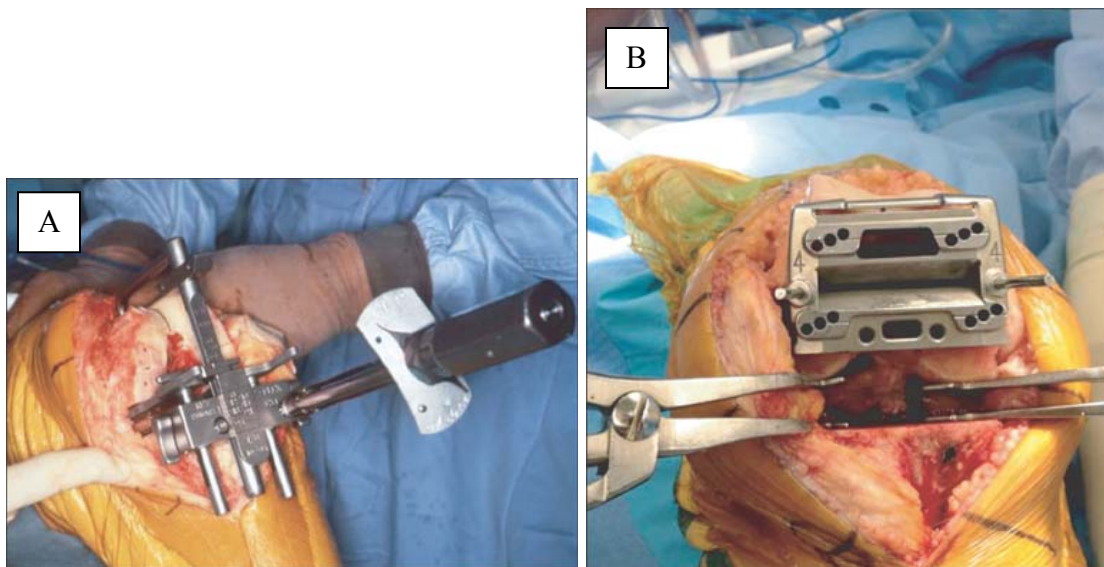


**Figure 3.2:** Ligament referencing technique: (a) Intraoperative photograph of a flexion gap tensioning jig placed into the flexion gap, tensioning the gap, and positioned parallel to the transepicondylar axis before the anterior and posterior femoral resections are performed (b) Intraoperative photograph demonstrating placement of the anteroposterior femoral cutting block parallel to the resected proximal tibia with each collateral ligament tensioned to create a rectangular flexion gap (Daines & Dennis, 2014).

These steps describe the generalized steps of a total knee replacement and do not take every aspect of the procedure into consideration. Depending on the severity of the damage ligaments may be resected during the procedure. If this occurs a different TKR design may have to be used to achieve the respective knee stability (Liddle et al., 2013). TKR designs will be addressed in the next section of this work with ligament stability being a significant factor.

### *3.2 Different TKR Designs and Functions*

There exists a substantial number of differing total knee replacement designs each of which has an intended use for a specific patient injury or based on a design or novelty concept. However, all TKR's typically have both a femoral component that is typically metal and a tibial component that is generally a polyethylene insert. This section will summarize the most common design types and will give a basic understanding to what function each type provides.

#### *3.2.1 Fixed Bearing Implants vs. Mobile Bearing Implants*

The most common and frequently used total knee replacement is the fixed bearing implant. This implant is considered fixed because of the way the polyethylene insert is attached. The tibial insert is rigidly attached, or fixed, to a metal plate that is attached to the tibia (Huang, Liao, & Cheng, 2007). The femoral component is then able to rotate over the polyethylene surface. The basic principle of mobile bearing implants is that the tibial insert is allowed some degree of movement at the interface between the baseplate

and the tibial insert. This movement is typically an internal and external rotation, however, there are also some designs that allow for an anterior and posterior displacement (Huang et al., 2007).

Fixed bearing implants are most commonly used because they are ideal for satisfying basic functionality and range of motion over a long period of time with minimal wear. They have been the gold standard in knee replacements for many years, and so many surgeons are hesitant to work with a different design. They are designed to have a high conformity along the bearing surface which provides low contact stresses on the polyethylene insert (Huang et al., 2007). This should increase the life span of the insert as degradation would be decreased. Unfortunately, the fixed bearing implants result in a high torque at the bone to implant interface (Huang et al., 2007). This high torque may put the implant at risk for loosening, a possible catastrophic mechanism of failure. Not only that, but it has been noted that under moderate rotational malalignment of the tibial component increased contact stresses on the polyethylene insert occur (Matsuda, White, Williams, McCarthy, & Whiteside, 1998).

Based on this the mobile bearing implant was implemented hoping to reduce polyethylene wear, reduce torque along the implant bone interface, and also improve kinematics by increasing the range of motion (W. C. H. Jacobs et al., 2012). The ability for the mobile bearing implant to rotate during knee flexion may also counterbalance possible tibial component malalignments (Huang et al., 2007). The increased range of motion in both axial rotation and displacement requires greater support from the soft tissue surrounding the articulation (W. Jacobs, Anderson, Limbeek, & Wymenga, 2004).

If these soft tissues cannot withstand the applied forces there is an increased risk of implant dislocation. Additionally, an increased risk for wear may exist in mobile bearing implants at the tibial cup and tibial base interface (W. C. H. Jacobs et al., 2012).

### *3.2.2 PCL Retaining vs. PCL Substituting*

The role that the posterior cruciate ligament (PCL) holds in the knee is significant to the overall stabilization. Therefore, when a total knee replacement is performed it is a common conception that the PCL is a requirement for a successful implant. Because of this the most popular TKR's have been PCL retaining and PCL substituting implants. Although these implants were originally designed as fixed implants, both fixed and mobile bearing designs are now available.

PCL retaining implants preserve the natural PCL to function along with the TKR. The implants require precise soft-tissue balancing and are dependent on the health of the PCL at the time of surgery (Pritchett, 2011). Waslewski et al reported incapacitating instability in a PCL retaining implant in a study that examined deficient PCL's and total knee replacements (Waslewski, Marson, & Benjamin, 1998). These risks of instability have led many surgeons to prefer PCL substituting designs.

PCL substituting implants use a cam-post system to substitute for the PCL. This substitution induces posterior femoral translation (Moonot et al., 2009), which may enhance the efficiency of the extensor mechanism (Parsley, Conditt, Bertolusso, & Noble, 2006), something that will be discussed in further detail in the next section of this chapter. The tibial post that notches with the femur has been reported to have a high

incidence of damage at the contact surfaces (Moonot et al., 2009), and when impingement between the tibial post and femur results, there has been a noted correlation in failure and increased wear (Haas, 2006).

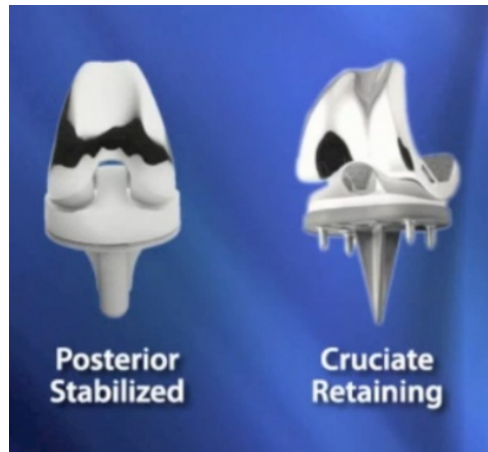


**Figure 3.3** PCL retaining implant with tibial post (right) and PCL substituting implant (left) (MicroPort Orthopedics)

### *3.2.3 Medial Pivot Implants*

Studies have shown that there exists minimal movement of the medial femoral condyle with posterior translation of the lateral femoral condyle in the natural knee during flexion (Asano et al., 2001; Dennis, Mahfouz, Komistek, & Hoff, 2005). This motion induces a medial pivot motion or medial centered rotation in the knee (Moonot et al., 2009). The medial pivot total knee replacement is structured around this concept. The femoral component of the medial pivot TKR has a single radius of curvature, while the tibial insert exhibits a spherical medial compartment and a cylindrical lateral condyle

(Moonot et al., 2009). The spherical medial condyle allows for rotation during flexion while the lateral condyle provides a means of stabilization as well as posterior rolling and sliding. The shape of the medial condyle also provides anterior/posterior stability as the single radius curvature ensures a high conformity (Moonot et al., 2009). In addition to increasing the stability of the knee it is believed that this design may provide more natural kinematics and reduce stress on the polyethylene inserts (Pritchett, 2011).

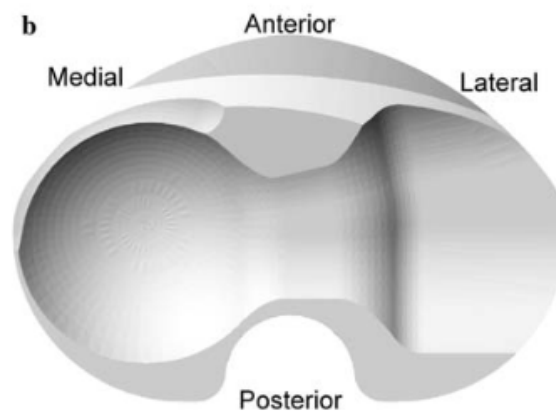


**Figure 3.4** Tibial insert of a medial pivot total knee replacement showing the spherical medial condyle and cylindrical lateral condyle (Moonot et al., 2009)

#### *3.2.4 High Flexion Total Knee Replacement's*

Standard TKR's are typically considered to allow approximately 120 degrees of flexion of the leg (Banks et al., 2003). Although a substantive movement suitable for walking, high flexion activities such as squatting, kneeling and sitting cross-legged are not possible (Mulholland & Wyss, 2001). The development of high-flexion knee implants to provide a larger range of motion was an exciting and necessary step in the evolution of total knee replacements.



High flexion implants are designed very similarly to standard TKR's, allowing for both PCL retaining and PCL substituting implants. In a comparison between high flexion PCL retaining and high flexion PCL substituting designs, both reported extremely high Knee Scores, with the PCL substituting design demonstrating greater range of motion, patient satisfaction, and decreased posterior knee pain at passive flexion (Yagishita et al., 2012). The significant design change in these implants versus standard TKR's is a change in the posterior sagittal femoral geometry. This geometry is designed to prevent the occurrence of polyethylene edge loading during deep flexion (Zelle, Janssen, Van Eijden, De Waal Malefijt, & Verdonschot, 2011). Although this intended geometry should provide the necessary conditions to achieve increased flexion angles, studies have shown that flexion angles may be significantly impacted by more than just design; including the patient, surgical technique, knee kinematics, perioperative complications, and postoperative physical therapy (Dennis, Komistek, Scuderi, & Zingde, 2007).

### *3.2.5 Constraint in Total Knee Replacement's*

Many different total knee replacement designs exist, yet each design follows a certain form or principle. One principle that must be satisfied is that of constraint. Constraint in relation to TKR's is a measure of the resistance to a particular degree of freedom (Walker & Sathasivam, 2000). An entirely unconstrained TKR would be problematic, however, unconstrained implants are generally considered those that can move freely assuming no ligaments are restricting motion. Based on this unconstrained implants are largely encapsulated by PCL retaining implants. A partially constrained

implant would include many PCL substituting implants, as these implants are partially constrained by the cam-post system. Fully constrained TKR's are typically considered to have very conforming bearing surfaces, or be hinged implants, as their motion is completely self-constrained.

Hinged implants are indicated for use in the presence of severe bone loss with global instability or if highly comminuted distal femoral fractures exist (Pour, Parvizi, Slenker, Purtill, & Sharkey, 2007). Although early designs of the implant allowed only for rotation in flexion or extension causing significant torque at the bone-implant interface, newer designs allow for rotation as well as incorporate fluted stems with variable offsets for improved alignment (Barrack, 2001). Modern hinged knee systems offer an excellent substitute for patients that have repeated failed TKR's or are at a high risk of a typical primary TKR failing. For patients that do not have sufficient ligaments to properly constrain an implant, the hinged mechanism provides the appropriate level of constraint necessary (Hernández-Vaquero & Sandoval-García, 2010).

When discussing constraint in TKR's ligaments are not the entire consideration. Tibial insert conformity is also a frequently debated issue. Conformity as related to knee implants describes the degree to which the angle of the femoral component aligns with the angle of the tibial insert. It is noted that increased conformity between the TKR components has the potential to decrease wear (Fregly, Marquez-Barrientos, Banks, & DesJardins, 2010). A tibial insert that is entirely flat would be considered to be unconstrained, assuming no friction (Walker & Sathasivam, 2000). However, for dished

implants that have non-linear curves, constraint would be increased (Walker & Sathasivam, 2000).

The goal of a total knee replacement is to reproduce the constraint demonstrated in the natural knee. A similar constraint is desired so as to reduce the risk of altering kinematics. Each of the various TKR designs hopes to replicate that constraint within their mechanism of action. Unfortunately, even if the natural geometry were duplicated, achieving the same constraint level may be impossible because of differing coefficients of friction (Walker & Sathasivam, 2000).

### *3.2.6 Unicompartamental Knee Replacement's*

The popularity of TKR's is due to their long term success in patients. However, as modern medicine advances, so does the surge towards minimally invasive surgical techniques. Unicompartamental knee replacements (UKA's) (Figure 3.3) continue to gain popularity because of the mini-incision technique that can be utilized for implantation (Pandit, Jenkins, Barker, Dodd, & Murray, 2006). A UKA is a procedure in which only a single compartment of the knee is replaced, leaving the other compartment, the ligaments, and the patellofemoral anatomy intact (Heyse et al., 2014). Most commonly it is the medial compartment that is replaced because it is more likely to be affected by osteoarthritis. This minimally invasive approach is said to give lower perioperative morbidity and earlier recovery (Borus & Thornhill, 2008). Other advantages may include preservation of bone stock, improved range of motion, reduced blood loss, and decreased costs (Bert, 2005).

Another reason for the more recent rise in the use of UKA's is the potential functional benefits that are provided. As was previously discussed in the section on medial pivot implants, flexion of the natural knee results in an internal rotation of the tibia around a medial pivot with no anteroposterior rollback in the medial condyle and posterior rollback in the lateral condyle (Heyse et al., 2014). These kinematics are incredibly complex and very difficult to replicate. Because a significant portion of the natural knee is preserved, the kinematics of a UKA should be very close to that of a natural knee. Heyse et al found that femoral rollback patterns after UKA were very close to that of the natural knee, with slight kinematic changes attributed to the loss of the conforming medial meniscus and a mismatch in material and geometry. These results may indicate that UKA's are a better initial option for patients. Younger patients may especially be inclined to begin with a UKA, as they are much more likely to need a revision procedure, and conversion of a UKA to a TKR is typically considered a lot more simple than a revision TKR (Heyse, Khefacha, Peersman, & Cartier, 2012).

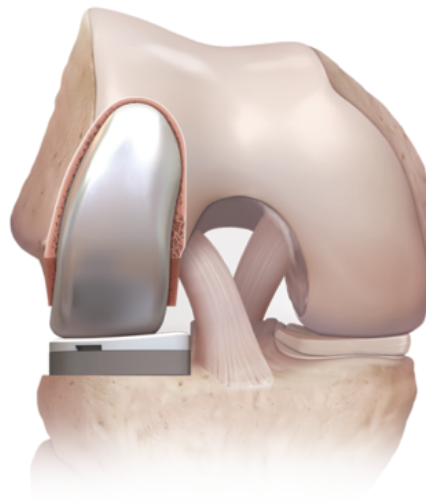


**Figure 3.5** Unicompartmental Knee Implant (Arthrex)

### *3.3 Femoral Design Features*

The functionality of total knee replacements is dictated by both the femoral and tibial components. As discussed previously, variations in the tibial insert are largely encapsulated by fixed versus mobile implants and the conformation that the tibial insert provides. This section will focus on the features that influence the femoral component design.

#### *3.3.1 Single-Axis vs. Multi-Axis Designs*

Femoral component designs are based primarily on anatomical observations of native femoral geometry and the flexion/extension axis of natural knees (Gunston, 1971). Multi-axis femurs are based on the geometrical configurations of the natural knee. Multiple radii of curvature are incorporated into the design in order to mimic the spiral path that it is believed that the instantaneous center of rotation follows (Shenoy et al., 2013; Wang, Simpson, Chamnongkich, Kinsey, & Mahoney, 2005). Multi-axis designs have been attributed to mid-flexion instability and altered patellofemoral kinematics (Shenoy et al., 2013). However, multi-axis designs may increase femoral flexion range of motion because of the decreasing radius of curvature at higher degrees of flexion (Chandran et al., 2009). Single-axis designs, on the other hand, are designed with the idea that there exists only one location for the axis of rotation. This concept is based on the premise that two simultaneous rotations are occurring about fixed axes (Churchill, Incavo, Johnson, & Beynnon, 1998). The hypothesis believes that the axis of flexion and extension is fixed to the femur while tibial internal and external rotations occur about an

axis fixed in the tibia (Churchill et al., 1998; Hollister, Jatana, Singh, Sullivan, & Lupichuk, 1993). Surprisingly, single-axis femoral designs typically result in kinematics that more closely match that of the normal knee.

### *3.3.2 The Extensor Mechanism*

The extensor mechanism was briefly referred to in the section on knee joint anatomy because its function is directly related to the structure of the knee. The knee extensor mechanism is important to patients as it plays a significant role in the stand to sit and sit to stand motion, something that patients do on a regular basis (Wang et al., 2005). The patella functions as a spacer between the tendon and the point of extension and flexion, extending the moment arm of the quadriceps tendon (Browne, Hermida, Bergula, Colwell, & D'Lima, 2005). It acts as a lever adjusting the magnitude and direction of the quadriceps tendon, ultimately affecting the mechanical advantage during knee extension (Kaufer, 1971; Yamaguchi & Zajac, 1989). The ability of this extensor mechanism to affect the quadriceps tendon is termed the mechanical efficiency. Mechanical efficiency is dependent on the tibiofemoral anteroposterior position, the patellar ligament angle, and the quadriceps to patella ligament force ratio (Draganich, Andriacchi, & Andersson, 1987).

Therefore, implant designs can greatly influence this mechanism as they dictate the point of rotation, or the exact size of the moment arm created (Krevolin, Pandy, & Pearce, 2004). An implant with the center of rotation located more posteriorly may result in a larger moment arm. Browne et al determined that a design with a longer extensor

moment arm reduced the required quadriceps forces to extend the knee and also reduced patellofemoral compressive forces.

In a study comparing the effects on the knee extensor mechanism between single-axis and multi-axis knee implants, patients that had single-axis designs had significantly less anterior knee pain when rising from a seated position starting at 6 weeks and maintained this through 2 years (Mahoney, McClung, dela Rosa, & Schmalzried, 2002). Because anterior knee pain has been associated with decreased extensor mechanism efficiency (Browne et al., 2005), this may indicate that a single-axis femoral design may reduce the quadriceps force needed for a sit to stand movement. Conceptually this would appear to be true, as a single-axis implant would have a larger moment arm at 120 degrees of flexion than a multi-axis implant. Also, the single-axis design typically has a more posterior flexion axis during the entire functional range increasing the moment arm (Wang et al., 2005). Based on multiple studies it would appear that the single-axis knee implant design has the most positive effects increasing the moment arm based on geometry alone.

### *3.3.3 Posterior Femoral Rollback*

The normal knee undergoes femoral rollback with the screw home mechanism (Chandran et al., 2009). As discussed previously femoral rollback occurs to a lesser degree in the medial condyle, with increased femoral rollback in the lateral condyle resulting in a medial pivot. This rollback occurs in the normal knee because of the geometry of the tibial and femoral components, as well as the function of the posterior

cruciate ligament (Chandran et al., 2009). Femoral rollback results in both the medial pivot of the knee as well as an enhancement of the extensor mechanism. Femoral rollback is required for increased flexion (Chandran et al., 2009), and thus should be exhibited in knee replacements.

Reduction of complications with the patellar component in total knee replacements remains a significant concern for many surgeons. Damage to the patellar component due to high compressive forces often results in pain to the patient and possibly even implant failure (Churchill, Incavo, Johnson, & Beynnon, 2001). Reducing patellar compressive forces via enhancement of the extensor mechanism remains the best solution (Churchill et al., 1998). Because increased femoral rollback results in a higher moment arm, increasing the femoral rollback, especially during degrees of high flexion, may be important.

Multi-axis femoral components appear to consistently produce early femoral rollback, while single-axis implants are significantly more dependent on other factors (Nozaki, Banks, Suguro, & Hodge, 2002). A major factor that may affect femoral rollback is the type of implant used between PCL retaining or PCL substituting. PCL substituting designs have been found to generate fairly consistent and significant femoral rollback when compared to the PCL retaining implants (Fantozzi, Catani, Ensini, Leardini, & Giannini, 2006; Shimizu, Tomita, Yamazaki, Yoshikawa, & Sugamoto, 2014). In addition, variations in the cam-post mechanism in PCL substituting implants may also affect the degree to which femoral rollback occurs (Chandran et al., 2009).



### *3.3.4 Ligament Interactions*

The ligaments of the knee play an integral role in the overall kinematics. The femoral attachments of the cruciate ligaments, the anterior cruciate ligament, the posterior cruciate ligament, and the tibial attachments of the cruciate ligaments results in a four-bar linkage (Shenoy et al., 2013). This four-bar linkage dictates our instantaneous center of rotation. As the knee is flexed from full extension, the instantaneous center of rotation will translate posteriorly (Shenoy et al., 2013). When the cruciate ligaments are damaged they may not function properly, and ultimately regular kinematics may be affected. In instances of damaged cruciate ligaments during knee replacements, the ligaments are frequently excised and a PCL-substituting design is incorporated. These PCL-substituting designs, as described previously, use a cam-post mechanism to induce proper femoral rollback. Significant variation in posterior rollback may occur between different implant designs (Chandran et al., 2009).

Although the PCL substituting designs are able to achieve femoral rollback, they do not account for other ligaments that may have been resected. It has been noted that both the knee geometry and the ligament geometry must be maintained to regain normal knee motion (Wilson, Feikes, & O'Connor, 1998). During a total knee replacement procedure, the anterior cruciate ligament is typically excised. Although most implants are designed to be used without the ACL, removal of this ligament will have implications on the kinematics of the knee.

The collateral ligaments also play a significant role in the function of the knee after a TKR. The medial and lateral collateral ligaments act to stabilize the knee during

flexion and extension (Ghosh, Merican, Iranpour, Deehan, & Amis, 2012). Both ligaments are often resected, however, it is becoming more common to retain these ligaments (Fuchs et al., 2004). Ghosh et al found that the collateral ligaments (both MCL and LCL) slackened more than normal following a total knee replacement, and these length changes were increased by femoral component flexion and extension. This slackening could lead to varus and valgus instability, altering the functionality of the implant.

### *3.4 Anatomical and Surgical Alignment*

The alignment of a total knee replacement is critical to the success of the procedure. Malalignment of the implant can result in severe wear of the polyethylene component, component loosening, and ultimately revision surgery (Werner, Ayers, Maletsky, & Rullkoetter, 2005). In this section surgical alignment techniques, possible errors, and methods of advancing precision are discussed.

#### *3.4.1 Surgical Alignment*

TKR's are an invasive procedure that require an incision of approximately 8 – 10 inches. Once the incision is made and the patella is rotated outside of the joint cavity the process for alignment begins immediately. The implant is considered ideally aligned when it is located perfectly within the coronal, sagittal and axial planes, the femoral component is matched to the tibial component in rotation, the joint line is at the desirable level, while the soft tissues are balanced in both flexion and extension to produce the

optimal stability without limiting range of motion, and the patella is tracking in the correct plane (Sikorski, 2008). These qualifiers all interact, and so changes in any of them could alter the kinematics of the knee.

Alignment of a total knee replacement is referenced to either theoretical axes or anatomical landmarks (Sikorski, 2008). The mechanical axes of the leg is a straight line drawn from the center of the femoral head to the center of the ankle (Figure 3.4).

Anatomical axes also exist running through the center of both the femur and the tibia (Shenoy et al., 2013). For alignment of the femoral component the distal one-third of the medullary canal is used as a reference axis. In addition, the anterior cortex of the femur, the intercondylar groove of the femur, and the plane of the posterior aspects of the femoral condyles can be used (Sikorski, 2008). Alignment of the tibial component utilizes the proximal two-thirds of the tibial medullary canal, the anterior cortex of the tibial flare, and lines connecting the posterior cruciate ligament to the tibial tuberosity (Sikorski, 2008). One of the most useful tools for knee alignment is the transepicondylar axis of the femur, which provides clearly defined anatomical landmarks while also maintaining the role as the mechanical axis around which knee flexion occurs (Sikorski, 2008). An additional method for surgeons to align TKR's is soft-tissue tension. This methodology is completed by aligning the tibial component along the mechanical axis, and then placing the femoral component based on the position that the femur assumes when the ligaments are in tension (Sikorski, 2008). Regardless of what methodology is used it is imperative that correct ligament balancing is achieved as ligaments that do not

exude enough tension may result in joint subluxation or dislocation but those that exhibit too much tension may induce increased wear or limit range of motion (Sikorski, 2008).

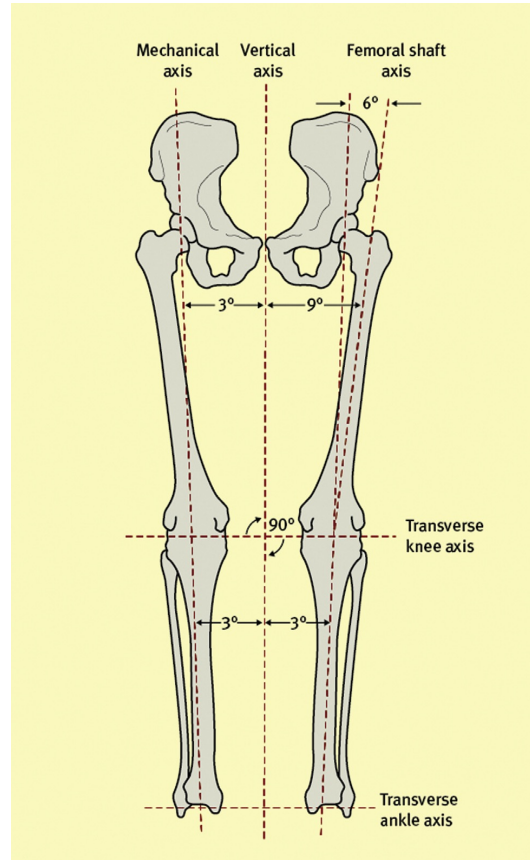


**Figure 3.6** Anatomical and mechanical axes of the leg (Shenoy et al., 2013)

Conventional methods of TKR implantation rely on utilizing these anatomical landmarks and mechanical axes to place the implant. The femoral component placement is reliant on the placement of the drilled entry point for the intramedullary rod (Hungerford, 1995). This initial entry point may vary based on surgeon, patient, and implant being used. Once the intramedullary rod is placed the femoral cutting block is placed on top (Hungerford, 1995). The anterior and posterior cuts that are made at this

point dictate femoral rotation. Most conventional knee systems utilize a sizing jig that has pins that are aligned perpendicular to Whiteside's line and parallel to the transepicondylar axis (Hungerford, 1995). The alignment jig is placed based on the anterior and posterior aspects of the femoral condyle. Once the cutting block is properly aligned the surgeon can make the cuts to the femur that will ultimately play a significant role in the alignment and femoral rotation. The dictated femoral rotation plays a significant role in patellofemoral kinematics as well (Shenoy et al., 2013). Alignment of the tibial component may utilize either an intramedullary alignment jig or an extramedullary alignment jig (Hungerford, 1995). The intramedullary technique is typically preferred unless extreme bowing of the tibia exists. The extramedullary alignment jig is used in this case, however, may be more technically demanding with large or obese patients (Hungerford, 1995).

#### *3.4.2 Known Errors in Surgical Alignment*

Conventional methods of TKR alignment often has significant variability depending on surgeon, surgical technique, patient, and implant used. Restoration of the correct mechanical axes of the leg is crucial to the success of the implant and health of the patient (Bellemans et al., 2005). Unfortunately, traditional techniques are believed to be greatly limited in their accuracy in determining the key landmarks associated with optimal alignment (Hoffart, Langenstein, & Vasak, 2012). Most of these systems still rely on surgeon judgement to verify the alignment and stability of the joint after the procedure (Hoffart et al., 2012).

When the intramedullary rod is placed for the femoral component errors can easily be made. If the entry hole is placed to laterally, a more valgus cut can be made, while a more varus cut may be made for a medially placed entry (Hungerford, 1995). These miscalculations may result in errors in the soft tissue balancing that may affect knee kinematics (Lotke & Ecker, 1977). Another study indicated that the surgeon should align the total knee implant in a neutral or slightly valgus position in order to increase the likelihood of implant survival (M A Ritter, Faris, Keating, & Meding, 1994). A posterior entry point may result in flexion of the distal femoral cut and an anterior entry point may induce an extended distal cut (Hungerford, 1995). The location and size of the distal cut influences the size of the component, which may put the patient at risk for periprosthetic fracture (Merrill A Ritter et al., 2005). Femoral rotation is also important for not only proper knee rotation but to ensure proper patellar tracking. An internally rotating femoral component may negatively influence patellar tracking while also creating a lateral laxity with tightness on the medial side during flexion (Hungerford, 1995). An excessive external rotation of the femoral component may result in the opposite, with ligament laxity medially and tightness laterally (Hungerford, 1995). Both instances would require significant ligament balancing to attempt to fix the problem, and will most likely cause a limitation to the functional range of motion (Hungerford, 1995).

Alignment on the tibial component presents its own challenges. When a patient is large or obese identification of anatomical landmarks may be very difficult. If a varus cut is made the patient may experience tightness on the lateral aspect of their knee during extension and flexion (Hungerford, 1995). Errors to the posterior slope may result in even

more significantly damaging outcomes. Too excessive of a posterior slope may result in instability of the knee during rotation, while if the cut is not sloped enough the knee may be too tight during rotation resulting in decreased range of motion (Hungerford, 1995). In addition, tibial rotation must be optimized to ensure the correct force distribution through the patella tendon (Nicoll & Rowley, 2010). Extreme internal rotation of the tibia could cause dislocation of the patella while too much external rotation could induce impingement leading to pain and reduced functionality (Nicoll & Rowley, 2010).

#### *3.4.3 Methods to Advance Surgical Precision*

It has been determined that TKR's with a postoperative mechanical axis of less than 3 degrees varus or valgus have better long term survival rates (Bargren, Blaha, & Freeman, 1983; Lotke & Ecker, 1977; M A Ritter et al., 1994). Because of significant variations in patients including bone deformity, bone wear, and patient obesity, conventional methods of TKR alignment result in varied outcomes (Pang et al., 2009). The integration of computer-assisted navigation techniques has been found to produce more consistent alignment correction and also reduce outliers during implant placement (Pang et al., 2009). One study noted a better functional outcome at five years using computer-assisted technology, with significant differences in the rotational alignment between the computer-assisted and conventional techniques (Hoffart et al., 2012). Other studies noted no significant difference in the outcome between conventional and computer-navigated systems (Kim, Kim, & Yoon, 2007).

The exact methods of the computer-navigated surgery differ slightly depending on the type of system used, however each system is similar on a whole. Based on this premise we will describe the procedure dictated by Hoffart et al to gain an understanding of the concept. A midline skin incision is made with a medial parapatellar arthrotomy being used. An imageless navigation system is then used to assess the bony landmarks. Based on these landmarks the cutting guides can be placed where the guiding system tells them to be placed. The femoral bone cuts are then also made using computer guidance. The system will then go as far as to suggest the optimal implant size, indicating the optimal alignment of the implant in relation to landmarks. A standard extramedullary guide was then used to make the tibial cuts and ligament balancing was used to optimize flexion and extension. Other systems also have a navigation system to check the alignment of the tibial cutting blocks before any cuts are made (Chan & Teo, 2012).

Another new technology that is being used in total knee replacement procedures use magnetic resonance imaging (MRI) or CT scans to custom fit a knee replacement to the patient (Chan & Teo, 2012; Spencer, Mont, McGrath, Boyd, & Mitrick, 2009). Using a sagittal MRI scan of the arthritic knee three-dimensional models of the arthritic knees could be developed (Spencer et al., 2009). Bone and cartilage defects could then be filled in while femoral and tibial components could be shape-matched and aligned to the model (Spencer et al., 2009). Based on this custom cutting guides could be machined prior to the surgery making it easier for the surgeon to find the optimal placement. Unfortunately, it has been reported that if proper alignment is not achieved there exists similar problems to conventional methods (Chan & Teo, 2012). However, if combined with computer-



assisted navigation it could be used to ensure ideal alignment, and any deficiencies or errors can be corrected (Chan & Teo, 2012).

Many studies have evaluated the efficacy of computer assisted techniques and although some found no difference in accuracy the overall consensus was an increase in accuracy. Most of these studies emphasize the fact that current mechanical instrumentation does not result in consistently accurately aligned TKR's (less than 3 degrees), but computer-assisted techniques have been found to allow measurement of the steps of the TKR with great accuracy and precision (less than 1 degree) (Stulberg, 2003). Patient specific guides have been shown to also improve accuracy and may even limit the number of steps required by the surgeon to complete the surgery (Krishnan, Dawood, Richards, Henckel, & Hart, 2012). However, when evaluated for cost-effectiveness it is suggested that cost-effectiveness would only be reached if it resulted in a significant decrease in the rate of revision procedures (Slover, Rubash, Malchau, & Bosco, 2012).

### *3.5 TKR Testing*

The approval process for total knee replacements is very extensive. As with any medical device, especially implants, TKR's must be approved by the FDA before they can ever be implanted in a patient. This section will detail standards, testing techniques, and design variables that are known to affect the success of implants.

### *3.5.1 TKR Standards*

In order for an implant to be approved by the FDA for use inside of a patient it must meet basic standards of design as well as testing. These standards are dictated by multiple organizations, the most prominent of which include the ISO (International Standards Organization) and ASTM (American Society for Testing and Materials). For purposes of this thesis I will specifically discuss ASTM standards in regards to TKR's, although as dictated by FDA requirements for class II devices both standards meet the same FDA qualifications (Health, 2003).

ASTM standard F2083-12, Standard Specification for Knee Replacement Prosthesis provides basic descriptions of materials and prosthesis geometry for total and unicondylar knee replacement designs ("ASTM F2083-12, Standard Specification for Knee Replacement Prosthesis," 2012). The first standard outlined in this specification is that of the material used to create the device. The standard requires that the material meets the necessary requirements for mechanical strength, corrosion resistance, and biocompatibility. Lists of materials are provided that are acceptable and if the material is not one of those listed it must be equal to or better than one on the list.

The next specification outlines performance standards. The component is expected to function as intended by the manufacturer and must be able to withstand both static and dynamic loads for the intended use and environment without compromising this function. It goes on to further define specifications for each component and the associated test method required for that component. These include specifications for the tibial base plate (including additional tests for mobile bearing implants), contact area and

pressure distributions at various flexion angles, the flexion-extension range of motion of at least 0 to 110 degrees, constraint data for internal-external rotation, anterior-posterior displacement, and medial-lateral displacement, evaluation of the integrity of all modular components, understanding of the wear performance for the articulating surfaces, and understanding of the characteristics of the debris generated.

Dimensions of TKR components must be labeled based on a certain figure and with specific terms previously outlined. All appropriate dimensions are required to be designated including any mobility features or mechanical stops. The tolerance and methods of measurement must also conform to industry practice.

Finishing of the components must also be followed. Metal bearing components cannot have a roughness higher than 0.10  $\mu\text{m}$ . Polymeric bearing surfaces cannot have a surface roughness greater than 2  $\mu\text{m}$ . Packaging standards are also noted, requiring an adequate description of overall size and shape on the packaging material.

When actually testing the components both the ISO and ASTM have listed standards. Again, with focus on the ASTM standard F1715-00 Standard Guide for Wear Assessment of Prosthetic Knee Designs in Simulator Devices, a guide covering laboratory methods for evaluating wear properties of materials or devices is explained (“ASTM F1715 - 00 Standard Guide for Wear Assessment of Prosthetic Knee Designs in Simulator Devices,” 2006).

The methods dictated in this guide are intended for use in a range of knee simulators with varying applied forces and kinematics. This test is preferred over basic wear screening tests because it can use the actual implant geometry and material to run

the tests. This guide offers a combination of implant designs and materials wear rates, however, the sheer number of combinations makes it impossible to specify all conditions. The intent of the guide is to provide reference materials for a comparative evaluation of wear rates between historically used materials and the materials under question. These materials would have all been tested under the same conditions to ensure accuracy.

### *3.5.2 TKR Simulation*

Testing TKR's and evaluating their performance is an arduous task. As mentioned previously there exists many different methods of testing implants, and so they need to be standardized as much as possible to evaluate functional performance.

One of the most frequently used methods of TKR wear testing is in a knee simulator. Knee simulators offer the benefit of reproducing in-vivo conditions, simulating the kinematics and forces experienced by the actual implant and allowing for the assessment of long-term reliability of the bearing surfaces (J L Lanovaz & Ellis, 2008). Although kinematics are not completely replicated, studies have shown that knee wear in the simulator is similar to wear observed in vivo (Walker et al., 2000). One consideration is that differing geometries of implants have been shown to result in different kinematics in knee simulators even with the same input forces (Dean, Haider, Walker, DesJardins, & Blunn, 2006). Based on this it may be beneficial to customize the input forces based on implant design (Dean et al., 2006). Unfortunately laboratory testing of knee implants can be an expensive and time consuming process that may not be beneficial to conducting an iterative experiment to alter geometry (J L Lanovaz & Ellis, 2008).

Because the kinematics in the knee are still a topic of debate, many systems have attempted to classify knee kinematics using cadaveric simulators. It is based on studies like these that a general consensus of minimal medial condyle translation has come about (Blaha, Mancinelli, Simons, Kish, & Thyagarajan, 2003). However it is of interest to note that when a natural knee in a cadaveric study is placed under wear testing conditions as specified by ISO displacement standards increased internal tibial rotation as well as anterior tibial translation rather than posterior tibial translation were noted (Sutton, Werner, Haider, Hamblin, & Clabeaux, 2010). These significant variations may provide a reason as to why many wear test results are not consistent even when following the same ISO protocols (Sutton et al., 2010). So although we have a better understanding of in vivo kinematics, there is still significant difficulty in applying those kinematics into a simulated environment.

A method of testing knee replacements that is becoming more frequently used with the advance of technology is computational modeling. Finite element method (FEM) modeling now allows for dynamic simulations that may allow researchers to find values that cannot be found experimentally (Godest, Beaugonin, Haug, Taylor, & Gregson, 2002; Joel L Lanovaz & Ellis, 2009). Not only that but these methods of experimentation allow for an iterative approach that could be used to alter implant designs. A problem that may exist with computational models is the accurate prediction of wear. Most computational models use contact pressure independent wear factors, focusing mainly on sliding distance and load as dictated by Archard's wear law (Abdelgaied et al., 2011). However, other mechanisms of wear exist most notably contact pressure and cross-shear

(Abdelgaied et al., 2011). Although significant difficulty exists in recreating all six degrees of freedom within a knee implant and measuring the appropriate wear, computational modeling of implants is not limited by mechanical forces and thus has a greater chance of achieving an ideal simulation.

### *3.5.3 Instron Stanmore Knee Simulator*

One of the direct aims of this study was to create a method of determining the ideal femoral axis for TKR wear testing. Our lab utilizes the Instron Stanmore Knee Simulator to conduct long-term knee replacement wear tests. This section will overview the functional components of this simulator.

The four station Instron Stanmore knee wear simulator was originally designed by the University College London Department of Biomedical Engineering at Stanmore Royal National Orthopaedic Hospital. The simulator applies controlled forces in the axial, anterior/posterior, and interior/exterior axes while also applying a flexion/extension motion (Instron, n.d.). The simulator utilizes 6 degrees of freedom, 4 controlled and 2 unconstrained, to attempt to recreate the kinematics of the natural knee (J. D. DesJardins, Walker, Haider, & Perry, 2000). It conforms to ISO standard ISO 14243 “Wear of Total Knee Joint Prosthesis, Loading and Displacement Parameters for Wear Testing Machines and Corresponding Environmental Conditions for Test”, and has been incredibly useful for measuring gravimetric wear in knee implants over the course of a walking cycle. However, because the flexion/extension axis does not move but remains static, choosing an axis for multi-axis femoral components must be optimized so that the kinematics are

not compromised (J. DesJardins & Rusly, 2011). If significant proximal/distal camming occurs because of poor axis selection unintended proximal/distal piston loading, unintended anterior/posterior displacement due to altered posterior rollback, and internal/external rotation may occur in the system (J. DesJardins & Rusly, 2011). Therefore, it may be critical to identify optimal flexion axes, as changes in kinematics have been associated with changes in wear patterns (J. D. DesJardins, Banks, Benson, Pace, & LaBerge, 2007; Harman et al., 2009; McEwen et al., 2005).

#### *3.5.4 Design Variables that May Affect Longevity*

The success of total knee replacements has been impressive enough that it is the best option for patients suffering with osteoarthritis. However, long-term failure is still very common and improvements in the various variables that impact this failure is being constantly addressed. Debris induced osteolysis is believed to be a significant potential long-term failure mechanism, and so is frequently considered in regards to implant design, kinematics, material, and lubrication (McEwen et al., 2005).

With regards to kinematics of a TKR, it is generally believed that to reproduce physiological wear patterns the natural kinematics of the knee are required (Walker et al., 1997). In addition, TKR kinematics are believed to be a function of the femoral component and tibial insert shapes (Dennis, Komistek, Stiehl, Walker, & Dennis, 1998; Sathasivam & Walker, 1998; Soudry, Walker, Reilly, Kurosawa, & Sledge, 1986). Based on these concepts the design of the implant and the outputted kinematics that determine wear patterns are intrinsically linked. This gives rise to the idea of TKR design

optimization based on various factors, something that has been shown to improve upon commercially available implants (Willing & Kim, 2011).

As discussed previously current knee replacement implants can be divided into two major groups, fixed and mobile bearing. In a study that directly compared these two implants it was found that mobile bearing implants exhibited reduced wear rates when compared to fixed bearing implants most likely due to a redistribution of knee motion to two articulating surfaces with more linear motions at each surface (McEwen et al., 2005). It is of note to point out that it has been stated that the geometry of the implant may influence kinematics more than any other factor (Pandit et al., 2005). Therefore, when considering the shape of the tibial insert the use of a curved design reduced wear compared to more flat-on-flat components (McEwen et al., 2005). The benefit of flatter components is that greater posterior femoral rollback is achieved giving more natural kinematics, while more curved components reduce contact stress on the tibial insert potentially reducing wear (Liu et al., 2011; Ranawat, 2003; Wimmer, Laurent, Haman, Jacobs, & Galante, 2012). Other design differences may be that of the PCL retaining versus PCL substituting designs. It is noted that studies have claimed that both give rise to more normal knee kinematics (Abdel, 2011), and so much debate exists between the two. Supporters of the PCL retaining implants claim that these implants maintain normal kinematics, protect the bone-cement interface from shear stress, and provide greater passive knee flexion along with enhanced quadriceps power (Clark et al., 2001; Pereira, Jaffe, & Ortiguera, 1998; Sorger et al., 1997). Researchers that instead support PCL retaining implants make the point that substitution increases the ease of ligament



balancing allowing for a more conforming tibiofemoral articulation as well as allowing for a replication of the posterior femoral rollback present in natural kinematics (Freeman & Railton, 1988). Each of these designs has pros and cons, and further research is required to fully understand the effects of each in vivo.

### *3.5.5 Summary of Aims and Introduction*

The knee joint is a complex joint with movement largely dictated by the anatomy of the bones. During flexion of the knee a medial pivot motion occurs along with a lateral femoral rollback. This rollback aids in the extensor mechanism reducing the required quadriceps force. Osteoarthritis is a common knee pathology that greatly limits knee function and is best treated using a total knee replacement. Many different TKR designs exist, with a significant difference existing in the geometry of the implants. The success of TKR's is not only dictated by design, but also the proper alignment by the surgeon. Improper alignment may result in kinematics that the implant designer did not intend. In order to test implants prior to patient implantation, wear tests are conducted utilizing knee wear simulators. Alignment of the implants for simulation may greatly impact the wear results, and so should be optimized.

The aim of this study was to determine the effect of femoral axis alignment on bearing migration in multiple TKR geometries. Using 3D scans of implants, a computational model was developed to track the lowest femoral contact-point during flexion over 400 possible axes.



## CHAPTER FOUR: MATERIALS

This chapter will detail the relevant materials used to complete this thesis. All of the materials and equipment that are discussed in this section directly affected the results. Intrinsic equipment that simply aided the research (such as the computer system that processed the data) are not discussed.

### *4.1 TKR Implants*

For my study I utilized seven previously wear tested total knee replacements. Because each of these implants was used on our Stanmore Knee Simulator they were all attached to phenolic blocks. These implants are detailed in the table below.

**Table 4.1** Femoral Component Descriptions

Implant Name	Implant Picture	Implant Type	Axis	Constraint	Orientation	Condyle Symmetry
					Size	
SulzerMedica Natural-Knee® System		PCL- Retaining	Multi- Axis	No constraint specification	Right	Symmetric
					M/L: 75 mm A/P: 55 mm	
CenterPulse Natural-Knee® II System		PCL- Retaining	Multi- Axis	No constraint specification	Right	Larger Medial Condyle
					M/L: 75 mm A/P: 65 mm	

<p>Biomet Maxim® Instrument System (BIOMET)</p>		<p>PCL- Retaining</p>	<p>Multi- Axis</p>	<p>Femoral Constrained (increased conformity)</p>	<p>Right M/L: 69 mm A/P: 65 mm</p>	<p>Increased Medial Curvature</p>
<p>Wright Medical Advance® Knee System (Systems)</p>		<p>Medial Pivot PCL- Retaining</p>	<p>Single Axis</p>	<p>Increased Tibial Conformity</p>	<p>Left M/L: 70 mm A/P: 60 mm</p>	<p>Symmetric</p>
<p>Ortho Development Balanced Knee® System (ODEV)</p>		<p>PCL- Substituti ng Posterior Stabilized</p>	<p>Multi- Axis</p>	<p>Tibial Post constraint</p>	<p>Left M/L: 67 mm A/P: 58 mm</p>	<p>Symmetric</p>
<p>Stryker Triathlon® Knee System (Triathlon Total Knee)</p>		<p>PCL- Retaining High- Flexion</p>	<p>Single- axis with high flex axis</p>	<p>Increased conformity without reducing constraint</p>	<p>Left M/L: 69 mm A/P: 62 mm</p>	<p>Larger Medial Condyle</p>
<p>Zimmer NexGen® Complete Knee Solution Legacy® (Zimmer)</p>		<p>PCL- Substituti ng</p>	<p>Multi- Axis</p>	<p>No constraint specification</p>	<p>Left M/L: 68 mm A/P: 61 mm</p>	<p>Symmetric</p>

#### *4.2 NextEngine 3D Laser Scanner*

In order to create the 3D models of our knee implants we needed a standardized system. We decided to use the NextEngine 3D laser scanner because of its ease of use and relatively high tolerance. The NextEngine scanner has an accuracy of 0.005 inches or 0.127 mm (“NextEngine 3D Laser Scanner”).

#### *4.3 3Matic STL*

In order to prepare our 3D scanned model for simulation we needed to use 3Matic STL. 3Matic STL allows you to make design modifications, design simplifications, 3D texturing, remeshing, as well as allows for forward engineering directly on STL, scanned, and CAD data (Taylor, n.d.). For our purposes we used 3Matic to repair missing or poorly scanned regions of our femoral components and prepare our data for finite element analysis.

#### *4.4 COMSOL Multiphysics*

Computational simulation was carried out in COMSOL Multiphysics, a platform for physics-based modeling and simulation (COMSOL, n.d.). COMSOL allows for coupled or multiphysics phenomena, making it an excellent tool for a comprehensive analysis. The simulations completed as part of this research project were all done in solid mechanics and so incorporated only one type of physics, but future work may require more extensive analysis.

#### 4.4.1 Model Physics

Although our model is a finite element model, the simulation is being run as a rigid body which means that deformation is not being accounted for. This stiff component will only contribute to the dynamic properties of the structure through its mass and moment of inertia (COMSOL, n.d.). Because of this the physics behind our model is fairly simple. This section will give an overview of the physics and equations that are dictating the movement of our model, as well as an overview of the solvers that are calculating the translation of the model.

The simulation is a time dependent solid mechanics model with a prescribed rotation of a rigid body. The equations that define our rigid body include:

$$F = -m \frac{d^2 u}{dt^2} \quad (\text{Equation 1})$$

$$M = -I \frac{d^2 \varphi}{dt^2} \quad (\text{Equation 2})$$

$$I = \int \left( (X_d * X_d) E_3 - X_d * X_d^T \right) \rho dV \quad (\text{Equation 3})$$

$$u_c = u + (R - I)(X_c - X'_c) \quad (\text{Equation 4})$$

$$b = \frac{\Omega}{|\Omega|} \sin\left(\frac{\varphi}{2}\right) \quad (\text{Equation 5})$$

$$a = \cos\left(\frac{\varphi}{2}\right) \quad (\text{Equation 6})$$

$$\varphi = \frac{2\pi}{360} * t \quad (\text{Equation 7})$$

In these equations  $F$  is force,  $m$  is mass,  $u$  is displacement,  $M$  is momentum,  $I$  is area moment of inertia,  $\varphi$  is angle of rotation,  $E_3$  is an identity matrix,  $X_d$  is global coordinates with respect to center of rotation ( $X_c$ ),  $\rho$  is the density of the material,  $R$  is a special

coordinate defined by  $a$  and  $b$ , and  $t$  is time. *Equation 7* defines the rotation of the object as one degree of rotation per second. This angle of rotation can be used to find  $a$  and  $b$ , which in turn can be utilized to find the global coordinate matrix. Once COMSOL has determined the global coordinate matrix, a global evaluation of the minimum  $z$  coordinate can be used at each time step that correlates with one degree of rotation to find the coordinates of the lowest point of contact.

The location of the component during rotation is approximated using Newton's method. Newton's method is described as a root finding algorithm using the first few terms of the Taylor series(Weisstein, n.d.). Therefore, the method of determining the locations of the coordinates is not exact, but rather an approximation. The approximation steps end based on a tolerance factor of 1, with a maximum of 4 iterations as recommended by COMSOL.

Time-stepping is used as part of the model in order to produce a more accurate approximation. By utilizing the previous results the next value can be approximated. For our model BDF (Backward Differential Formula) was used with an order of accuracy between one and five (COMSOL, n.d.). BDF was the best choice for our model because it is used for smoother solutions without any expected sharp turns or changes. The stability of BDF allows for larger analysis with less risk of variability than generalized alpha methods (Note: analysis compared both methods and the same approximations were given for each) (COMSOL, n.d.).

#### 4.5 MATLAB

MATLAB is a high level language and interactive environment that allows for numerical computation and visualization (“MATLAB - The Language of Technical Computing,” n.d.). It gives us the ability to utilize mathematical functions to process large amounts of data for both thorough analysis and graphic displays.

#### 4.6 Alignment Jig

In order to validate our computational results and also prepare the knee wear simulator for simulation we used an alignment jig (Figure 4.1) that allows us to properly align the femoral component on the simulator bracket. The alignment jig measures proximal/distal displacement, anterior/posterior displacement, as well as medial/lateral displacement in ten degree increments. This allows us to ensure that the minimal P/D camming occurs during the simulation.

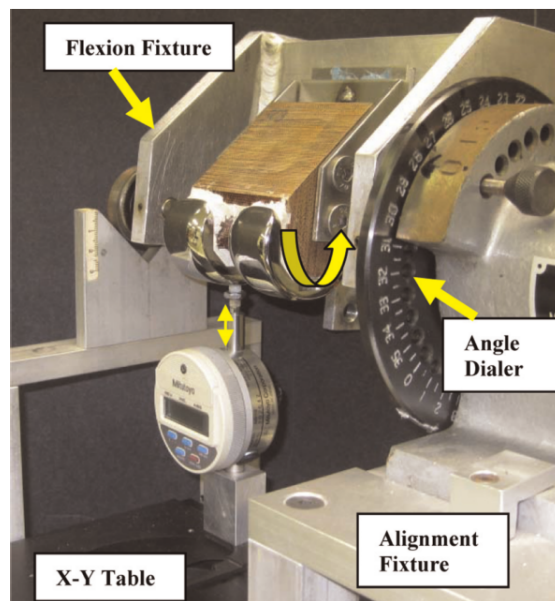


**Figure 4.1:** Alignment jig used for alignment of femoral components

## CHAPTER FIVE: METHODS

The materials previously described were used on each femoral component that was detailed. This chapter will describe the steps necessary to develop our femoral meshes for finite element analysis, the method of setting up a model in COMSOL Multiphysics, and the subsequent method for ideal alignment on the femoral bracket. Post-processing methods using Matlab will also be described.

### *5.1 NextEngine 3D Laser Scanner*

To use the scanner the object is positioned in front of the scanner. It does not need to be placed in or on the scanner so objects that are to be scanned are not limited by size. To create the three-dimensional model the image is simply captured from multiple views and then each facet is combined using NextEngine's ScanStudio software. The software is able to easily put the objects together to form our 3D model. The model takes approximately two minutes to process for each view, with a minimum of twelve views recommended for a complete model ("NextEngine 3D Laser Scanner"). The NextEngine scanner has an accuracy of 0.005 inches or 0.127 mm ("NextEngine 3D Laser Scanner"). This tolerance was suitable for our needs. The scanner then outputs 3D files in STL format and can be incorporated into the next step.



## 5.2 3Matic STL

The use of 3Matic begins by importing the 3D scanned STL files into 3Matic. 3Matic works very well with STL formats and is able to easily open the file. STL formatted objects are made up of a mesh of triangles rather than rectangles or tetrahedrons, which many other programs require. Once the file is open the first step is to run the 'Auto Fix Wizard' that 3Matic supplies. This unique tool is able to fix many problems in the scan, and can save considerable time.

One problem that the wizard is unable to fix is 'bad edges' (Figure 5.1) and so these must be adjusted manually. Experience goes a long way in locating these 'bad edges' as they typically congregate around any sharp edges or areas that may have been difficult to scan. The 'bad edge' will appear as a bright red hole within the model. Once located the areas around the edge can be selected by 'marking' them. These areas can then be deleted. Using the 'smooth curve' function the surface of the hole can be smoothed by changing the size of the triangles around the hole. The smooth surface of the hole allows for fixing of the hole using either the 'fix hole normal' or 'fix hole freeform' functions. If the hole is along a flat surface or the hole is very large it is recommended to use the 'fill hole normal' function. However, if the hole is along a curved edge and is not too big it is recommended to use the 'fill hole freeform' function. Once it is believed that all of the bad edges have been accounted for and fixed the 'Auto Fix Wizard' can be run again. If bad edges still exist after running the simulation and none appear to be on the surface of the object there is a good chance that complexities exist inside of the model. It

is recommended that a hole is made in a spot that will allow for vision within the model, and any bad edges on the inside of the model can then be fixed.

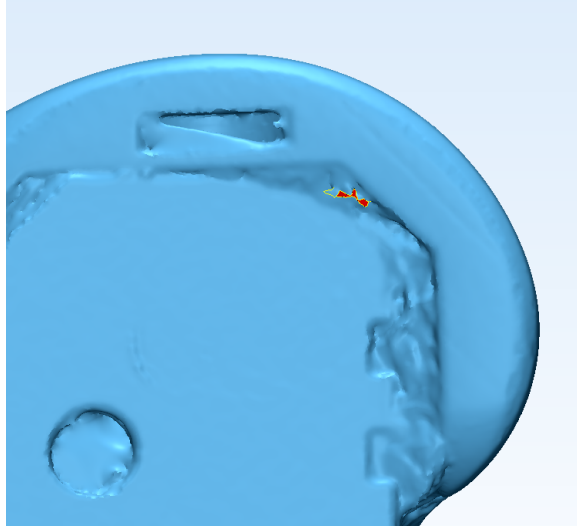


**Figure 5.1** Bad edges located in difficult to scan areas of the implants need to be fixed in order to create a defined mesh.

Once no ‘bad edges’ exist as depicted by the ‘Auto Fix Wizard’ most likely there will be ‘overlapping triangles’ that the wizard is unable to converge. In order to eliminate these the function ‘mark double triangles’ can be utilized. All of the double triangles within the model will now be highlighted. The function ‘mark broader area’ needs to be used for each triangle to create a small area around which the overlapping triangles exist. This marked area can then be deleted. Utilizing the ‘smooth curve’ function along with one of our ‘fix hole’ functions the overlapping triangles should be eliminated.

After running ‘Auto Fix Wizard’ once again another problem that may present itself is multiple ‘shells’. A ‘shell’ within the model is a 3D object that is self-standing. For our purposes we wanted to make sure that only one shell existed. Locating these extra

shells can be done using the 'Surfaces' tab. By clicking on 'Surface' then 'shells to surface sets' you convert each shell into its own surface. At this point each of the surfaces can be located in the tree, and any additional surfaces that are not a part of the desired object can be deleted. Once again 'Auto Fix Wizard' can be run to confirm that no additional 'shells' exist.

Once no errors are apparent and the 'Auto Fix Wizard' has 0 errors listed for each possible problem the model can be prepared for export. The first step in this is to merge all of the surfaces so that only one surface is present. Next the condyles must be prepared so that separate analysis can be run on each condyle in our simulation. This can be done using the 'Mark Wave Brush' tool. Using a diameter of 10 mm the brush is run along the length of each condyle. Once the surfaces are marked the 'smooth border' operation is utilized. This will output three surfaces as part of the single model, with each condyle being its own surface or boundary and the rest of the object being the third surface.

The object now needs to be finely remeshed so that the tolerance of the scans is not affected. By finely remeshing only the condyles (the surface that we will be analyzing) we are able to reduce the file size so that errors do not persist in COMSOL Multiphysics. To do this the 'Auto Remesh' function is utilized. Leaving the elements at the defaults (0.3 mm shape quality, 0.05 max geom error) the local remesh tab is used. Condyles 1 and 2 are added to the local remesh list and the values 1.0 mm for max edge length and 2.0 mm for influence area are used. These values meet the 3Matic recommended values that will not affect tolerance. This 'local remesh' can then be added to the 'remesh' that is being run, after which Condyle 1 and 2 need to be deleted from the

local remesh marking area. Once this is done ‘Apply’ can be entered. A very fine mesh should be noted on the condyles with a rougher mesh around the rest of the object. Once again it is recommended that the ‘Auto Fix Wizard’ is run as some minor errors may have developed in the remesh. The wizard should solve any problems that may have occurred, but if it does not the previous steps should be followed to resolve them. In order to run finite element analysis on an object a volume must be present. Currently the object is simply a ‘surface’ and so a ‘volume mesh’ must be applied. This is done by using the ‘create volume mesh’ tool. Tolerances are again based on 3Matic recommendations. With an ‘Aspect ratio’ of 25, condyles 1 and 2 are applied to the local remesh area with 1.0 mm max edge length and 3.00 mm influence arc. Once this mesh is applied in the model tree there should appear both ‘Surfaces’ and ‘Volumes’ under the component.

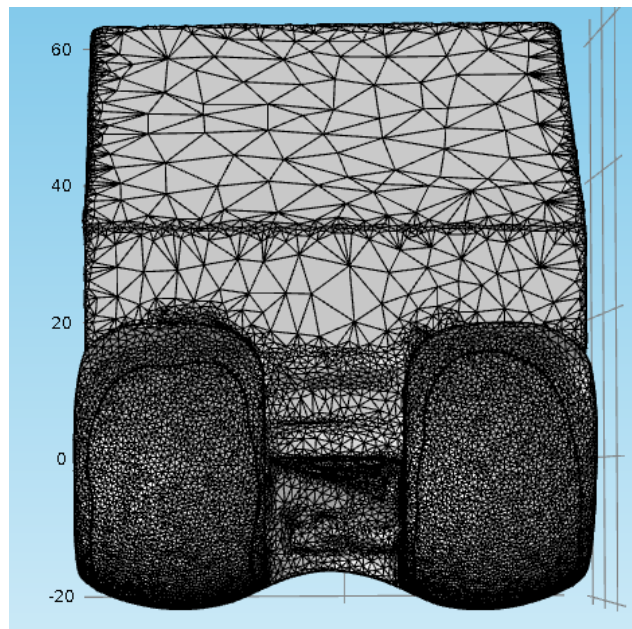


**Figure 5.2** Two-tone mesh created to keep the file size small while having a fine mesh over the area of analysis.

The final step before export to COMSOL is the alignment of the implant. The implant should already be aligned along the x-axis by the methods of 3D scanning. The next alignment needs to align the implant in the y-z plane so that rotation can be defined. In order to do this 'Plane to Plane Align' can be used. In the 'Plane on Fixed Entity' box, the 'xy plane' under the 'World Coordinate System' can be used. For the 'Plane on Moving Entity', the piece of the block between the two femoral condyles can be used by right clicking and choosing 'fit triangle'. This piece of the implant can be used because it is parallel to the zero degree alignment of the implant.

The model is now ready for export to COMSOL and can be done simply. Selecting 'Export to Comsol' and choosing 'both surface and volume mesh' will output a file that COMSOL is capable of reading. This step was done for all seven components.

### *5.3 COMSOL Multiphysics Model*

Setting up the model to run our simulations can be done very simply. This section will cover the steps for setting up the model in COMSOL based on the previously described physics that dictate the model.

When COMSOL is first opened the first step will be to select the type of study that needs to be run. Using 3D Model Wizard, select 'Solid Mechanics' and then hit study. After that select 'time-dependent' and enter done.

Once the study is set up the first step will be to import the exported file from 3Matic STL. Under 'Component 1' right click on 'Mesh 1' and select 'Import' (note: the file exported was a mesh not a geometry, so no geometry for this file will exist). In the

settings window select the correlating file and choose 'Import'. The 3D scanned file should now appear in the graphics window.

Next, the parameters and variables can be set. Under 'Global', then 'Definitions', select 'Parameters'. The parameters for this simulation will be 'ap' defined as 0 [mm] and 'pd' defined as 0 [mm]. These parameters will later be used to define our possible axes of rotation. Then click 'Variables' and the first variable will be 'omega' with a value of ' $2\pi/360$ [s/rad]'. The next variable will be 'theta' and is defined as ' $\text{omega}\cdot t$ '. In this instance 'theta' will be our angle of rotation at any time 't'.

The component must have a defined material so that an analysis can be run. For the purposes of this simulation the material properties are not taken into account. To keep the model simplified 'Structural Steel' is selected as the material. Under 'Component 1' click the geometry tab and change the units to millimeters.

Each condyle must now be defined so that measurements can be taken along both the medial and lateral condyle. To do this a minimum coupling operator is used. Under 'Component 1', right click 'Definitions' and select 'Component couplings' and then 'Minimum'. In the settings window select 'Boundary' and then in the Graphics window select the medial condyle. The same steps are followed for the lateral condyle.

At this point the physics can be added to the model. Right click 'Solid Mechanics' and select 'Material Models' followed by 'Rigid Domain'. In the Model Builder window right click 'Rigid Domain' and select 'Prescribed Displacement/Rotation'. Also be sure to select the model in the graphics window so that the physics applies to the component. Next click on 'Prescribed Displacement/Rotation' and the settings of these physics can be

adjusted. In the settings window adjust the 'Center of Rotation' to 'user defined'. In the 'Global coordinates of center of rotation' field enter '0' for x, 'ap' for y, and 'pd' for z. This defines our anterior/posterior displacement along the y-axis, and our proximal/distal displacement along the z-axis. In the 'Prescribed Displacement at Center of Rotation' field check each box for displacement in all three directions, however, leave the displacement at 0 m. This ensures that the object will rotate. In the 'Prescribed Rotation at Center of Rotation' field select 'Prescribed rotation at center of rotation' from the drop down menu. In the 'Axis of rotation' field enter '1' for x, and '0' for y and z. This defines the axis that our model will rotate around. Because of our previous alignment steps we want the model to rotate around the x-axis. The 'Angle of rotation' can be defined as '-theta'. This final step is negative because of the direction that we want the model to rotate. This will complete the physics for the model.

The time-dependent parameters now need to be set for the model. In the Model Builder window expand 'Study 1' and select 'Step 1: Time Dependent'. In the settings window under 'Study Settings' set the time as 'range(0,1,120)'. This will make the component rotate 120 degrees at 1 degree per second. Also, check the 'include geometric nonlinearity' checkbox. This ensures that COMSOL calculates the spatial coordinates of deformation.

To ensure convergence the solver configurations need to be adjusted. Right click 'Study 1' and select 'Show Default Solver'. Expand 'Solver Configurations' and then expand 'Solution 1'. Now click on 'Time-Dependent Solver 1' and open 'Time Stepping'. Under this tab adjust the method to BDF (as described previously) in the pull

down window. Next, looking back in the Model Builder window under ‘Time Dependent Solver 1’ select ‘Fully Couple 1’. Under ‘Method and Termination’ adjust ‘Nonlinear method’ to ‘Constant (Newton)’.

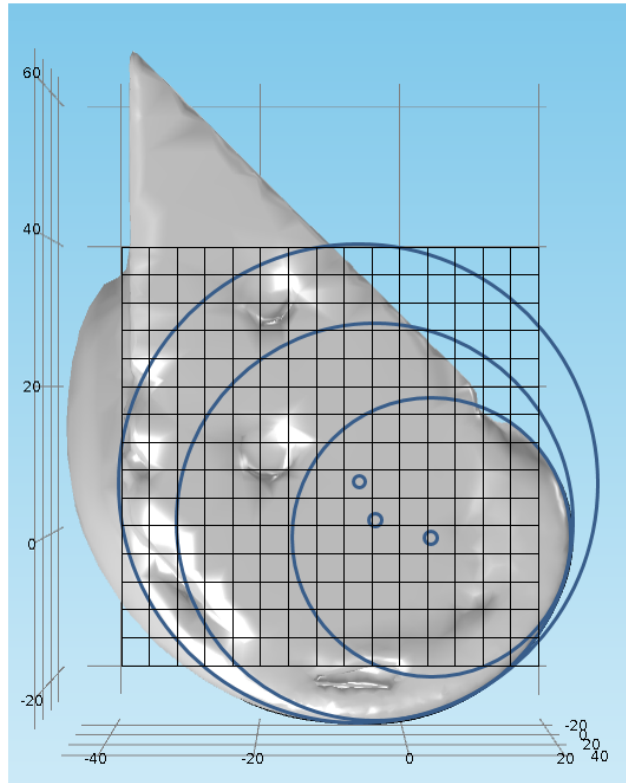


**Figure 5.3** Estimated geometrical axes for CenterPulse NKII.

The final step is setting up a parametric sweep to evaluate the rotation along multiple axes. In order to complete this step the geometrical axes of the components needs to be determined (Figure 5.3). In order to do this a snapshot of the images can be taken in COMSOL along the yz-plane. Using Microsoft Word’s shape function, the axes can be approximated by aligning circles along the femoral condyles of the implants. Once the axes of rotation are determined, a 20mm by 20mm square can be generated to



incorporate all of the axes, especially in the regions between 0 and 60 degrees of rotation. Using this 20 x 20 window the parametric sweep can be generated by right clicking 'Study 1' and selecting 'Parametric Sweep'. Under study settings select 'ap' and set the range for movement along the y-axis. Complete this step for pd for movement along the z-axis. Once all of these steps are completed the model can be run by entering 'Compute'. This simulation for four hundred axes should take approximately two hours. At the completion of the simulation the displacement can be noted visually by the color of the component showing a clear axis of rotation.

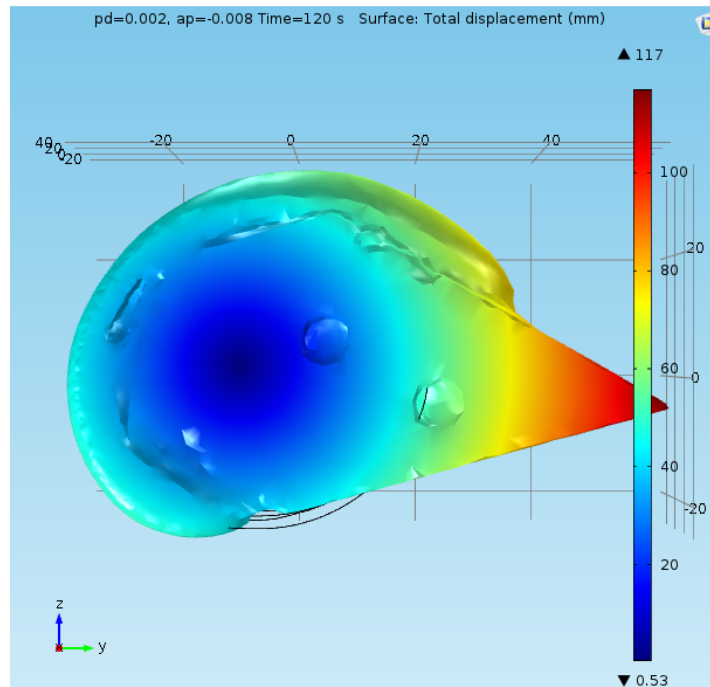


**Figure 5.4** Visualized displacement of CenterPulse NKII at P/D 2mm and A/P -8mm.

Note the dark blue circle at the center of the implant dictating the axis of rotation.

Once the simulation is done running the results need to be outputted. To do this, click on the results tab and choose 'Global Evaluation'. In the 'Global Evaluation' settings window choose the parametric data set. Unfortunately, due to an error in COMSOL's system there is a limit to how much data can be outputted at once, therefore we must break up our outputs. In the same window where the drop down tab for 'pd' appears, select manual. The output will be broken up into 5 components to keep it to less than 10,000 readings per output. For the first output the numbers '1,2,3,4' will be output, then '5,6,7,8' etc. all the way up to 20. In the expression field six expressions will be entered for each of the manual output numbers. These are 'minop1(z,x)', 'minop1(z,y)', 'minop1(z,z)', 'minop2(z,x)', 'minop2(z,y)', 'minop2(z,z)'. These expressions indicate the condyle being analyzed (minop1 or minop2), determination of the minimum point of contact in the z axis (minop1(z,\_)), and then finally dictate what point of location to output (minop1(z, x or y or z)). These are all output into tables and can then be imported into excel for further analysis using Matlab programming. These steps are repeated for all seven femoral components.

#### *5.4 MATLAB Post Processing*

In order to process the large amount of data outputted algorithms in MATLAB were generated. Because each of the outputs could be easily compiled into six columns (time, A/P axis location, P/D axis location, x-axis location, y-axis location, z-axis location) the MATLAB sorting algorithm just had to separate the output into a 400 x 121 matrix (400 possible axes of rotation and 121 degrees of rotation) for the x, y, and z axis

locations of minimal contact. With each column now corresponding to a separate axis of rotation, averages, standard deviations, and maximums and minimums could now be determined. Also, graphs to demonstrate the data could be outputted. In order to streamline the alignment process, the ideal axis could be singled out, and the radius of the implant at 0 and 90 degrees of rotation could be determined.

### *5.5 Alignment of the Femoral Components for Wear Testing*

With the radius of the implant at 0 degrees flexion and 90 degrees flexion alignment of the femoral component on the simulator bracket is very simple. Using an alignment jig previously created in our lab the proximal/distal displacement, anterior/posterior displacement, and medial/lateral displacement of the implant at the lowest point of contact can be located. The first step is to attach the femur to the bracket without any additional spacers. Next the bracket is attached to the alignment jig and rotated to 90 degrees. The tool used to measure the minimal contact point or proximal/distal displacement needs to be zeroed against the bearing of the bracket. Because the bearing has a radius of 21 mm the P/D displacement measured can be added to 21 mm to determine the radius of the implant. The radius can now be measured at 90 degrees flexion and can be compared to the MATLAB outputted radius required for ideal axis alignment. The radius should be a few millimeters less than the ideal radius. By finding the difference between these two values it can be determined how many spacers are needed. The spacers have a thickness of 1 mm, and so adjustment of the ideal axis can only be done in 1 mm increments. Once the additional spacers have been added

alignment at 0 degrees can be completed. This is done by manually adjusting the height of the implant until the exact radius outputted by the algorithm is found. In order to validate the axis selection measurements of the lowest point of contact are measured in 10 degree increments and compared to the COMSOL outputs.

## CHAPTER SIX: RESULTS

The first results to be studied was the verification of our model. Next, because this study yielded a significant portion of data we chose to present in two ways: 1) the ideal axes of femoral rotation at 60, 90, and 120 degrees flexion for each tested implant, and 2) the relationship between proximal/distal translation and anterior/posterior translation between differing implants. The three aims of the study are satisfied and validated with the data produced in the results.

### *6.1 Mathematical Model Comparison*

Although the data output by the model may inherently provide verification of the data, creation of a mathematical model and comparison to the simulation data would do a better job of pointing out any significant errors. In order to mathematically verify our model the Wright Medical Advance® Knee System was analyzed. Because this implant is a single axis femoral component (up until about 100 degrees of flexion), mathematical displacements between 0 and 90 degrees of flexion could be more easily determined. Based on the below graphic (Figure 6.1), the data in Figure 6.2 could be produced. This data is determined by simply adding the distance of translation. For example, translation 2 mm anteriorly and 1 mm proximally results in a displacement of  $1 + 2 = 3$  mm. On the other hand, translation 2 mm anteriorly and 1 mm distally results in a displacement of  $-1 + 2 = 1$  mm.

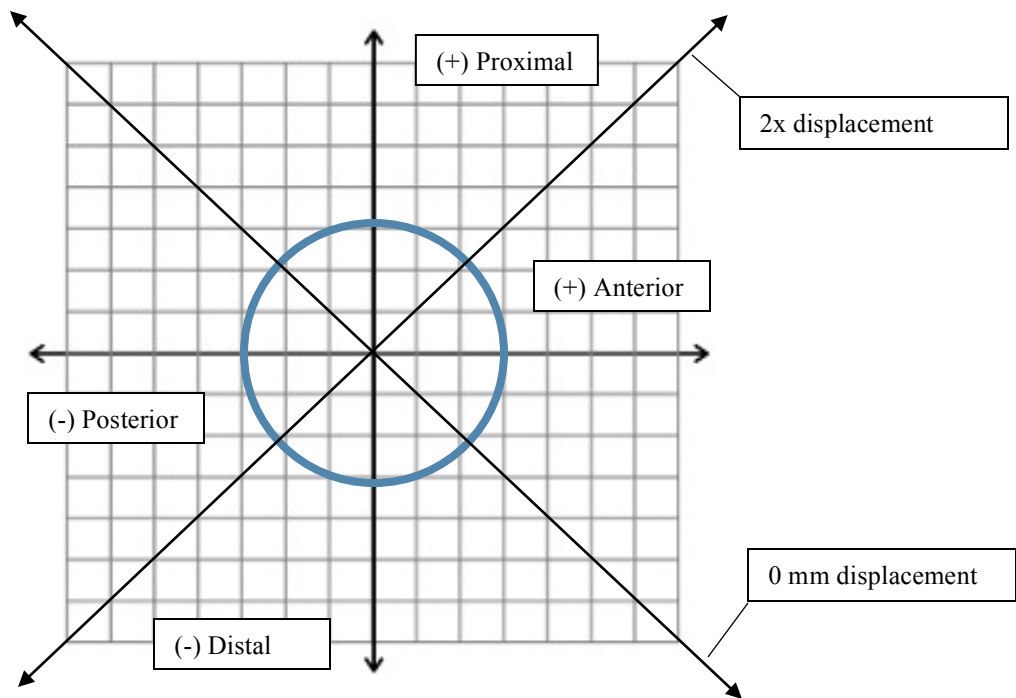


**Figure 6.1:** Graphic for measuring P/D migration of circle at ideal axis of rotation. A/P or P/D translation results in an equivalent displacement between 0° and 90° flexion.

Orthogonal displacement is either 0mm or double the translation.

0	1	2	3	4	5	6	7	5
-1	0	1	2	3	4	5	4	7
-2	-1	0	1	2	3	3	5	6
-3	-2	-1	0	1	2	3	4	5
-4	-3	-2	-1	0	1	2	3	4
-5	-4	-3	-2	-1	0	1	2	3
-6	-5	-4	-3	-2	-1	0	1	2
-7	-6	-5	-4	-3	-2	-1	0	1
-8	-7	-6	-5	-4	-3	-2	-1	0

**Figure 6.2:** Mathematically determined P/D displacement of single-axis implant at 0° - 90° Flexion for 81 possible femoral axes with the ideal axis highlighted.

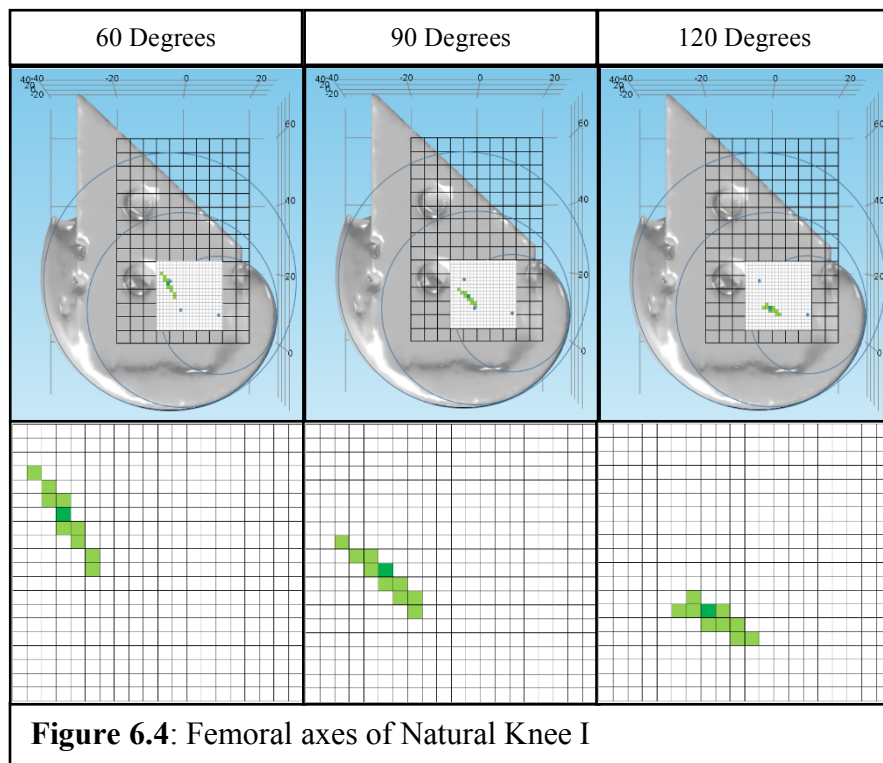
0.0	1.0	2.0	3.0	4.0	5.0	6.0	7.0	8.0	9.0	10.0	11.0	12.0	13.0	14.0	15.0	16.0	17.0	18.0	19.0	
-1.0	0.0	0.9	2.0	3.0	4.1	5.0	6.0	7.0	8.0	9.0	10.0	11.0	12.0	13.0	14.0	15.0	16.0	17.0	18.0	
-2.0	-0.9	0.0	1.1	2.0	2.9	4.1	5.0	6.0	7.0	8.0	9.0	10.0	11.0	12.0	13.0	13.9	14.3	16.0	17.0	
-3.0	-2.0	-1.0	0.0	1.0	2.0	3.0	4.0	5.0	6.0	7.0	8.0	9.0	10.0	11.0	12.0	13.4	14.0	14.9	15.9	
-4.0	-3.0	-2.0	-1.0	0.0	1.1	2.1	3.1	3.8	5.0	6.0	7.0	8.0	9.0	10.0	11.0	12.0	13.0	14.0	15.0	
-5.0	-4.0	-3.0	-2.0	-1.1	0.0	0.7	1.8	3.0	4.0	5.0	6.0	7.0	8.0	9.0	10.0	11.0	11.7	13.0	14.0	
-5.9	-5.0	-4.1	-3.0	-2.3	-0.9	0.0	1.0	1.9	3.0	3.9	5.1	6.0	7.0	8.0	9.0	10.0	11.0	12.0	12.9	
-7.0	-6.0	-4.9	-4.0	-3.1	-2.3	-1.0	0.0	0.9	2.0	3.0	3.9	5.1	6.0	7.0	8.0	9.0	10.0	11.0	12.0	
-8.4	-7.0	-5.9	-5.0	-4.0	-3.0	-2.0	-1.8	-0.1	1.0	2.0	3.0	4.0	5.1	6.0	7.0	8.1	9.0	10.0	11.0	
-9.1	-8.0	-6.9	-6.0	-5.0	-4.0	-3.0	-1.3	-1.1	0.0	1.0	2.0	2.8	4.0	4.9	6.0	5.9	8.1	9.0	10.0	
-	-	-	-	-	-	-	-	-	-	0.0	1.0	2.0	2.8	4.0	4.9	6.0	7.0	8.5	9.0	
10.0	-9.0	-7.9	-7.0	-6.0	-5.1	-4.0	-3.4	-2.7	-1.0	0.0	1.0	2.3	3.0	4.0	4.9	6.0	7.0	8.5	9.0	
-	-	-	-	-	-	-	-	-	-	-1.0	0.0	0.9	2.0	3.1	3.8	5.0	6.0	7.0	8.0	
11.0	10.0	-9.0	-8.0	-7.0	-6.1	-5.0	-4.0	-3.0	-1.9	-1.0	0.0	0.9	2.0	3.1	3.8	5.0	6.0	7.0	8.0	
-	-	-	-	-	-	-	-	-	-	-3.0	-2.0	-1.1	0.0	1.1	2.0	3.0	4.0	5.0	5.9	7.0
12.0	10.9	-9.9	-9.0	-7.9	-7.0	-6.0	-5.4	-4.1	-3.0	-2.0	-1.1	0.0	1.1	2.0	3.0	4.0	5.0	5.9	7.0	
-	-	-	-	-	-	-	-	-	-	-3.0	-2.0	-1.0	0.3	1.0	1.9	3.0	3.9	5.1	6.0	
13.0	12.0	11.0	10.0	-9.0	-8.8	-7.0	-6.1	-5.0	-4.1	-3.0	-2.0	-1.0	0.3	1.0	1.9	3.0	3.9	5.1	6.0	
-	-	-	-	-	-	-	-	-	-	-4.1	-3.0	-2.0	-1.1	0.1	1.0	2.5	3.1	3.1	5.0	
14.0	12.9	12.0	11.1	10.0	-9.0	-8.0	-7.3	-6.0	-5.1	-4.1	-3.0	-2.0	-1.1	0.1	1.0	2.5	3.1	3.1	5.0	
-	-	-	-	-	-	-	-	-	-	-5.0	-2.2	-3.0	-2.0	-1.0	-0.2	1.0	2.0	2.9	3.9	
14.9	14.0	13.0	11.9	11.0	10.0	-9.0	-7.8	-7.1	-7.6	-5.0	-2.2	-3.0	-2.0	-1.0	-0.2	1.0	2.0	2.9	3.9	
-	-	-	-	-	-	-	-	-	-	-6.0	-4.9	-4.2	-3.0	-2.0	-1.3	1.2	1.0	1.8	2.1	
16.0	15.0	13.9	13.0	12.0	11.0	10.0	-9.0	-8.0	-7.0	-6.0	-4.9	-4.2	-3.0	-2.0	-1.3	1.2	1.0	1.8	2.1	
-	-	-	-	-	-	-	-	-	-	-7.0	-6.2	-4.5	-4.5	-3.0	-1.5	-1.3	0.0	1.0	2.0	
17.0	16.1	15.1	14.0	13.0	12.0	10.7	-9.9	-8.9	-8.0	-7.0	-6.2	-4.5	-4.5	-3.0	-1.5	-1.3	0.0	1.0	2.0	
-	-	-	-	-	-	-	-	-	-	-8.0	-7.1	-6.0	-5.2	-4.0	-3.0	-2.3	-1.0	0.0	0.0	
18.0	17.0	15.5	14.9	12.7	12.9	12.0	11.0	10.0	-9.0	-8.0	-7.1	-6.0	-5.2	-4.0	-3.0	-2.3	-1.0	0.0	0.0	
-	-	-	-	-	-	-	-	-	-	-9.0	-8.0	-6.9	-6.0	-5.7	-4.0	-2.9	-2.0	-1.0	-0.2	
19.0	18.2	17.0	16.0	14.9	13.9	12.9	12.4	11.3	10.5	-9.0	-8.0	-6.9	-6.0	-5.7	-4.0	-2.9	-2.0	-1.0	-0.2	

**Figure 6.3:** P/ D displacement of 400 possible axes of rotation of Wright Medical Advance® Knee System Flexion at 0° – 90° flexion with ideal axis highlighted.

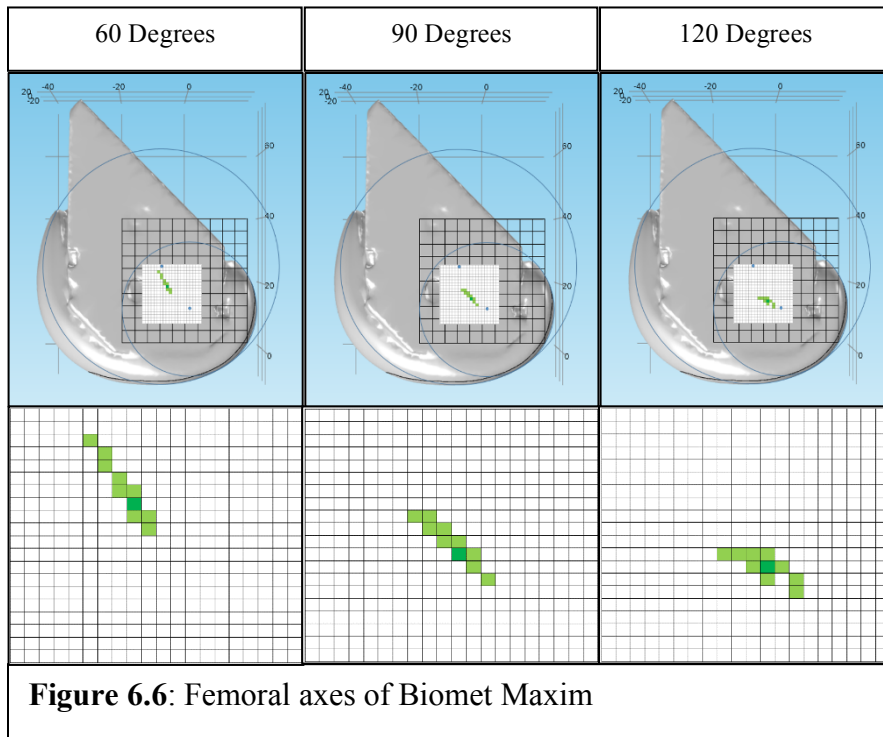
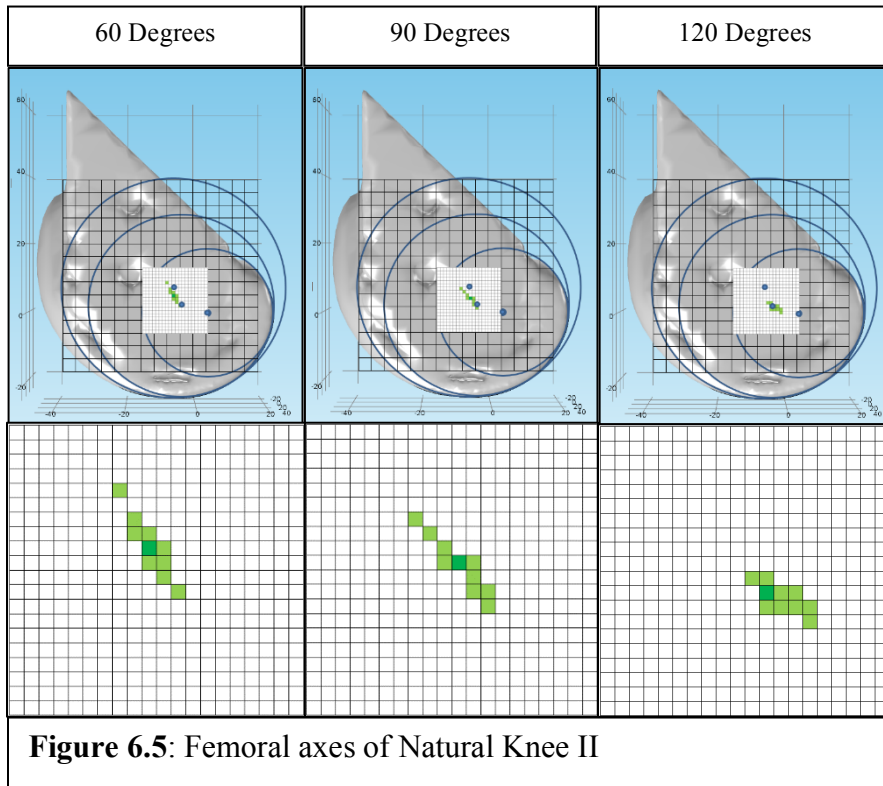
### 6.2 Ideal Axes of Femoral Rotation

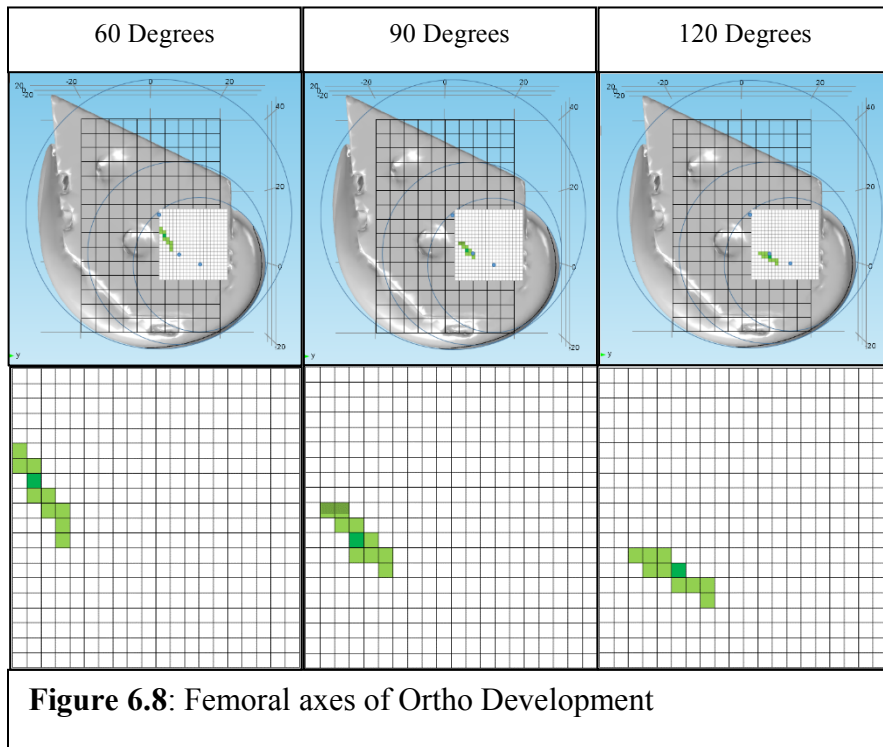
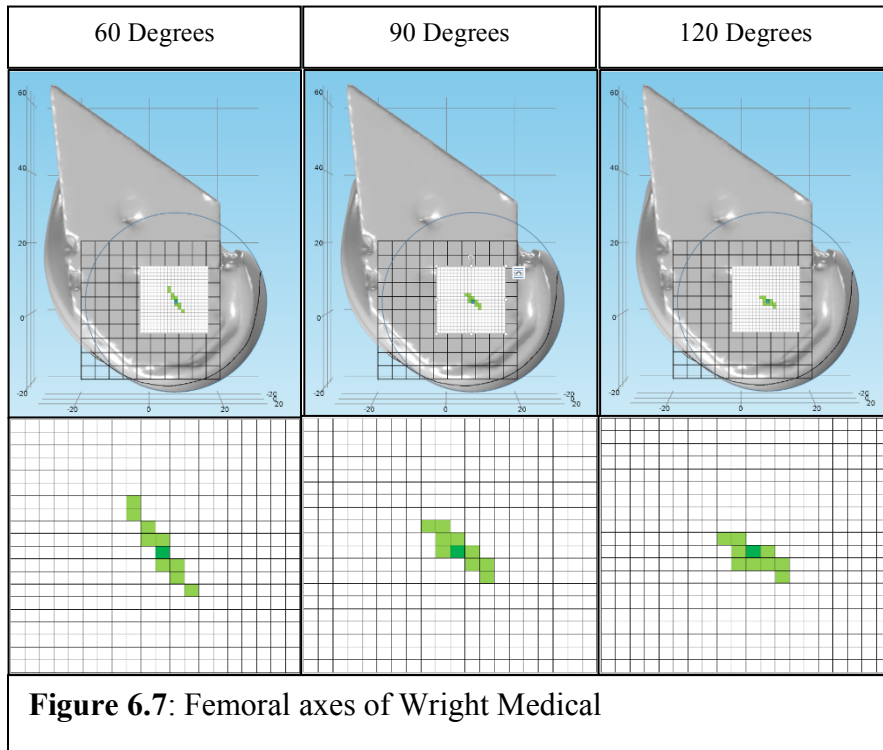
The methods of creating a 3D model and then using finite element analysis to simulate rotation allowed for the determination of minimal proximal/distal bearing migration. By determining the maximum and minimum points of contact between 0 and

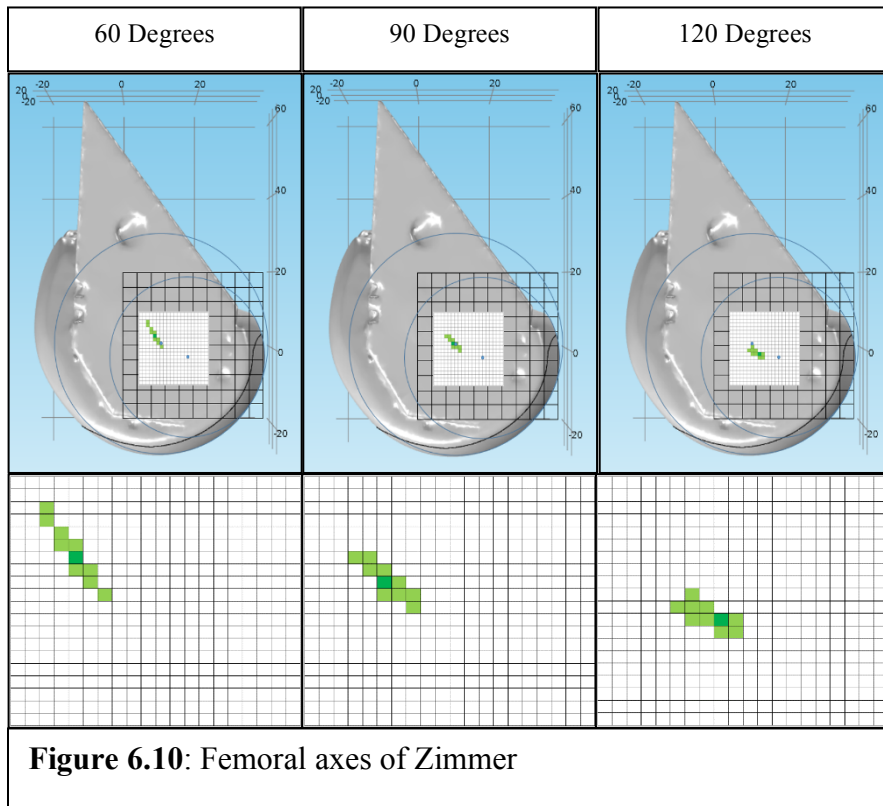
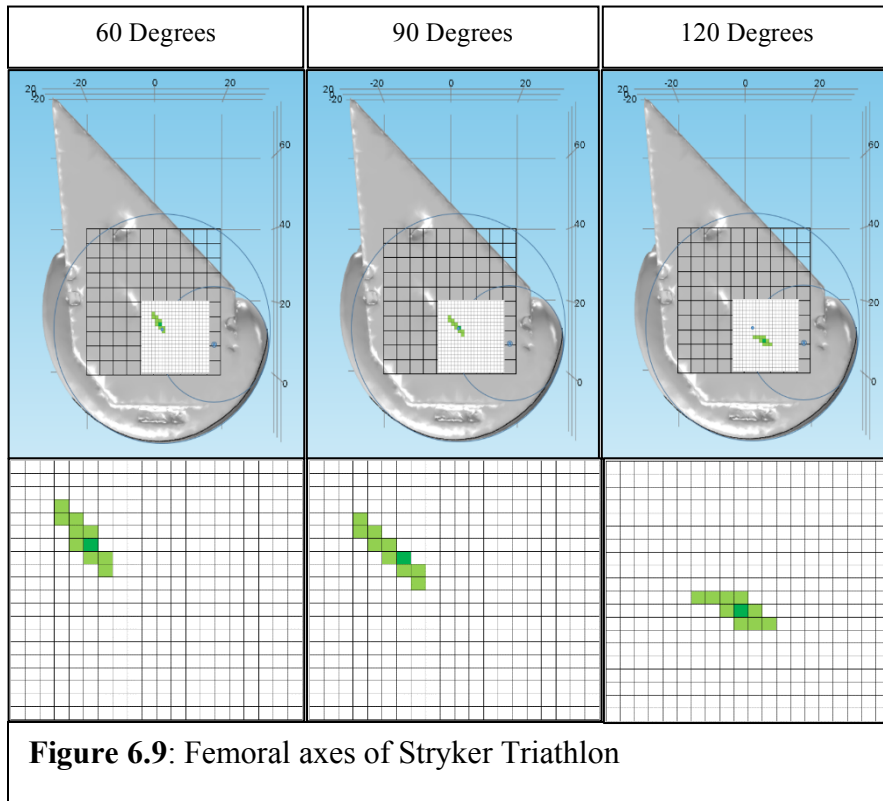
60, 0 and 90, and 0 and 120 degrees of flexion and then finding the difference along each axis, the axis with minimum migration, as well as the ten other axes with minimum migration can be found. This data is outputted using the MATLAB algorithms previously discussed. These can be compared to the geometrical axes of the implants. Figures 6.4-6.10 demonstrate these ideal axes for the varying implants within the varying ranges of flexion.











Figures 6.4 – 6.10 demonstrate the movement of the ideal axes based on flexion and in comparison to the geometrical axes. These ideal axes are based purely on proximal/distal migration. However, in order to view the numerical displacement for each possible femoral axis 3D plots can be generated. These plots allow for a greater distinction between the different possible axes. For example, some implants may have multiple axes within less than 0.127 mm (our tolerance) and so the ideal axis could include all of them, while other implants may have only a single axis that truly minimized P/D displacement. These may also present patterns within the data associated with the geometry of the implants. These graphics (Figure 6.11) are outputted using a MATLAB algorithm that plots the displacements against the axis locations. It should be noted that differences in shapes may occur because of range of axis selection, as the ideal axis is not always located within the center of this range.

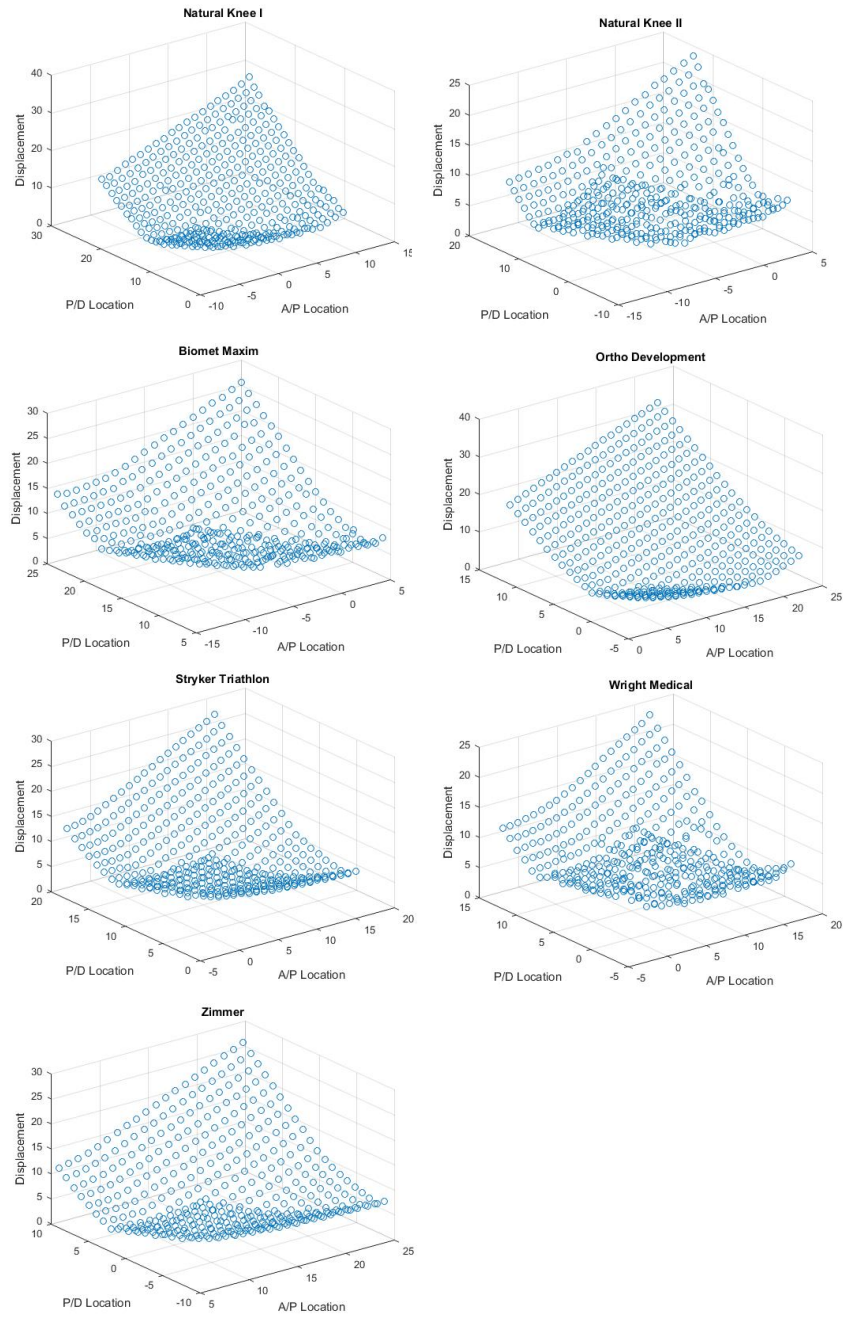


**Figure 6.11:** Proximal/distal displacements at each possible femoral axis in 3-D for all seven implants.

The next step in the analysis is to utilize the data from the ideal axis to determine the ideal alignment of the implants for wear simulation. Using the computed radius of the implant at 0 and 90 degrees the implants can be properly aligned on the simulator bracket using the alignment jig shown in Figure 5.5. Table 6.1 shows the P/D camming for the computational and measured analysis, as well as the correlation between the computed migration and actual migration. These results may also act as validation of our 3D scanned model and simulation.

**Table 6.1:** Computational versus measured proximal/distal bearing migration with the associated correlation value between the two sets of data

	Max P/D Camming at 60°	Max P/D Camming at 60°	Correlation
	Computational	Measured	R
NKI	0.33	0.54	0.9959
NKII	0.204	0.597	0.9072
Biomet Maxim	0.4601	0.763	0.9923
Wright Medical	0.124	0.119	0.9421
Ortho Develop	0.238	0.624	0.9939
Stryker Triathlon	0.149	0.100	0.9982
Zimmer	0.096	0.083	0.9928

### 6.3 P/D and A/P Translation at Varying Femoral Axes

Proximal/distal displacement was determined at four hundred possible axes. This data could be used to determine the effect on P/D displacement by selecting different axes. Table 6.2 reports the mean P/D displacements and standard deviations of the 10 axes with the minimum migrations (as depicted in Figures 6.1-6.7) as well as the migration at the ideal axis for comparison. This data has a tolerance of 0.127 mm based on the scanner tolerances.

**Table 6.2:** Proximal/Distal displacement at ideal axis for each implant and flexion range.

The mean and standard deviations of the 10 axes with the lowest P/D displacements are reported for each implant and flexion range.

Flexion	P/D Migration at Ideal Axis (mm) ( $\pm 0.127$ mm)			Mean P/D from 10 Best Axes (mm) ( $\pm 0.127$ mm)			Standard Deviation P/D from 10 Best Axes (mm)		
	60°	90°	120°	60°	90°	120°	60°	90°	120°
NKI	0.356	0.954	1.683	0.638	1.357	2.181	0.123	0.200	0.325
NKII	0.194	0.510	1.319	0.515	1.038	1.934	0.171	0.321	0.334
Biomet	0.503	1.009	1.205	0.719	1.257	1.926	0.100	0.149	0.361
Wright	0.093	0.130	0.932	0.453	0.820	1.466	0.173	0.361	0.371
Ortho	0.308	0.827	1.380	0.591	1.214	1.866	0.160	0.236	0.291
Stryker	0.189	0.708	1.89	0.493	0.948	2.473	0.176	0.225	0.288
Zimmer	0.107	0.480	1.317	0.472	0.962	1.903	0.187	0.264	0.327

Anterior/posterior displacements at the axes deemed ideal based on minimal P/D displacements are also reported for each implant and each flexion range. This data has a tolerance of 2 mm based on standardization of data. Error exists because of bumpy surfaces of implants created by the 3D scanner.

**Table 6.3:** Anterior/Posterior displacements at ideal axis based on minimum P/D displacement for each implant and flexion range. The mean and standard deviations of the 10 axes with the lowest P/D displacements are reported for each implant and flexion range.

Ideal Axis for 60° Flexion	A/P Migration at Ideal Axis (mm) ( $\pm 2$ mm)			Mean A/P from 10 Best Axes (mm) ( $\pm 2$ mm)			Standard Deviation P/D from 10 Best Axes (mm)		
	60°	90°	120°	60°	90°	120°	60°	90°	120°
NKI	6.066	7.806	10.851	6.620	8.796	11.414	0.869	0.896	0.999
NKII	1.748	4.824	7.412	3.033	5.604	8.138	1.220	1.547	1.234
Biomet	6.820	9.049	9.858	6.901	8.706	10.285	0.649	1.082	1.614
Wright	1.987	1.987	5.589	3.492	3.516	6.148	1.250	1.110	1.818
Ortho	4.878	6.777	8.630	5.618	7.420	9.087	0.572	0.739	1.038
Stryker	3.645	5.174	12.886	4.405	6.628	13.210	0.704	1.379	1.180
Zimmer	2.001	4.452	9.079	3.460	4.941	10.042	1.329	0.848	1.399

Anterior/posterior displacement data was graphed at the ideal femoral rotation axis for 60° and 120° flexion for all of the implants. The patterns of anterior and posterior displacement can be considered (Appendices B.1-B.7).



The ideal axis was also translated in various directions with the lowest contact point anterior/posterior motion being tracked. This data allowed for the recognition of changing contact point motion with varying axis selection

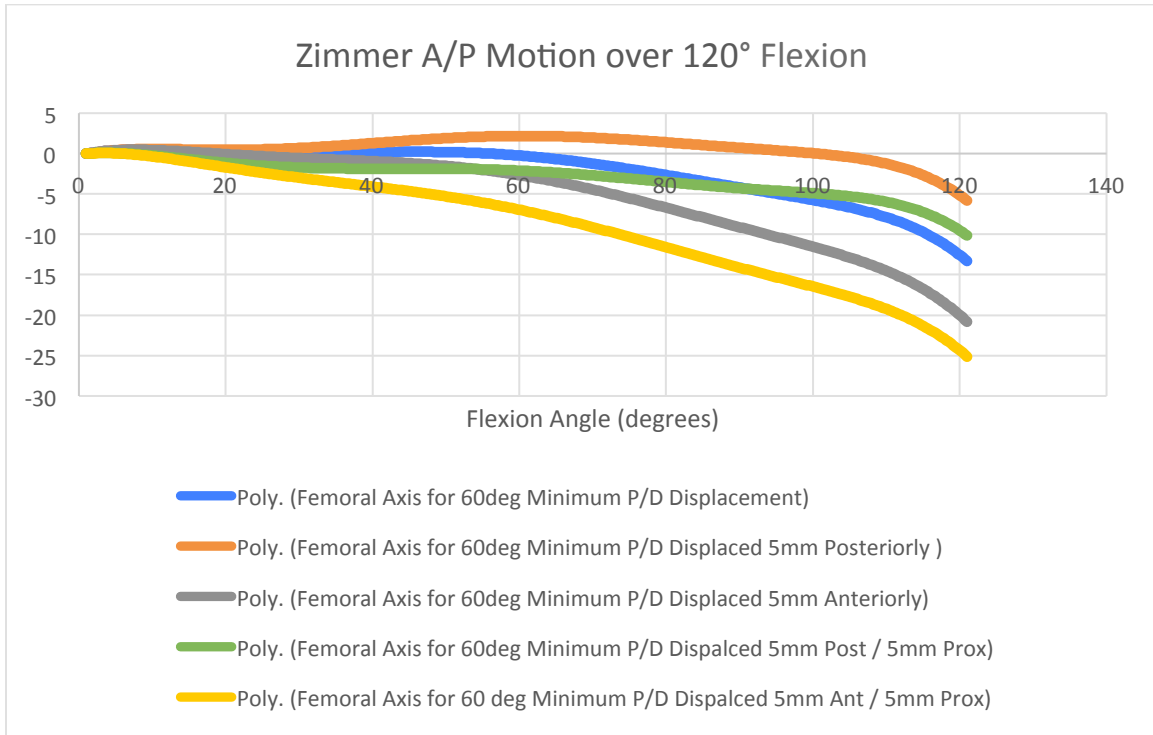


**Figure 6.12:** A/P displacement at the ideal axes and translated axes for 120 degrees flexion for the Zimmer knee. Note: anterior displacement is (-) y-axis displacement with (+) y-axis displacement relating to posterior displacement.

Single-axis versus multi-axis knee designs were considered and compared by translating the flexion axis both anteriorly and posteriorly. This could indicate possible variations between designs in tolerance for axis selection.

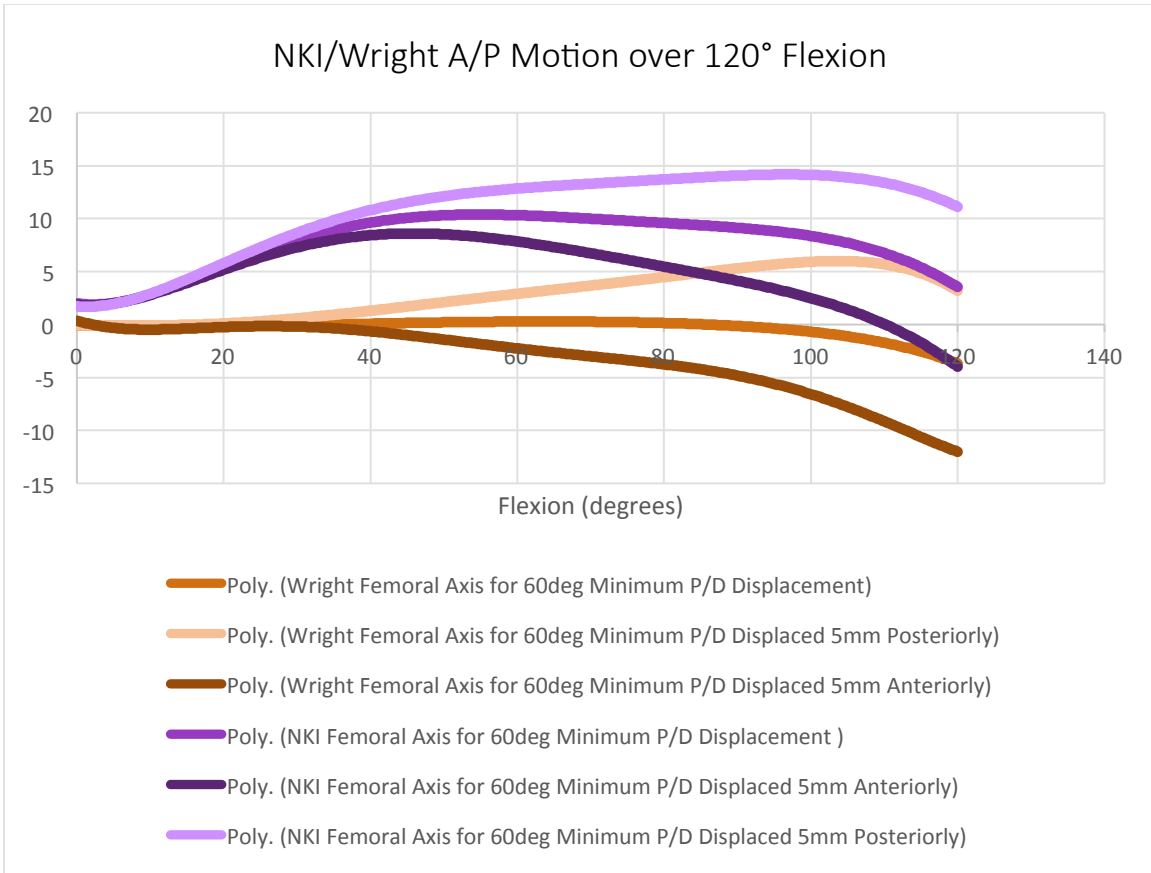


**Figure 6.13:** A/P displacement at the ideal axes and translated axes for 120 degrees flexion for the NKI (multi-axis) and Wright (single-axis) knee designs. Note: anterior displacement is (-) y-axis displacement with (+) y-axis displacement relating to posterior displacement.

## CHAPTER 7: DISCUSSION

The results of this study are unique in that they more comprehensively define possible femoral axis selection than any other previous study. In addition, literature appears to focus on effects that geometry can have on kinematics and minimizing surgeon error, but little literature exists on the specific effects that choosing the wrong femoral axis may have. The methods of conducting the study are verified with the outputted data, and relationships between proximal/distal displacement, anterior/posterior displacement, and implant geometry are discussed.

### *7.1 Verification of 3D Model and Simulation Model*

The first aim of this study was to utilize 3D scans in order to analyze knee implants. These 3D models were generated using the NextEngine 3D scanner and then edited and prepared for our simulation using 3Matic STL. The next aim of the study was to use these models to simulate rotation in COMSOL. Unfortunately, the 3Matic components could not be verified prior to use in COMSOL, and so verification must be done in multiple steps to ensure both steps are accurate. Therefore, verification of the models was done in two ways: 1) studying the data of a single axis implant, and 2) comparing the simulation data to actual measured data using an alignment jig.

The first method of verification was done using the Wright Medical Advance® Knee System, as this implant is a single axis implant (up to around 100 degrees of flexion). In a single axis knee system, if the ideal axis is chosen, it can be expected that

zero displacement is noted in the proximal/distal and anterior/posterior directions. Also, we would expect the ideal axis to remain unchanged at all ranges of femoral flexion. Because the implant has a simple geometry it can also be worked out mathematically what displacement should occur at differing axes of rotation. In order to mathematically verify this model flexion at 0 degrees and 90 degrees needs to be determined. Using MATLAB this data was output and rounded to the nearest tenth of a millimeter (Figure 6.3). This data could then be compared to the mathematical estimates (Figure 6.2) based on Figure 6.1. When rotating around a single axis any anterior, posterior, proximal, or distal displacement will result in an equal proximal/distal or anterior/posterior displacement in terms of location at 0 degrees flexion minus location at 90 degrees flexion. However, orthogonal displacement will have varied results depending on whether proximal/distal and anterior/posterior displacement are being measured. For our purposes we measured proximal/distal displacement and noted that orthogonal translation resulted in either a doubled displacement, or a displacement of 0. When our simulation data (Figure 6.3) is compared to these mathematical determinations the data appears to follow very strongly, with only slight deviations existing perhaps due to approximation errors. Based on this analysis we were satisfied with proceeding and continued to verify the model.

The next method of verification, still using the Wright Medical Advance® knee, was to ensure that the ideal axis of rotation was consistent between 0° - 60°, 0° - 90°, and 0° - 120° flexion. As is depicted in Figure 6.7, these axes remain consistent and so the model can be further validated.

Lastly, it was necessary to analyze both the P/D displacements and A/P displacements, because in a single axis implant the displacements would be identical, with the only difference being in opposite orthogonal translations. To determine if these maximum minus minimum displacements were equivalent with the ideal axis equal to approximately zero, the data for 0° - 60° flexion were compared (Figure A.1 and Figure A.2). It was immediately apparent that some discrepancies may exist in the anterior/posterior displacement data. While the P/D data is centered with a minimum displacement of approximately 0.09 mm (with a tolerance of 0.127mm) the A/P data had a minimum displacement of approximately 1.99 mm. When the displacement is graphed over the entire flexion range it can be seen that an oscillation is occurring (Figure A.3). In order to determine what was causing this oscillation the locations of the minimum displacements were plotted one by one using the COMSOL 3D plot function (Figure A.4). Using this function it was apparent that an oscillation in the anterior/posterior direction was occurring due to a non-smooth surface of the implant. Although unfortunate, this ruled out a possible COMSOL simulation error, and so the COMSOL model could be given a final validation of functionality. The bumpy surface on the scan was therefore due to an error in either the 3D Scan or the mesh created using 3Matic STL. In order to determine if the mesh created was not fine enough and was affecting tolerances, the Wright Medical implant was remeshed in 3Matic with a mesh one order of magnitude finer (Figure A.5). This mesh created was 10x finer than the 3Matic recommended mesh size because of the large size file that it created. This fine mesh was then ran through the COMSOL simulation and results were outputted. The outputted

results were identical to the results of the previous mesh, and so the problem was narrowed down to an inaccuracy in the 3D scanner.

The bumpy surface of the implant did not appear to affect the P/D data, but only affected A/P data because of the orientation of the bumps. Although this affects the tolerances of the results, the trends that exist within the results are still accurate. In order to account for this error, the oscillations of the Wright Medical implant can be used for standardization. Because the oscillations between all implants are similar in size when compared, a tolerance of  $\pm 2$  mm can be applied to all A/P data. Although not ideal this will allow us to still note trends in the data.

In summary, we were able to validate the functionality of both the creation of the 3D mesh using 3Matic and the creation of the simulation model using COMSOL Multiphysics by verifying the accuracy of the results. We did determine, however, that some inaccuracies exist in the method of 3D scanning.

### *7.2 Location of Ideal Axes of Femoral Rotation*

The identification of the ideal axes of femoral rotation based on minimal P/D camming motion is perhaps one of the strongest aspects of this study. In all simulations the data appeared consistent and reliable. We chose to analyze this data by both presenting the ideal axis and the following 9 best axes and by graphing the displacement of each axis in a 3-D representation. We were also able to use this data to satisfy our third aim by using the data to properly align our femoral components for wear simulation.

Figures 6.4-6.10 give an excellent demonstration of the outlook of our experiment. These figures show the grid of axes that were used to rotate the implants and the subsequent ideal axes for minimal P/D bearing migration. It can be immediately noticed that in the multi-axis designs (Figures 6.4-6.6 and 6.8-6.10) the ideal axis moves depending on the range of flexion. This is obviously due to the geometry of the implants, as the ideal axis of rotation moves posteriorly as the range of flexion increases to account for the reducing radius of curvature of the implants. It also appears as if the ideal axis of rotation moves posteriorly as the flexion range increases, again to account for the changing geometry of the implants. Another point to note is that the range of ideal axes appears to travel orthogonally, as was previously discussed with Figures 6.1-6.3. This can especially be seen in the single-axis implant (Figure 6.7), where at 0° - 60° flexion the axes are perfectly orthogonal, but as very slight geometrical changes occur the range of ideal axes begins to congregate. If the axes are studied closely it is noted that there is a significant shift in ideal axes between 90° and 120° flexion for the Stryker Triathlon® knee. Because the Stryker Triathlon knee is designed for high-flexion, this may be a result of those design changes. Further analysis of some other data may enhance this significance.

The changing ideal axis between each range of flexion for each implant may be of significance to a clinician as alignment of TKR's need to be optimized depending on each patient's needs. A patient that has a high level of activity will more likely have increased satisfaction with an implant that provides a higher degree of flexion (Willing & Kim, 2011). More significantly, wear tests that utilize only a single axis of rotation need to

consider the ideal axis based on their range of flexion. For example, the wear tests done in our lab conform to the standards for a walking cycle, and so only induce 60 degrees of flexion, therefore, it would be in our best interest to utilize the ideal axis for 60 degrees of rotation.

Figure 6.11 shows off the magnitude of the P/D displacements at each possible axis of rotation. Although it is difficult to note any significant differences in magnitude of P/D displacement due to the variations in the location of the minimal displacement, it can be seen that the CenterPulse Natural Knee® and the Wright Medical Advance® knee appear to have increased curvature around the entire implants. This may be due to a more constant radius of curvature within each component. Increased curvature in the graphs may also indicate a decreased tolerance for axis selection, as translating the axis would result in more significant displacements.

The next aspect of our study involved applying these ideal axes to the actual implants for proper alignment for simulation in the Instron Stanmore knee simulator. The radius (from the axis of rotation to the lowest point of contact on the femur) was found computationally for each implant at 0° and 90° flexion. Using the alignment jig (Figure 5.5) these femurs could be properly aligned and then P/D displacements could be measured in 10° increments. Table 6.1 illustrates these results with correlations in the data computed for each implant. For each implant the computed and measured data was found to be significantly correlated (>0.80), with similar P/D camming motions. It is interesting to note that between 0° and 60° flexion the Wright Medical implant, Stryker implant, and the Zimmer implant appear to approximately have a single radius (within



tolerance of 0.127 mm). The data is not exact between the computed and measured simulations because of the translation of the ideal axis into the actual simulation. Anterior/posterior alignment of the implant can only be done in 1 mm increments using metal spacers, and so this radius could not be perfectly replicated. However, this data is still very impressive, and acts not only as further verification of our computational model but also acts to satisfy our third aim. There now exists an exact method to align our femoral components before wear simulation that will allow for consistent results between varying implants. Not only this but utilizing the computational results the P/D motion that will be occurring can be characterized. This may allow for a greater understanding of wear patterns that occur in TKR simulations.

### *7.3 Relationship between P/D and A/P Translation on Varying Implants*

Because both proximal/distal and anterior/posterior displacement data is recorded along varying axes for multiple implants, a significant amount of analysis can be done. This section will discuss patterns that are recognized within P/D and A/P data between the various implants, and will also explore the relationship between P/D and A/P displacement.

The proximal/distal data is summarized in Table 6.2. This table lists the displacement at the ideal axis, as well as the mean displacements among the 10 lowest displacement axes (as seen in Figures 6.4-6.10), and then the standard deviation between these axes. This table presents a significant amount of data and so must be very carefully studied to recognize patterns.

It is of interest to study the data for 0°-60° flexion, because a few of the implants hold an approximate single-axis of rotation over this range. When looking at the minimal displacement at the ideal axis it appears as if the Natural Knee II, the Wright Medical knee, the Stryker knee, and the Zimmer knee are all very close to having a single radius in this flexion range. And when the standard deviation is considered for each of these knees, it is noted that the standard deviation is higher for all four of these knees compared to the others. In fact, there appears to be a clear pattern in that the implant with the highest P/D displacement at 60° (Biomet Maxim®) has the lowest standard deviation between each of the lowest 10 possible axes. When Figure 6.11 is considered the curvature of those graphs for the implants with a more constant radius of curvature would explain this pattern in standard deviations. This leads to the idea that although implants with a single radius have minimized P/D bearing migration at the ideal axis, there is less tolerance in the selection of axes, thus potentially resulting in a higher variability in performance of the implants depending on alignment. However, it is of note to indicate that within the 10 axis selection range the mean displacement is still lower for the implants with an approximate single axis than those with multiple axes. This would indicate that if P/D bearing migration is the most important factor in implant selection a single-axis implant would still be preferred.

As further consideration is given to the higher flexion ranges it is apparent that the Stryker Triathlon® Knee has the largest change between flexion ranges. The implant starts as a single-axis but then ends up having nearly 2 mm of P/D displacement at the ideal axis. Stryker describes this knee as a single-axis knee with a high-flexion axis

(“Primary Knee Systems - Triathlon Total Knee : Stryker,” n.d.). As Zelle et al described, the geometry of this implant is supposed to reduce polyethylene edge loading. The reason for this increased P/D displacement in the high flexion ranges may be due to the shape of the tibial inserts in high-flexion implants, as it is reported that modern high-flexion implants typically have an increased posteriorly beveled tibial insert (Bollars et al., n.d.). This sudden increase in P/D displacement can also be noted in the Wright Medical, Zimmer, and NKII implants, all designed as a single axis implant within the 0°-60° flexion ranges. These drastic changes in P/D displacement again are most likely due to tibial insert geometry, but this high conformity design could in theory increase shear forces on the femoral component encouraging implant loosening (Bollars et al., n.d.).

Table 6.3 can be considered to gain an understanding of the A/P displacements in our implants. It should first be noted that all numbers are only estimates with a tolerance of  $\pm 2$  mm due to the oscillations. Also, these migration numbers only tells us what is occurring in rotation about a single axis. Therefore, these exact numbers do not give significant understanding to A/P migration in multi-axis implants in vivo. Also, although the lowest point of contact can be measured, the mechanisms of motion (whether rotation, gliding, etc.) are unknown. However, for wear testing consideration these numbers may be of significant use. Because increased migration has the potential to be associated with wear, being able to quantify the migration of the implant and then compare it to the wear test results may allow for wear patterns to be addressed. Similarly, understanding this lowest contact-point motion and then comparing it to wear results may allow for a determination of the type of movement occurring. In Table 6.3 it can be seen

that at lower flexion ranges the single-axis implants have minimal A/P migration. Also, the high-flexion Stryker implant appears to have a significant change in A/P displacement similar to the change it exhibited in P/D displacement. No significant patterns were presented in the standard deviation data, perhaps due to the error range. Therefore, when a single-axis method is being used to test these implants, the single-axis designs may exhibit the least amount of A/P migration at lower flexion ranges (such as the walking cycle), but as the flexion range increases the difference in A/P migration is reduced.

The next aspect of A/P migration that should be considered is the migration identified for each implant at the ideal axes for both 60° and 120° flexion. Although these displacements are not an accurate measure of in vivo displacement, they can be further used for testing relying on single axis purposes and can also be compared to one another for noted patterns. As displayed in Figure 6.12 axis selection for single axis testing purposes can have significant effects on A/P displacement. This figure shows when the ideal axis for 60° of flexion is selected, motion beyond 60° results in anterior displacement of the lowest contact point. This indicates that no femoral rollback would occur in this simulation, which may skew wear results. When the ideal axis for 120° flexion is considered, posterior translation of the lowest contact point is noted to an extent. Therefore, if posterior femoral rollback is a significant consideration in the wear results, axis selection should perhaps be altered to induce this ideal posterior translation, rather than minimize P/D camming. When studying the results of all implants (Figures B.1-B.6), similar patterns are noted. Furthermore, when these implants are compared to each other, it can be noted that in the femoral components that have multiple axes of

rotation throughout the entire flexion range, A/P displacement patterns are affected less by axis selection. Therefore, this may indicate that implants with a more constant changing radius of curvature have a higher tolerance to alignment error in regards to A/P displacement patterns.

#### *7.4 Future Research*

This study demonstrated a few obvious limitations that future research should seek to address. A 3D scanner with higher tolerances should be used to eliminate the bumpy femoral component surface. This step could give greater accuracy in these experimental results, as well as any other future computational testing.

In order to gain a greater understanding of in vivo conditions for anterior/posterior displacement, a simulation should be developed where rotation is applied along the geometry of the implant. Although this would take away from the usefulness for wear testing, it would complement the understanding gained of the proximal/distal motion in implants. Also, it would be of great interest to quantify the effect that altered axis of rotation has on femoral rollback. Because femoral rollback is directly related to the extensor mechanism, it could be possible to quantify the increased quadriceps force required when a femoral rotation axis is used that decreases femoral rollback.

Another aspect that could be addressed is the articulation of the femoral component on the tibial component. This could be tested for both in vivo kinematics and wear simulator kinematics. Because in vivo kinematics are difficult to define it may be more feasible to apply the measured kinematics of the knee simulator into a

computational model to observe the movement of the lowest contact point on the tibial surface. This may give extremely useful insight into observed wear patterns in the simulations. There would also be potential to take this a step further and determine contact pressures that result because of the applied kinematics.

## CHAPTER EIGHT: CONCLUSIONS

Based on the results of this study it can be statistically concluded that a 3D scanned model can be created and used to computationally simulate rotation in femoral knee components. These results could then be used to ideally align femoral components for minimized proximal/distal bearing migration for knee wear simulation both reliably and consistently.

For multi-axis knee designs, ideal alignment to reduce P/D displacement for single-axis rotation purposes is dependent on the range of flexion, with the ideal axis located orthogonally and moving posteriorly as that flexion range increases. Single-axis knee designs were found to have a lower tolerance to varied femoral axis selection, however, still exhibited lower mean proximal/distal displacements than multi-axis designs. Also, implants designed for high-flexion exhibited more proximal/distal displacement than any other design at the ideal flexion axes for the largest range of flexion. Anterior/posterior displacement patterns in single-axis rotation simulations were found to be inconsistent with ideal in vivo kinematics. If femoral rollback is the most significant factor being tested, it may be beneficial to align the implants based on A/P migration instead of P/D displacement. Also, A/P displacement patterns in implants with multiple axes of rotation are affected less by the femoral axis selection.

It is imperative to understand the factors being tested in single-axis wear simulations, and align the knee implants accordingly. This study clearly showed that alignment of the femoral axis affects both proximal/distal and anterior/posterior migration.

## CHAPTER NINE: APPENDICES



## Appendix A

### Model Verification

15.00	14.50	13.13	13.03	12.97	12.50	11.98	11.50	11.00	10.50	9.99	9.50	8.99	8.50	7.99	7.50	7.00	6.50	6.05	5.61
14.10	13.59	12.85	12.67	12.13	11.57	11.13	10.63	10.03	9.62	9.13	8.63	8.13	7.63	7.13	6.62	6.12	5.65	5.22	5.10
13.26	12.71	12.26	11.76	11.42	10.20	10.27	9.76	9.26	8.76	8.26	7.76	7.26	6.45	6.00	5.55	5.21	4.81	4.59	4.58
12.39	11.88	11.40	10.52	10.37	9.32	9.27	8.86	8.34	7.90	6.99	6.88	6.39	5.89	5.52	5.01	4.44	4.21	4.06	3.91
11.54	11.01	10.53	10.03	9.32	9.12	8.54	8.03	7.42	7.03	6.53	6.03	5.53	4.99	4.52	4.06	3.81	3.69	3.53	3.17
10.67	10.14	9.62	9.14	8.66	8.17	7.26	7.18	6.67	6.04	5.61	5.16	4.66	4.16	3.67	3.42	3.31	3.12	3.00	2.85
9.80	8.58	8.80	8.30	8.10	7.07	6.86	6.33	5.80	5.30	4.66	4.23	3.80	3.29	2.91	2.93	2.78	2.67	2.91	3.34
8.28	8.44	7.93	7.43	6.85	6.29	5.94	5.44	4.87	4.44	3.94	3.33	2.92	2.71	2.55	2.49	2.68	3.10	3.49	4.38
8.04	7.57	7.06	6.56	6.05	5.57	5.11	4.66	4.14	3.56	3.06	2.57	2.34	2.31	2.45	2.87	3.30	3.72	4.15	4.58
7.20	6.70	5.56	5.68	5.19	4.70	4.31	3.71	3.12	2.74	2.20	2.15	2.52	2.63	3.19	3.47	3.90	4.63	4.76	5.17
6.33	5.86	5.20	4.86	4.34	2.71	3.48	2.84	2.08	1.98	1.99	2.37	2.76	3.21	3.68	4.29	4.51	4.94	5.39	5.73
5.47	4.99	4.34	3.81	3.48	3.04	2.47	2.03	1.82	2.18	2.56	2.96	3.41	3.61	4.26	4.81	5.31	5.63	5.99	6.43
4.63	4.11	3.11	3.17	2.68	3.41	2.34	1.99	2.35	2.96	3.19	3.67	4.01	4.42	4.90	5.31	5.74	6.29	6.61	7.00
3.90	4.45	3.01	2.65	2.29	3.00	2.22	2.55	3.11	3.49	3.67	4.19	4.56	5.04	5.39	5.88	6.36	6.84	7.29	7.73
3.55	2.99	2.60	2.15	2.17	2.74	3.22	3.44	3.61	4.01	4.31	4.88	5.35	5.66	6.25	6.70	7.16	7.63	8.88	8.53
2.81	2.57	2.24	2.45	2.90	4.39	3.71	3.89	4.33	4.50	5.14	5.62	6.15	6.59	6.96	7.50	7.84	8.40	8.86	9.39
2.61	2.54	2.84	3.11	3.42	3.87	5.45	4.67	5.12	5.63	6.02	6.65	6.88	7.37	7.88	8.28	8.73	9.19	9.65	10.03
3.35	3.28	3.43	3.78	4.21	4.59	5.13	6.80	6.81	6.23	6.78	7.50	7.71	8.15	8.61	8.76	9.52	9.99	10.44	10.89
3.57	3.78	4.53	4.55	4.94	5.30	5.81	7.34	6.27	7.14	7.54	8.29	9.15	8.87	9.36	9.86	10.34	10.75	11.23	11.67
4.15	4.48	5.16	5.28	5.68	6.02	6.45	7.01	7.48	7.71	8.14	8.84	9.29	9.74	10.20	10.67	11.09	11.58	12.00	12.40

**Figure A.1:** A/P displacement of Wright Medical Advance® Knee System between 0° - 60° flexion with ideal axis highlighted.

4.15	3.44	2.79	2.17	1.64	1.89	2.29	2.84	3.47	4.20	5.03	5.86	6.74	7.60	8.47	9.33	10.19	11.06	11.91	12.80
4.59	3.69	3.01	2.35	1.79	1.44	1.85	2.38	3.03	3.71	4.50	5.35	6.22	7.08	7.94	8.81	9.70	10.54	11.40	12.30
4.79	4.03	3.44	2.59	1.96	1.41	1.44	1.92	2.51	3.20	4.01	4.86	5.72	6.64	7.51	8.38	9.21	10.05	10.92	11.79
5.21	4.39	3.62	2.88	2.19	1.57	1.13	1.49	2.05	2.71	3.48	4.43	5.24	6.11	7.08	8.11	8.69	9.68	10.42	11.28
5.63	4.81	3.99	3.43	2.46	1.79	1.18	1.27	1.58	2.21	2.98	3.86	4.73	5.58	6.47	7.34	8.19	8.92	10.37	10.79
6.14	5.29	4.43	3.59	2.78	2.00	1.36	0.80	1.13	1.73	2.51	3.33	4.24	5.09	5.95	6.81	7.70	8.55	9.63	10.29
6.63	5.87	4.93	4.06	3.21	2.45	1.67	0.97	0.69	1.26	2.00	2.86	3.71	4.56	5.47	6.31	7.18	8.05	8.92	9.79
7.23	6.29	5.43	4.55	3.71	2.86	1.99	1.22	0.57	0.78	1.50	2.43	3.21	4.08	4.94	5.82	6.68	7.54	8.22	9.21
7.85	6.81	5.94	5.05	4.19	3.33	2.44	1.79	0.85	0.33	1.01	1.86	2.64	3.59	4.46	5.27	6.14	7.06	7.93	8.79
8.16	7.30	6.54	5.55	4.70	3.83	3.01	2.10	1.23	0.42	0.47	1.34	2.41	2.99	4.05	4.82	5.67	6.56	7.37	8.29
8.64	7.76	7.02	6.06	5.19	4.46	3.41	2.60	1.74	0.89	0.09	0.86	1.69	2.57	3.43	4.45	5.15	6.04	6.88	7.85
9.14	8.26	7.53	6.64	5.68	4.85	3.96	2.86	2.25	1.37	0.54	0.45	1.22	2.13	2.96	3.29	4.79	5.68	6.41	7.29
9.64	8.80	7.97	7.04	6.19	5.32	4.74	3.61	2.69	1.88	1.01	0.33	0.86	1.67	2.46	3.31	4.19	4.82	5.93	6.80
10.16	9.29	8.55	7.56	6.70	6.15	4.95	4.11	3.52	2.29	1.61	0.87	0.63	2.36	2.42	2.78	3.68	4.58	5.34	6.30
11.16	9.81	8.92	8.09	7.18	6.33	5.74	4.49	3.65	2.87	2.09	1.25	0.78	1.04	1.69	2.42	5.56	4.06	5.25	5.79
11.25	10.30	9.47	8.56	7.69	7.06	6.01	5.10	4.35	3.66	2.56	1.80	1.22	0.82	1.44	2.11	2.83	3.58	4.42	5.28
11.63	10.80	9.92	9.07	8.41	7.08	6.87	5.58	5.40	3.91	3.00	2.33	1.74	1.15	1.24	4.58	2.62	3.51	4.01	4.82
12.15	11.29	10.42	9.55	8.69	7.84	7.06	6.59	5.24	4.48	3.46	2.70	2.00	1.56	1.14	1.64	2.25	3.24	4.04	4.41
12.65	11.77	10.96	10.06	9.19	8.29	7.47	6.60	5.92	4.87	3.90	3.17	2.55	2.00	1.47	1.48	2.73	2.68	3.34	4.05
13.15	12.39	11.92	10.55	9.85	8.88	8.63	7.09	6.23	5.49	4.66	3.67	5.27	2.46	1.84	1.58	1.78	2.38	3.07	3.77

**Figure A.2:** P/d displacement of Wright Medical Advance® Knee System between 0° - 60° flexion with ideal axis highlighted.

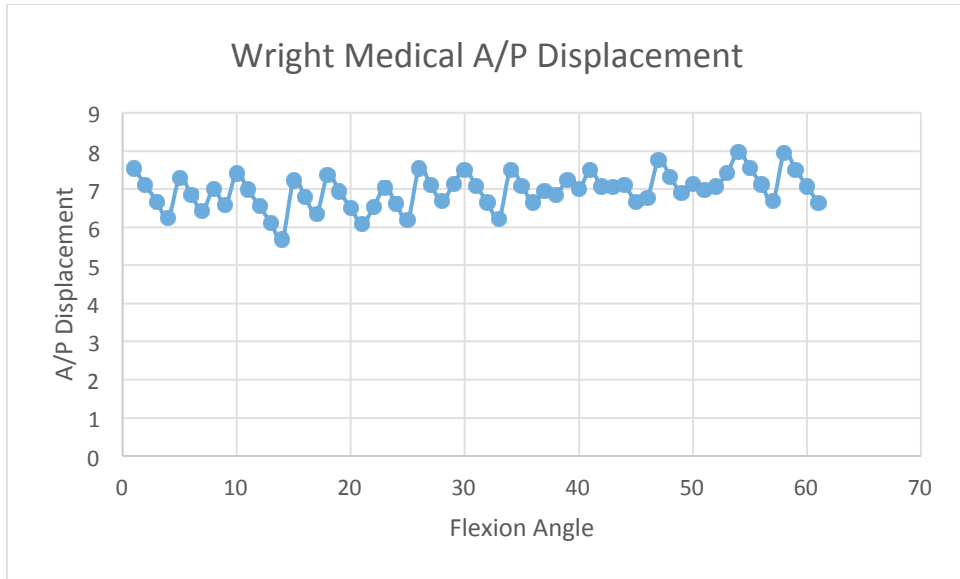


**Figure A.3:** A/P Displacement at ideal femoral axis between 0° - 60° flexion for Wright Medical Advance® Knee System.

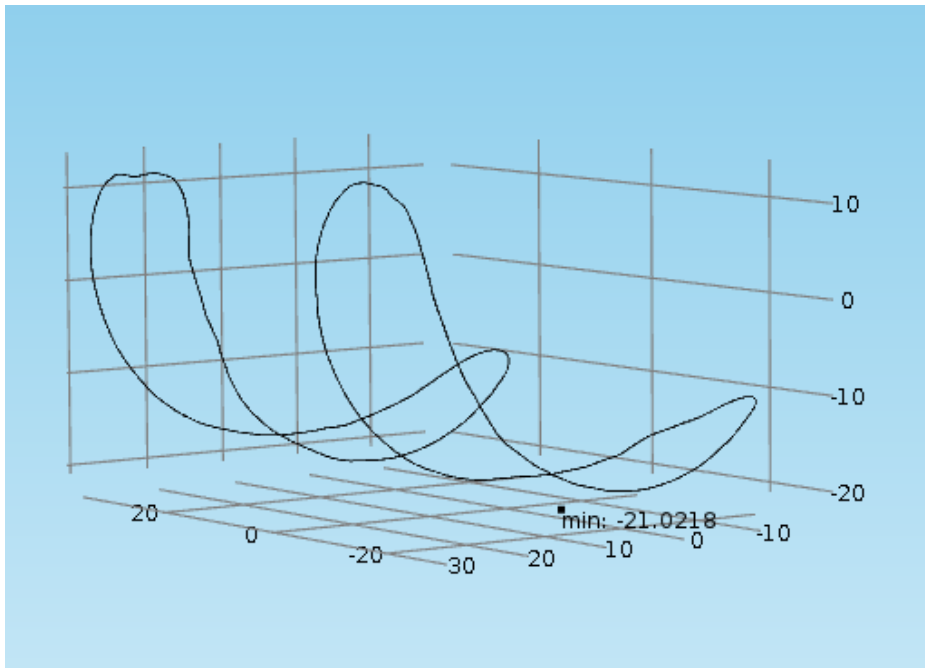


**Figure A.4:** Point of lowest contact in reference to knee geometry at 0° flexion. This can be plotted at each degree of flexion to recognize patterns.

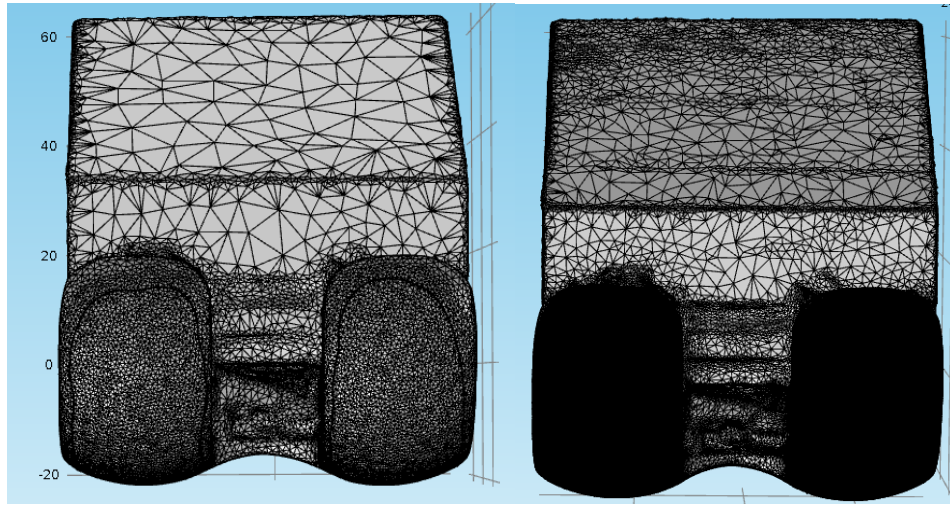


**Figure A.5:** Two meshes created in order to determine if bumpy surface was a result of mesh creation. The 3Matic recommended mesh is pictured on the left, with the mesh 10 times as fine pictured on the right.

Appendix B

A/P Displacement

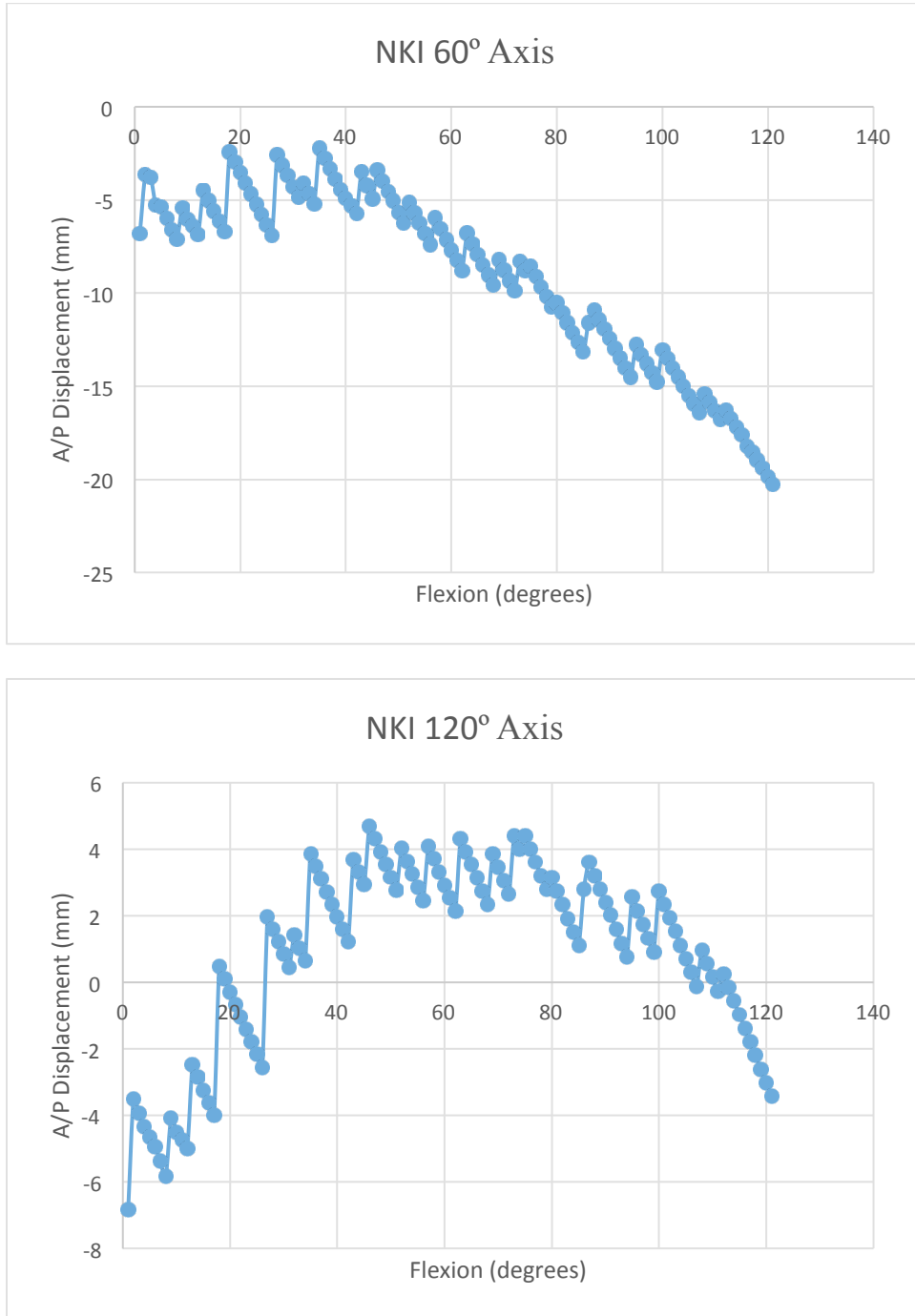


**Figure B.1:** A/P displacement of NKI at ideal axes for 60 and 120 degrees flexion.

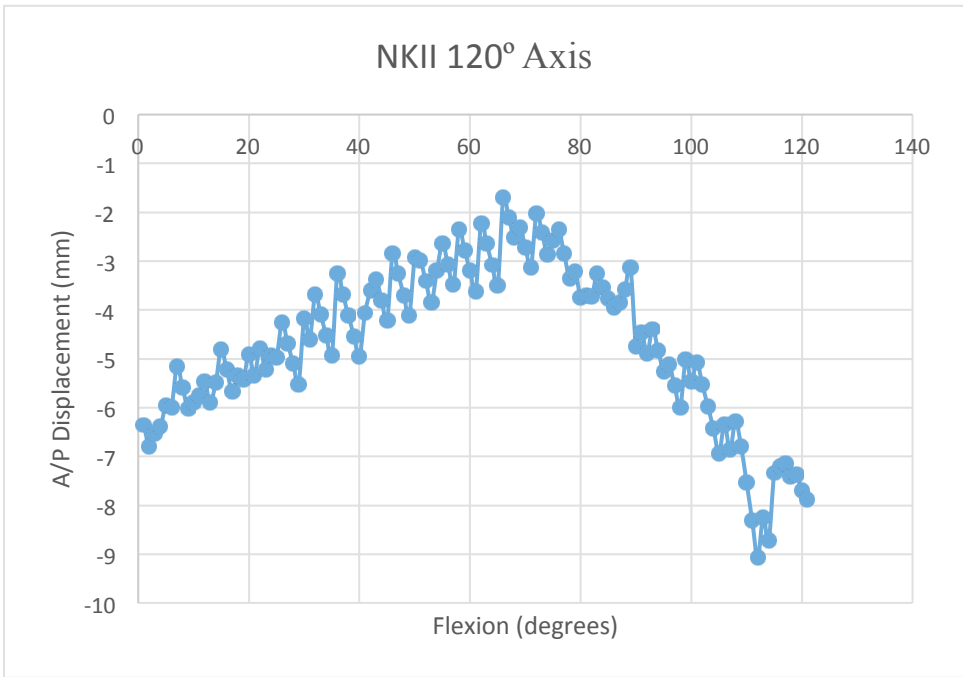
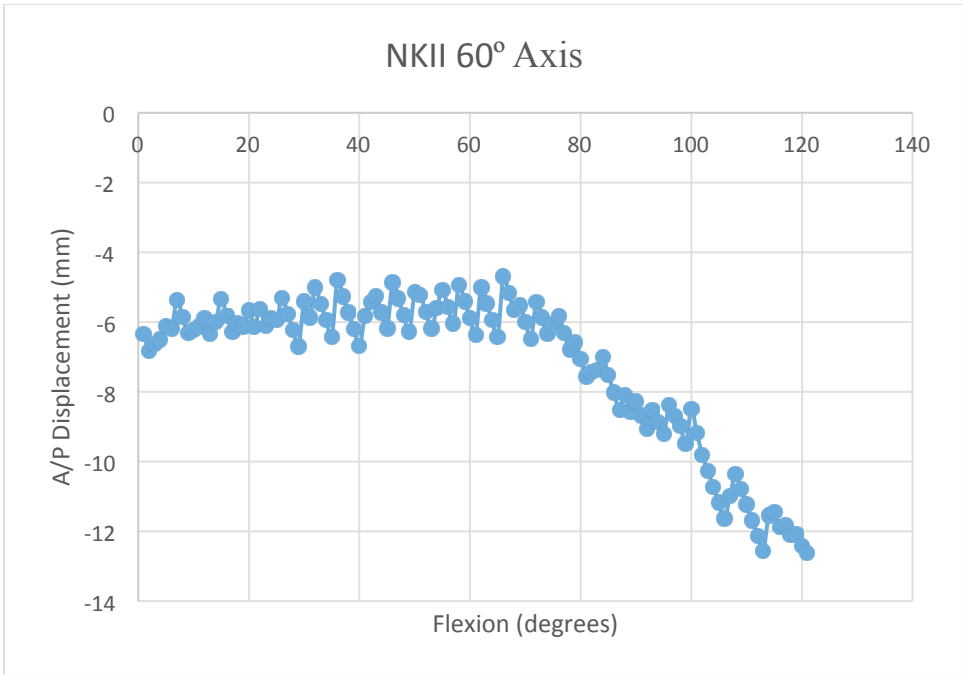


**Figure B.2:** A/P displacement of NKII at ideal axes for 60 and 120 degrees flexion.

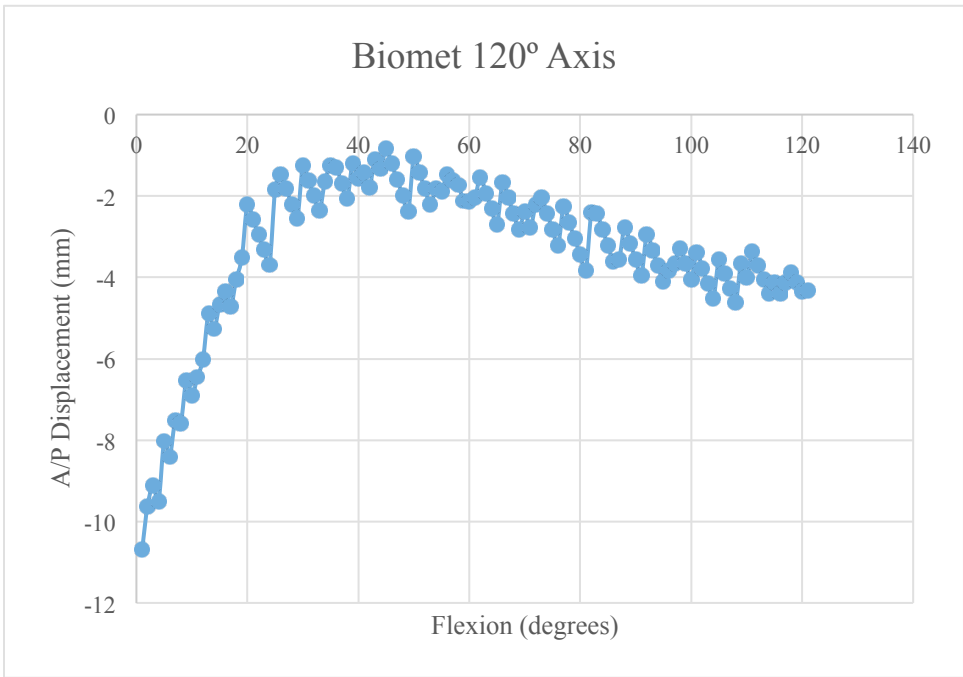
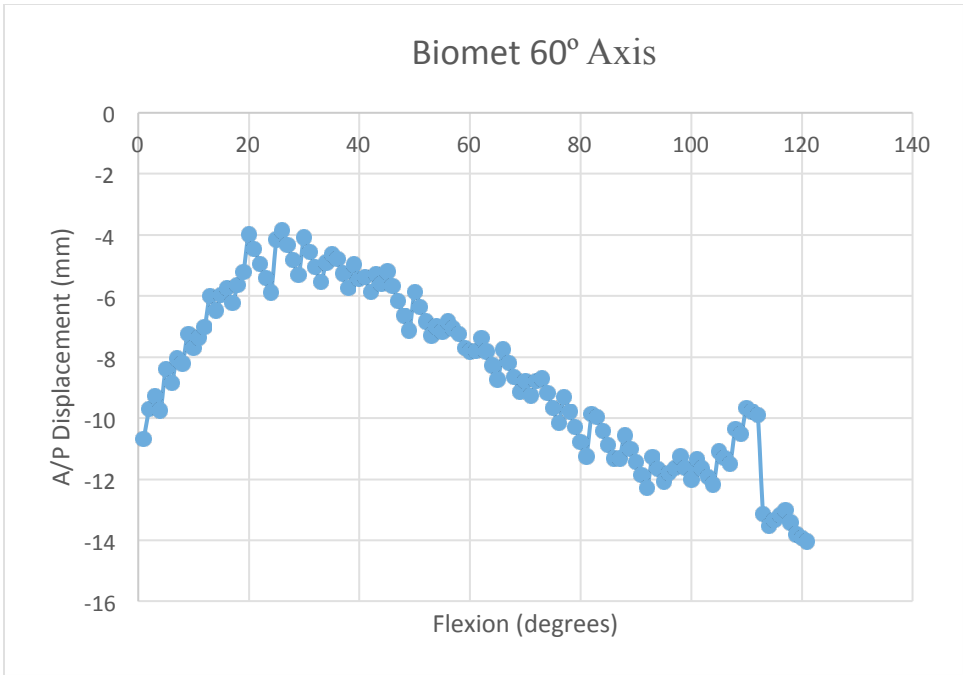


**Figure B.3:** A/P displacement of Biomet Maxim® at ideal axes for 60 and 120 degrees flexion.

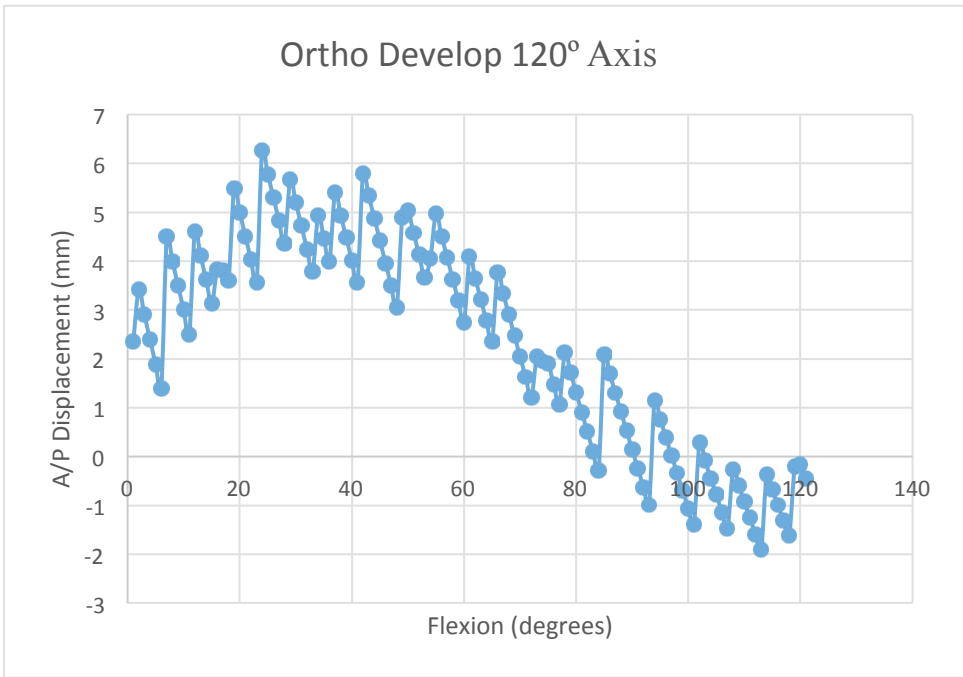
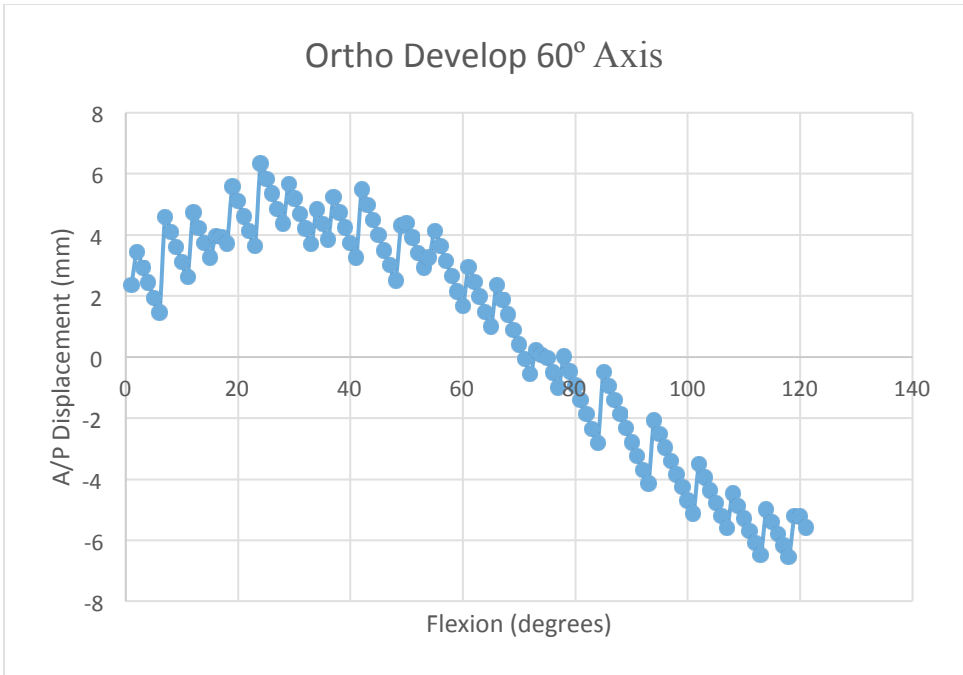


**Figure B.4:** A/P displacement of Ortho Development knee at ideal axes for 60 and 120 degrees flexion.



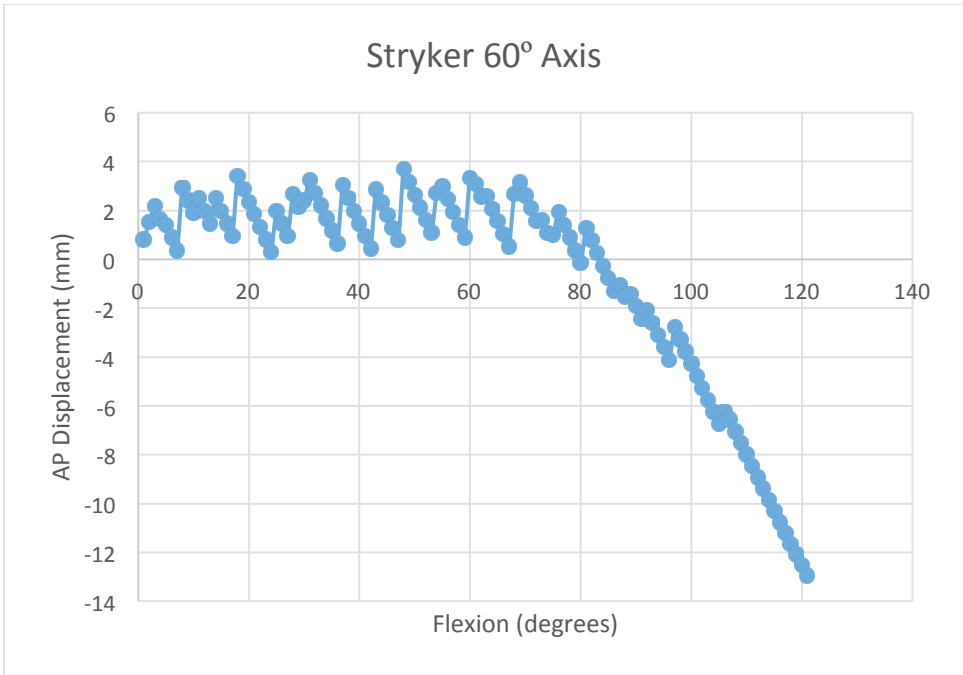


**Figure B.5:** A/P displacement of Stryker Triathlon® at ideal axes for 60 and 120 degrees flexion.

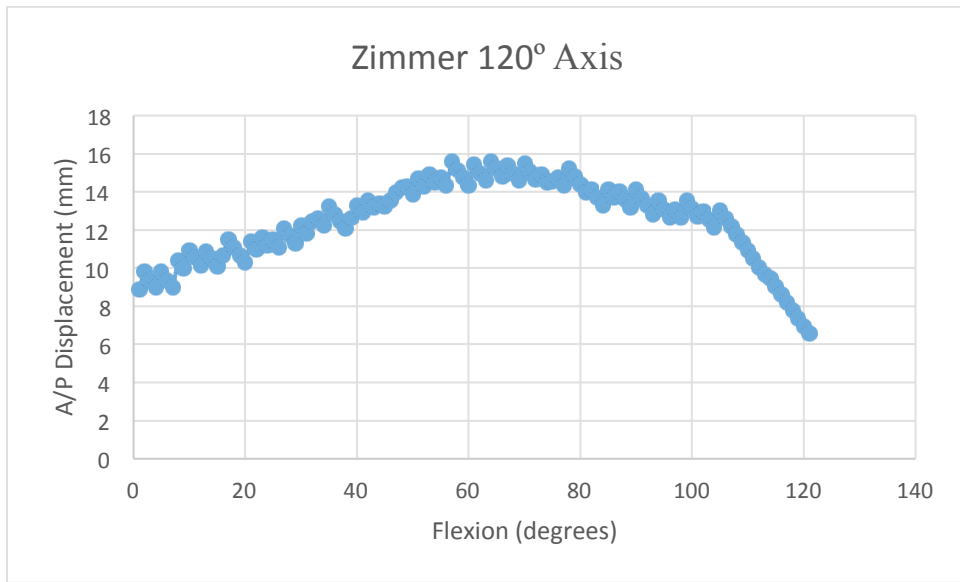
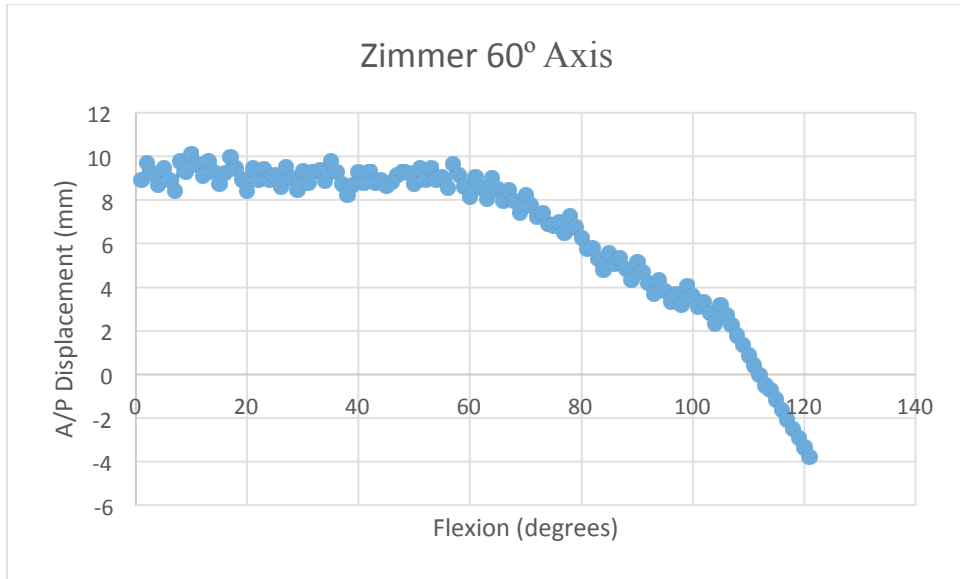


**Figure B.6:** A/P displacement of Zimmer Knee at ideal axes for 60 and 120 degrees flexion.

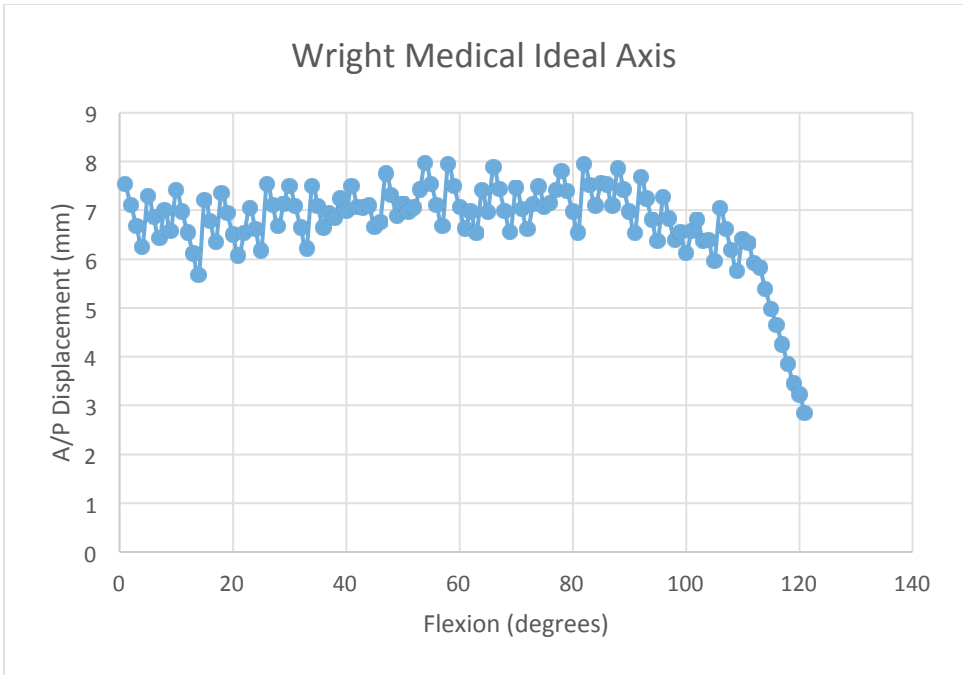


**Figure B.7:** A/P displacement of Wright Medical knee at ideal axis of flexion (same for all ranges).

## CHAPTER TEN: REFERENCES

- Abdel, M. P. (2011). Increased Long-Term Survival of Posterior Cruciate-Retaining Versus Posterior Cruciate-Stabilizing Total Knee Replacements. *The Journal of Bone and Joint Surgery*. <http://doi.org/10.2106/JBJS.J.01143>
- Abdelgaied, A., Liu, F., Brockett, C., Jennings, L., Fisher, J., & Jin, Z. (2011). Computational wear prediction of artificial knee joints based on a new wear law and formulation. *Journal of Biomechanics*, 44(6), 1108–1116. <http://doi.org/10.1016/j.jbiomech.2011.01.027>
- Asano, T., Akagi, M., Tanaka, K., Tamura, J., & Nakamura, T. (2001). In vivo three-dimensional knee kinematics using a biplanar image-matching technique. *Clinical Orthopaedics and Related Research*, (388), 157–166. <http://doi.org/10.1097/00003086-200107000-00023>
- ASTM F1715 - 00 Standard Guide for Wear Assessment of Prosthetic Knee Designs in Simulator Devices. (2006). Retrieved June 23, 2015, from <http://www.astm.org/DATABASE.CART/HISTORICAL/F1715-00.htm>
- ASTM F2083-12, Standard Specification for Knee Replacement Prosthesis. (2012). *ASTM International*. Retrieved from <http://www.astm.org/Standards/F2083.htm>
- Banks, S., Bellemans, J., Nozaki, H., Whiteside, L. A., Harman, M., & Hodge, W. A. (2003). Knee motions during maximum flexion in fixed and mobile-bearing arthroplasties. *Clinical Orthopaedics and Related Research*, (410), 131–138. <http://doi.org/10.1097/01.blo.0000063121.39522.19>
- Bargren, J. H., Blaha, J. D., & Freeman, M. A. (1983). Alignment in total knee arthroplasty. Correlated biomechanical and clinical observations. *Clinical Orthopaedics and Related Research*, (173), 178–183.
- Barrack, R. L. (2001). Evolution of the rotating hinge for complex total knee arthroplasty. *Clinical Orthopaedics and Related Research*, (392), 292–299.
- Bellemans, J., Vandenuecker, H., & Vanlauwe, J. (2005). (iv) Total knee replacement. In *Current Orthopaedics* (Vol. 19, pp. 446–452). <http://doi.org/10.1016/j.cuor.2005.09.007>
- Bert, J. M. (2005). Unicompartmental knee replacement. *The Orthopedic Clinics of North America*, 36(4), 513–522. <http://doi.org/10.1016/j.ocl.2005.05.001>

- Beynnon, B. D., Johnson, R. J., Abate, J. A., Fleming, B. C., & Nichols, C. E. (2005). Treatment of anterior cruciate ligament injuries, part I. *The American Journal of Sports Medicine*, 33(10), 1579–1602. <http://doi.org/10.1177/0363546505279913>
- BIOMET. (n.d.). AGC Total Knee System.
- Blackburn, T. A., & Craig, E. (1980). Knee anatomy: a brief review. *Physical Therapy*, 60(12), 1556–1560.
- Blaha, J. D., Mancinelli, C. A., Simons, W. H., Kish, V. L., & Thyagarajan, G. (2003). Kinematics of the human knee using an open chain cadaver model. *Clinical Orthopaedics and Related Research*, (410), 25–34. <http://doi.org/10.1097/01.blo.0000063564.90853.ed>
- Bollars, P., Surgeon, O., Innocenti, B., Kinematics, N., Labey, L., Kinematics, E., ... Orthopaedics, N. (n.d.). Femoral component loosening in high- flexion total knee replacement.
- Borus, T., & Thornhill, T. (2008). Unicompartmental knee arthroplasty. *The Journal of the American Academy of Orthopaedic Surgeons*, 16(1), 9–18.
- Browne, C., Hermida, J. C., Bergula, A., Colwell, C. W., & D'Lima, D. D. (2005). Patellofemoral forces after total knee arthroplasty: Effect of extensor moment arm. *Knee*, 12(2), 81–88. <http://doi.org/10.1016/j.knee.2004.05.006>
- Chan, K. Y., & Teo, Y. H. (2012). Patient-specific instrumentation for total knee replacement verified by computer navigation: a case report. *Journal of Orthopaedic Surgery (Hong Kong)*, 20(1), 111–4. Retrieved from <http://www.ncbi.nlm.nih.gov/pubmed/22535825>
- Chandran, N., Amirouche, F., Gonzalez, M. H., Hilton, K. M., Barmada, R., & Goldstein, W. (2009). Optimisation of the posterior stabilised tibial post for greater femoral rollback after total knee arthroplasty-a finite element analysis. *International Orthopaedics*, 33(3), 687–693. <http://doi.org/10.1007/s00264-008-0566-3>
- Churchill, D. L., Incavo, S. J., Johnson, C. C., & Beynnon, B. D. (1998). The transepicondylar axis approximates the optimal flexion axis of the knee. *Clinical Orthopaedics and Related Research*, (356), 111–118.
- Churchill, D. L., Incavo, S. J., Johnson, C. C., & Beynnon, B. D. (2001). The influence of femoral rollback on patellofemoral contact loads in total knee arthroplasty. *The Journal of Arthroplasty*, 16(7), 909–918. <http://doi.org/10.1054/arth.2001.24445>

- Clark, C. R., Rorabeck, C. H., MacDonald, S., MacDonald, D., Swafford, J., & Cleland, D. (2001). *Posterior-stabilized and cruciate-retaining total knee replacement: a randomized study. Clinical orthopaedics and related research.*
- Collado, H., & Fredericson, M. (2010). Patellofemoral pain syndrome. *Clinics in Sports Medicine.* <http://doi.org/10.1016/j.csm.2010.03.012>
- COMSOL. (n.d.). Multiphysics Simulation Software - Platform for Physics-Based Modeling. Retrieved June 24, 2015, from <https://www.comsol.com/comsol-multiphysics>
- Daines, B. K., & Dennis, D. A. (2014). Gap balancing vs. measured resection technique in total knee arthroplasty. *Clinics in Orthopedic Surgery, 6*(1), 1–8. <http://doi.org/10.4055/cios.2014.6.1.1>
- Das, S. K., & Farooqi, A. (2008). Osteoarthritis. *Best Practice & Research. Clinical Rheumatology, 22*(4), 657–675. <http://doi.org/10.1016/j.berh.2008.07.002>
- Dean, S., Haider, H., Walker, P., DesJardins, J., & Blunn, G. (2006). Effects of Patient and Surgical Alignment Variables on Kinematics in TKR Simulation Under Force-Control. *Journal of ASTM International.* <http://doi.org/10.1520/JAI100248>
- Dennis, D. A., Komistek, R. D., Scuderi, G. R., & Zingde, S. (2007). Factors affecting flexion after total knee arthroplasty. *Clinical Orthopaedics and Related Research, 464*, 53–60. <http://doi.org/10.1097/BLO.0b013e31812f785d>
- Dennis, D. A., Komistek, R. D., Stiehl, J. B., Walker, S. A., & Dennis, K. N. (1998). Range of motion after total knee arthroplasty: The effect of implant design and weight-bearing conditions. *Journal of Arthroplasty, 13*(7), 748–752. [http://doi.org/10.1016/S0883-5403\(98\)90025-0](http://doi.org/10.1016/S0883-5403(98)90025-0)
- Dennis, D. A., Mahfouz, M. R., Komistek, R. D., & Hoff, W. (2005). In vivo determination of normal and anterior cruciate ligament-deficient knee kinematics. *Journal of Biomechanics, 38*(2), 241–253. <http://doi.org/10.1016/j.jbiomech.2004.02.042>
- DesJardins, J. D., Banks, S. A., Benson, L. C., Pace, T., & LaBerge, M. (2007). A direct comparison of patient and force-controlled simulator total knee replacement kinematics. *Journal of Biomechanics, 40*(15), 3458–3466. <http://doi.org/10.1016/j.jbiomech.2007.05.022>

- DesJardins, J. D., Walker, P. S., Haider, H., & Perry, J. (2000). The use of a force-controlled dynamic knee simulator to quantify the mechanical performance of total knee replacement designs during functional activity. *Journal of Biomechanics*, 33(10), 1231–1242. [http://doi.org/10.1016/S0021-9290\(00\)00094-4](http://doi.org/10.1016/S0021-9290(00)00094-4)
- DesJardins, J., & Rusly, R. (2011). Single flexion-axis selection influences femoral component alignment and kinematics during knee simulation. *Proceedings of the Institution of Mechanical Engineers, Part H: Journal of Engineering in Medicine*, 225(8), 762–768. <http://doi.org/10.1177/0954411911400534>
- Draganich, L. F., Andriacchi, T. P., & Andersson, G. B. (1987). Interaction between intrinsic knee mechanics and the knee extensor mechanism. *Journal of Orthopaedic Research : Official Publication of the Orthopaedic Research Society*, 5(4), 539–547. <http://doi.org/10.1002/jor.1100050409>
- Duthon, V. B., Barea, C., Abrassart, S., Fasel, J. H., Fritschy, D., & Ménétrey, J. (2006). Anatomy of the anterior cruciate ligament. *Knee Surgery, Sports Traumatology, Arthroscopy : Official Journal of the ESSKA*, 14(3), 204–213. <http://doi.org/10.1007/s00167-005-0679-9>
- Espregueira-Mendes, & Vieira Da Silva, M. (2006). Anatomy of the lateral collateral ligament: A cadaver and histological study. *Knee Surgery, Sports Traumatology, Arthroscopy*, 14(3), 221–228. <http://doi.org/10.1007/s00167-005-0681-2>
- Fagan, V., & Delahunt, E. (2008). Patellofemoral pain syndrome: a review on the associated neuromuscular deficits and current treatment options. *British Journal of Sports Medicine*, 42(10), 789–795. <http://doi.org/10.1136/bjsm.2008.046623>
- Fantozzi, S., Catani, F., Ensini, A., Leardini, A., & Giannini, S. (2006). Femoral rollback of cruciate-retaining and posterior-stabilized total knee replacements: In vivo fluoroscopic analysis during activities of daily living. *Journal of Orthopaedic Research*, 24(12), 2222–2229. <http://doi.org/10.1002/jor.20306>
- Flandry, F., & Hommel, G. (2011). Normal anatomy and biomechanics of the knee. *Sports Medicine and Arthroscopy Review*, 19(2), 82–92. <http://doi.org/10.1097/JSA.0b013e318210c0aa>
- Freeman, M. A., & Railton, G. T. Should the posterior cruciate ligament be retained or resected in condylar nonmeniscal knee arthroplasty? The case for resection., 3 Suppl The Journal of arthroplasty S3–S12 (1988). [http://doi.org/10.1016/S0883-5403\(88\)80002-0](http://doi.org/10.1016/S0883-5403(88)80002-0)

- Fregly, B. J., Marquez-Barrientos, C., Banks, S. A., & DesJardins, J. D. (2010). Increased conformity offers diminishing returns for reducing total knee replacement wear. *Journal of Biomechanical Engineering*, *132*(2), 021007. <http://doi.org/10.1115/1.4000868>
- Fuchs, S., Tibesku, C. O., Genkinger, M., Volmer, M., Laaß, H., & Rosenbaum, D. (2004). Clinical and functional comparison of bicondylar sledge prostheses retaining all ligaments and constrained total knee replacement. *Clinical Biomechanics*, *19*(3), 263–269. <http://doi.org/10.1016/j.clinbiomech.2003.11.004>
- Ghosh, K. M., Merican, A. M., Iranpour, F., Deehan, D. J., & Amis, A. A. (2012). Length-change patterns of the collateral ligaments after total knee arthroplasty. *Knee Surgery, Sports Traumatology, Arthroscopy*, *20*(7), 1349–1356. <http://doi.org/10.1007/s00167-011-1824-2>
- Godest, A. C., Beaugonin, M., Haug, E., Taylor, M., & Gregson, P. J. (2002). Simulation of a knee joint replacement during a gait cycle using explicit finite element analysis. *Journal of Biomechanics*, *35*(2), 267–275. [http://doi.org/10.1016/S0021-9290\(01\)00179-8](http://doi.org/10.1016/S0021-9290(01)00179-8)
- Goldblatt, J. P., & Richmond, J. C. (2003). Anatomy and biomechanics of the knee. *Operative Techniques in Sports Medicine*. <http://doi.org/10.1053/otsm.2003.35911>
- Goldring, M. B., & Goldring, S. R. (2007). Osteoarthritis. *Journal of Cellular Physiology*. <http://doi.org/10.1002/jcp.21258>
- Gunston, F. H. (1971). Polycentric knee arthroplasty. Prosthetic simulation of normal knee movement. *The Journal of Bone and Joint Surgery. British Volume*, *53*(2), 272–277. <http://doi.org/10.1097/01.blo.0000214423.59829.04>
- Haas, B. D. (2006). Tibial post impingement in posterior-stabilized total knee arthroplasty. *Orthopedics*, *29*(9 Suppl), S83–S85.
- Harman, M. K., Desjardins, J., Benson, L., Banks, S. A., Laberge, M., & Hodge, W. A. (2009). Comparison of polyethylene tibial insert damage from in vivo Function and in vitro wear simulation. *Journal of Orthopaedic Research*, *27*(4), 540–548. <http://doi.org/10.1002/jor.20743>
- Health, C. for D. and R. (2003). Search for FDA Guidance Documents - Class II Special Controls Guidance Document: Knee Joint Patellofemorotibial and Femorotibial Metal/Polymer Porous-Coated Uncemented Prostheses; Guidance for Industry and FDA. Center for Devices and Radiological Health. Retrieved from <http://www.fda.gov/RegulatoryInformation/Guidances/ucm072714.htm>



- Hernández-Vaquero, D., & Sandoval-García, M. A. (2010). Hinged total knee arthroplasty in the presence of ligamentous deficiency. In *Clinical Orthopaedics and Related Research* (Vol. 468, pp. 1248–1253). <http://doi.org/10.1007/s11999-009-1226-7>
- Heyse, T. J., El-Zayat, B. F., De Corte, R., Chevalier, Y., Scheys, L., Innocenti, B., ... Labey, L. (2014). UKA closely preserves natural knee kinematics in vitro. *Knee Surgery, Sports Traumatology, Arthroscopy*, 22(8), 1902–1910. <http://doi.org/10.1007/s00167-013-2752-0>
- Heyse, T. J., Khefacha, A., Peersman, G., & Cartier, P. (2012). Survivorship of UKA in the middle-aged. *Knee*, 19(5), 585–591. <http://doi.org/10.1016/j.knee.2011.09.002>
- Hoffart, H.-E., Langenstein, E., & Vasak, N. (2012). A prospective study comparing the functional outcome of computer-assisted and conventional total knee replacement. *The Journal of Bone and Joint Surgery. British Volume*, 94(2), 194–9. <http://doi.org/10.1302/0301-620X.94B2.27454>
- Hollister, A. M., Jatana, S., Singh, A. K., Sullivan, W. W., & Lupichuk, A. G. (1993). The axes of rotation of the knee. *Clinical Orthopaedics and Related Research*, (290), 259–268.
- Huang, C.-H., Liao, J.-J., & Cheng, C.-K. (2007). Fixed or mobile-bearing total knee arthroplasty. *Journal of Orthopaedic Surgery and Research*, 2, 1. <http://doi.org/10.1186/1749-799X-2-1>
- Hungerford, D. S. (1995). Alignment in total knee replacement. *Instructional Course Lectures*, 44, 455–468. <http://doi.org/10.1302/0301-620X.90B9.20793>
- Instron. (n.d.). BiomedicalBrochure. Retrieved June 24, 2015, from <http://www.inteszt.hu/PDF/01/BiomedicalBrochure.pdf>
- Jacobs, W., Anderson, P., Limbeek, J., & Wymenga, A. (2004). Mobile bearing vs fixed bearing prostheses for total knee arthroplasty for post-operative functional status in patients with osteoarthritis and rheumatoid arthritis. *Cochrane Database of Systematic Reviews (Online)*, (2), CD003130. <http://doi.org/10.1002/14651858.CD003130.pub2>
- Jacobs, W. C. H., Christen, B., Wymenga, A. B., Schuster, A., van der Schaaf, D. B., ten Ham, A., & Wehrli, U. (2012). Functional performance of mobile versus fixed bearing total knee prostheses: a randomised controlled trial. *Knee Surgery, Sports Traumatology, Arthroscopy : Official Journal of the ESSKA*, 20(8), 1450–1455. <http://doi.org/10.1007/s00167-011-1684-9>

- Kaufner, H. (1971). Mechanical function of the patella. *The Journal of Bone and Joint Surgery. American Volume*, 53(8), 1551–1560. <http://doi.org/10.2106/JBJS>.
- Kim, Y.-H., Kim, J.-S., & Yoon, S.-H. (2007). Alignment and orientation of the components in total knee replacement with and without navigation support: a prospective, randomised study. *The Journal of Bone and Joint Surgery. British Volume*, 89(4), 471–476. <http://doi.org/10.1302/0301-620X.89B4.18878>
- Krevolin, J. L., Pandy, M. G., & Pearce, J. C. (2004). Moment arm of the patellar tendon in the human knee. *Journal of Biomechanics*, 37(5), 785–788. <http://doi.org/10.1016/j.jbiomech.2003.09.010>
- Krishnan, S. P., Dawood, A., Richards, R., Henckel, J., & Hart, A. J. (2012). A review of rapid prototyped surgical guides for patient-specific total knee replacement. *Journal of Bone and Joint Surgery - British Volume*. <http://doi.org/10.1302/0301-620X.94B11.29350>
- Lanovaz, J. L., & Ellis, R. E. (2008). Dynamic simulation of a displacement-controlled total knee replacement wear tester. *Proceedings of the Institution of Mechanical Engineers. Part H, Journal of Engineering in Medicine*, 222(5), 669–681. <http://doi.org/10.1243/09544119JEIM366>
- Lanovaz, J. L., & Ellis, R. E. (2009). A cadaverically evaluated dynamic FEM model of closed-chain TKR mechanics. *Journal of Biomechanical Engineering*, 131(5), 051002. <http://doi.org/10.1115/1.3078159>
- Liddle, A. D., Pegg, E. C., & Pandit, H. (2013). Knee replacement for osteoarthritis. *Maturitas*. <http://doi.org/10.1016/j.maturitas.2013.03.005>
- Liu, Y. L., Lin, K. J., Huang, C. H., Chen, W. C., Chen, C. H., Chang, T. W., ... Cheng, C. K. (2011). Anatomic-like polyethylene insert could improve knee kinematics after total knee arthroplasty - A computational assessment. *Clinical Biomechanics*, 26(6), 612–619. <http://doi.org/10.1016/j.clinbiomech.2011.01.013>
- Lotke, P. A., & Ecker, M. L. (1977). Influence of positioning of prosthesis in total knee replacement. *The Journal of Bone and Joint Surgery. American Volume*, 59(1), 77–79.
- Mahoney, O. M., McClung, C. D., dela Rosa, M. A., & Schmalzried, T. P. (2002). The effect of total knee arthroplasty design on extensor mechanism function. *J Arthroplasty*, 17(4), 416–421. <http://doi.org/S0883540302608290> [pii]
- MATLAB - The Language of Technical Computing. (n.d.). Retrieved June 28, 2015, from <http://www.mathworks.com/products/matlab/features.html>

- Matsuda, S., White, S. E., Williams, V. G., McCarthy, D. S., & Whiteside, L. A. (1998). Contact stress analysis in meniscal bearing total knee arthroplasty. *The Journal of Arthroplasty*, *13*(6), 699–706. [http://doi.org/10.1016/S0883-5403\(98\)80016-8](http://doi.org/10.1016/S0883-5403(98)80016-8)
- McEwen, H. M. J., Barnett, P. I., Bell, C. J., Farrar, R., Auger, D. D., Stone, M. H., & Fisher, J. (2005). The influence of design, materials and kinematics on the in vitro wear of total knee replacements. *Journal of Biomechanics*, *38*(2), 357–365. <http://doi.org/10.1016/j.jbiomech.2004.02.015>
- Moonot, P., Mu, S., Railton, G. T., Field, R. E., & Banks, S. A. (2009). Tibiofemoral kinematic analysis of knee flexion for a medial pivot knee. *Knee Surgery, Sports Traumatology, Arthroscopy*, *17*(8), 927–934. <http://doi.org/10.1007/s00167-009-0777-1>
- Mulholland, S. J., & Wyss, U. P. (2001). Activities of daily living in non-Western cultures: range of motion requirements for hip and knee joint implants. *International Journal of Rehabilitation Research. Internationale Zeitschrift Fur Rehabilitationsforschung. Revue Internationale de Recherches de Readaptation*, *24*(3), 191–198. <http://doi.org/10.1097/00004356-200109000-00004>
- NexGen® Complete Knee Solution Legacy® Knee Posterior Stabilized. (n.d.). Retrieved July 2, 2015, from <http://www.zimmer.com/medical-professionals/products/knee/nexgen-posterior-stabilized-lps-flex-fixed.html>
- NextEngine 3D Laser Scanner. (n.d.). Retrieved June 22, 2015, from <http://www.nextengine.com/faq>
- Nicoll, D., & Rowley, D. I. (2010). Internal rotational error of the tibial component is a major cause of pain after total knee replacement. *The Journal of Bone and Joint Surgery. British Volume*, *92*(9), 1238–1244. <http://doi.org/10.1302/0301-620X.92B9.23516>
- Noyes, F. R., Heckmann, T. P., & Barber-Westin, S. D. (2012). Meniscus repair and transplantation: a comprehensive update. *J Orthop Sports Phys Ther*, *42*(3), 274–290. <http://doi.org/10.2519/jospt.2012.3588>
- Nozaki, H., Banks, S. A., Suguro, T., & Hodge, W. A. (2002). Observations of femoral rollback in cruciate-retaining knee arthroplasty. *Clinical Orthopaedics and Related Research*, (404), 308–314. <http://doi.org/10.1097/01.blo.0000030061.92399.b1>
- ODEV | Balanced Knee® System. (n.d.). Retrieved June 28, 2015, from <http://www.odev.com/products/knee/balanced-knee-system/>

- Pandit, H., Jenkins, C., Barker, K., Dodd, C. A. F., & Murray, D. W. (2006). The Oxford medial unicompartmental knee replacement using a minimally-invasive approach. *The Journal of Bone and Joint Surgery. British Volume*, 88(1), 54–60.  
<http://doi.org/10.1302/0301-620X.88B8.18225>
- Pandit, H., Ward, T., Hollinghurst, D., Beard, D. J., Gill, H. S., Thomas, N. P., & Murray, D. W. (2005). *Influence of surface geometry and the cam-post mechanism on the kinematics of total knee replacement. The Journal of bone and joint surgery. British volume* (Vol. 87).
- Pang, C. H., Chan, W. L., Yen, C. H., Cheng, S. C., Woo, S. B., Choi, S. T., ... Mak, K. H. (2009). Comparison of total knee arthroplasty using computer-assisted navigation versus conventional guiding systems: a prospective study. *Journal of Orthopaedic Surgery (Hong Kong)*, 17(2), 170–173.
- Parsley, B. S., Conditt, M. A., Bertolusso, R., & Noble, P. C. (2006). Posterior cruciate ligament substitution is not essential for excellent postoperative outcomes in total knee arthroplasty. *The Journal of Arthroplasty*, 21(6 Suppl 2), 127–131.  
<http://doi.org/10.1016/j.arth.2006.05.012>
- Pereira, D. S., Jaffe, F. F., & Ortiguera, C. (1998). Posterior cruciate ligament-sparing versus posterior cruciate ligament-sacrificing arthroplasty. Functional results using the same prosthesis. *The Journal of Arthroplasty*, 13(2), 138–144.  
[http://doi.org/10.1016/S0883-5403\(98\)90091-2](http://doi.org/10.1016/S0883-5403(98)90091-2)
- Phisitkul, P., James, S. L., Wolf, B. R., & Amendola, A. (2006). MCL injuries of the knee: current concepts review. *The Iowa Orthopaedic Journal*, 26, 77–90.
- Pour, A. E., Parvizi, J., Slenker, N., Purtill, J. J., & Sharkey, P. F. (2007). Rotating hinged total knee replacement: use with caution. *The Journal of Bone and Joint Surgery. American Volume*, 89(8), 1735–1741. <http://doi.org/10.2106/JBJS.F.00893>
- Primary Knee Systems - Triathlon Total Knee : Stryker. (n.d.). Retrieved June 28, 2015, from <http://www.stryker.com/en-us/products/Orthopaedics/KneeReplacement/Primary/Triathlon/005025>
- Pritchett, J. W. (2011). Patients Prefer A Bicruciate-Retaining or the Medial Pivot Total Knee Prosthesis. *Journal of Arthroplasty*, 26(2), 224–228.  
<http://doi.org/10.1016/j.arth.2010.02.012>
- Ranawat, C. S. (2003). Design may be counterproductive for optimizing flexion after TKR. *Clinical Orthopaedics and Related Research*, (416), 174–176.  
<http://doi.org/10.1097/01.blo.0000093028.56370.46>

- Ritter, M. A., Faris, P. M., Keating, E. M., & Meding, J. B. (1994). Postoperative alignment of total knee replacement. Its effect on survival. *Clinical Orthopaedics and Related Research*, (299), 153–156. <http://doi.org/10.1097/00003086-199402000-00021>
- Ritter, M. A., Thong, A. E., Keating, E. M., Faris, P. M., Meding, J. B., Berend, M. E., ... Davis, K. E. (2005). The effect of femoral notching during total knee arthroplasty on the prevalence of postoperative femoral fractures and on clinical outcome. *The Journal of Bone and Joint Surgery. American Volume*, 87(11), 2411–2414. <http://doi.org/10.2106/JBJS.D.02468>
- Rodkey, W. G. (2000). Basic biology of the meniscus and response to injury. *Instructional Course Lectures*, 49, 189–193.
- Sathasivam, S., & Walker, P. S. (1998). Computer model to predict subsurface damage in tibial inserts of total knees. *Journal of Orthopaedic Research*, 16(5), 564–571. <http://doi.org/10.1002/jor.1100160507>
- Shenoy, R., Pastides, P. S., & Nathwani, D. (2013). (iii) Biomechanics of the knee and TKR. *Orthopaedics and Trauma*, 27(6), 364–371. <http://doi.org/10.1016/j.mporth.2013.10.003>
- Shimizu, N., Tomita, T., Yamazaki, T., Yoshikawa, H., & Sugamoto, K. (2014). In Vivo Movement of Femoral Flexion Axis of a Single-Radius Total Knee Arthroplasty. *Journal of Arthroplasty*. <http://doi.org/10.1016/j.arth.2013.12.001>
- Sikorski, J. M. (2008). Alignment in total knee replacement. *The Journal of Bone and Joint Surgery. British Volume*, 90(9), 1121–1127. <http://doi.org/10.1302/0301-620X.90B9.20793>
- Slover, J. D., Rubash, H. E., Malchau, H., & Bosco, J. A. (2012). Cost-effectiveness analysis of custom total knee cutting blocks. *Journal of Arthroplasty*, 27(2), 180–185. <http://doi.org/10.1016/j.arth.2011.04.023>
- Snibbe, J. C., & Gambardella, R. A. (2005). Treatment options for osteoarthritis. *Orthopedics*, 28(2 Suppl), s215–s220.
- Sorger, J. I., Federle, D., Kirk, P. G., Grood, E., Cochran, J., & Levy, M. (1997). The posterior cruciate ligament in total knee arthroplasty. *J Arthroplasty*, 12(8), 869–879. [http://doi.org/10.1016/s0883-5403\(97\)90156-x](http://doi.org/10.1016/s0883-5403(97)90156-x)

- Soudry, M., Walker, P. S., Reilly, D. T., Kurosawa, H., & Sledge, C. B. (1986). Effects of total knee replacement design on femoral-tibial contact conditions. *J Arthroplasty*, *1*(1), 35–45. Retrieved from <http://www.ncbi.nlm.nih.gov/htbin-post/Entrez/query?db=m&form=6&dopt=r&uid=0003559575>
- Spencer, B. A., Mont, M. A., McGrath, M. S., Boyd, B., & Mitrick, M. F. (2009). Initial experience with custom-fit total knee replacement: Intra-operative events and long-leg coronal alignment. *International Orthopaedics*, *33*(6), 1571–1575. <http://doi.org/10.1007/s00264-008-0693-x>
- Stulberg, S. D. (2003). How accurate is current TKR instrumentation? *Clinical Orthopaedics and Related Research*, (416), 177–184. <http://doi.org/10.1097/01.blo.0000093029.56370.0f>
- Surgical Technique for TKR - Wheelless' Textbook of Orthopaedics. (n.d.). Retrieved July 2, 2015, from [http://www.wheelsonline.com/ortho/surgical\\_technique\\_for\\_tkr](http://www.wheelsonline.com/ortho/surgical_technique_for_tkr)
- Sutton, L. G., Werner, F. W., Haider, H., Hamblin, T., & Clabeaux, J. J. (2010). In vitro response of the natural cadaver knee to the loading profiles specified in a standard for knee implant wear testing. *Journal of Biomechanics*, *43*(11), 2203–7. <http://doi.org/10.1016/j.jbiomech.2010.03.042>
- Systems, S. M. K. (n.d.). Medial-Pivot and Stemmed Medial-Pivot Knee Systems A D VANCE®.
- Taylor, D. (n.d.). 3-maticSTL | Software for additive manufacturing. Retrieved June 22, 2015, from <http://software.materialise.com/3-maticSTL>
- Voos, J. E., Mauro, C. S., Wentz, T., Warren, R. F., & Wickiewicz, T. L. (2012). Posterior cruciate ligament: anatomy, biomechanics, and outcomes. *The American Journal of Sports Medicine*, *40*(1), 222–31. <http://doi.org/10.1177/0363546511416316>
- Walker, P. S., Blunn, G. W., Broome, D. R., Perry, J., Watkins, A., Sathasivam, S., ... Paul, J. P. (1997). A knee simulating machine for performance evaluation of total knee replacements. *Journal of Biomechanics*, *30*(1), 83–89.
- Walker, P. S., Blunn, G. W., Perry, J. P., Bell, C. J., Sathasivam, S., Andriacchi, T. P., ... Campbell, P. A. (2000). Methodology for long-term wear testing of total knee replacements. *Clinical Orthopaedics and Related Research*, (372), 290–301.

- Walker, P. S., & Sathasivam, S. (2000). Design forms of total knee replacement. *Proceedings of the Institution of Mechanical Engineers. Part H, Journal of Engineering in Medicine*, 214(1), 101–119. <http://doi.org/10.1243/0954411001535282>
- Wang, H., Simpson, K. J., Chamnongkich, S., Kinsey, T., & Mahoney, O. M. (2005). A biomechanical comparison between the single-axis and multi-axis total knee arthroplasty systems for the stand-to-sit movement. *Clinical Biomechanics*, 20(4), 428–433. <http://doi.org/10.1016/j.clinbiomech.2004.12.003>
- Waslewski, G. L., Marson, B. M., & Benjamin, J. B. (1998). Early, incapacitating instability of posterior cruciate ligament-retaining total knee arthroplasty. *The Journal of Arthroplasty*, 13(7), 763–767. [http://doi.org/10.1016/S0883-5403\(98\)90027-4](http://doi.org/10.1016/S0883-5403(98)90027-4)
- Weisstein, E. W. (n.d.). Newton's Method. Wolfram Research, Inc. Retrieved from <http://mathworld.wolfram.com/NewtonsMethod.html>
- Werner, F. W., Ayers, D. C., Maletsky, L. P., & Rullkoetter, P. J. (2005). The effect of valgus/varus malalignment on load distribution in total knee replacements. *Journal of Biomechanics*, 38(2), 349–355. <http://doi.org/10.1016/j.jbiomech.2004.02.024>
- Willing, R., & Kim, I. Y. (2011). Design optimization of a total knee replacement for improved constraint and flexion kinematics. *Journal of Biomechanics*, 44(6), 1014–1020. <http://doi.org/10.1016/j.jbiomech.2011.02.009>
- Wilson, D. R., Feikes, J. D., & Connor, J. J. (1998). Ligaments and articular contact guide passive knee flexion. *Journal of Biomechanics*, 31(12), 1127–1136. [http://doi.org/10.1016/S0021-9290\(98\)00119-5](http://doi.org/10.1016/S0021-9290(98)00119-5)
- Wimmer, M. A., Laurent, M. P., Haman, J. D., Jacobs, J. J., & Galante, J. O. (2012). Surface damage versus tibial polyethylene insert conformity: A retrieval study. In *Clinical Orthopaedics and Related Research* (Vol. 470, pp. 1814–1825). <http://doi.org/10.1007/s11999-012-2274-y>
- Woo, S. L. Y., Chan, S. S., & Yamaji, T. (1997). Biomechanics of knee ligament healing, repair and reconstruction. *Journal of Biomechanics*, 30(5), 431–439. [http://doi.org/10.1016/S0021-9290\(96\)00168-6](http://doi.org/10.1016/S0021-9290(96)00168-6)
- Yagishita, K., Muneta, T., Ju, Y. J., Morito, T., Yamazaki, J., & Sekiya, I. (2012). High-flex Posterior Cruciate-Retaining vs Posterior Cruciate-Substituting Designs in Simultaneous Bilateral Total Knee Arthroplasty. A Prospective, Randomized Study. *Journal of Arthroplasty*, 27(3), 368–374. <http://doi.org/10.1016/j.arth.2011.05.008>

Yamaguchi, G. T., & Zajac, F. E. (1989). A planar model of the knee joint to characterize the knee extensor mechanism. *Journal of Biomechanics*, 22(1), 1–10.  
[http://doi.org/10.1016/0021-9290\(89\)90179-6](http://doi.org/10.1016/0021-9290(89)90179-6)

Zelle, J., Janssen, D., Van Eijden, J., De Waal Malefijt, M., & Verdonschot, N. (2011). Does high-flexion total knee arthroplasty promote early loosening of the femoral component? *Journal of Orthopaedic Research*, 29(7), 976–983.  
<http://doi.org/10.1002/jor.21363>